

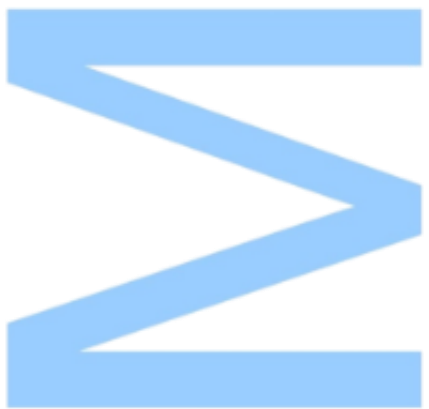


Response of *Solanum lycopersicum* L. to diclofenac – impacts on the plants' xenome and antioxidant mechanisms

Bruno Filipe Pereira de Sousa
Dissertação de Mestrado apresentada à
Faculdade de Ciências da Universidade do Porto em
Biologia Funcional e Biotecnologia de Plantas
2018

Response of *Solanum lycopersicum* L. to diclofenac
– impacts on the plants' xenome and antioxidant
mechanisms

Bruno Filipe Pereira de Sousa





Response of *Solanum lycopersicum* L. to diclofenac – impacts on the plants' xenome and antioxidant mechanisms

Bruno Filipe Pereira de Sousa

Mestrado em Biologia Funcional e Biotecnologia de Plantas

Departamento de Biologia

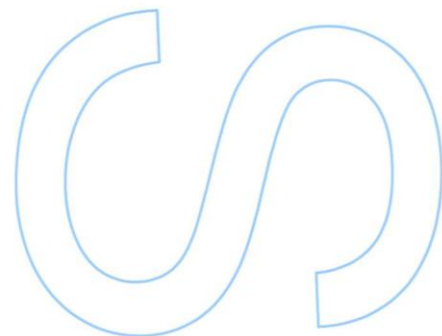
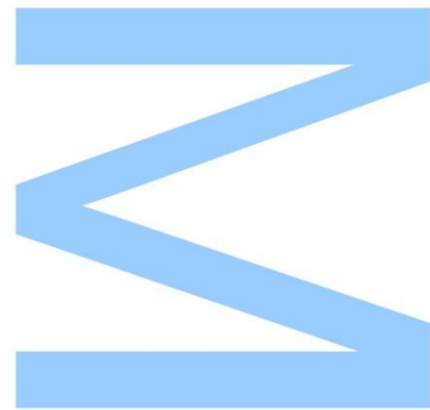
2018

Orientador

Jorge Teixeira, Professor Auxiliar, FCUP

Coorientador

Fernanda Fidalgo, Professora Auxiliar, FCUP

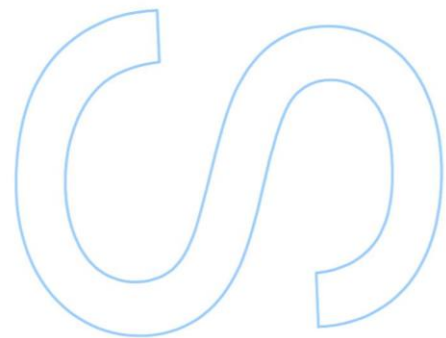
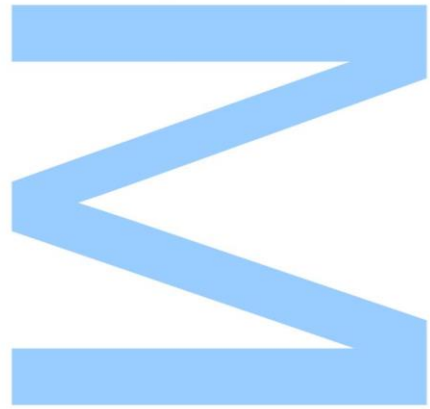




Todas as correções determinadas pelo júri, e só essas, foram efetuadas.

O Presidente do Júri,

Porto, ____ / ____ / ____



Data presented in the following scientific communication was used for the elaboration of this master dissertation:

- Sousa, Bruno; Lopes, Jorge; Leal, André; Fidalgo, Fernanda; Teixeira, Jorge., 2018. Role of tomato glutathione-S-transferase and the contribution of glutathione metabolism-related enzymes in response to diclofenac - molecular and biochemical approaches. IJUP 18 – Encontro de Jovens Investigadores da Universidade do Porto, Portugal. – **Awarded as the best oral communication in the Agrofood & Environment area.**

Agradecimentos

Após o término deste trabalho, chega a altura de agradecer a quem, à sua maneira, me ajudou a chegar a este ponto.

Ao Professor Doutor Jorge Teixeira, por ter aceite ser o meu mentor neste ano, pelo voto de confiança, pela motivação e por toda a ajuda que disponibilizou ao longo deste percurso, devo um grande agradecimento. À Professora Doutora Fernanda Fidalgo, um muito obrigado pela disponibilidade e sinceridade com que ajudou a direcionar este projeto. Um muito obrigado também ao Professor Doutor Manuel Azenha, pela ajuda com as quantificações do diclofenac e pela simpatia com que sempre me recebeu, e à Doutora Zélia pela ajuda na técnica do HPLC.

Ao Cris, que como membro mais velho deste laboratório, me fez sentir à vontade e bem-vindo, obrigado por toda a ajuda e boa disposição com que sempre nos agraciaste. À Maria, o meu “monstro” preferido, obrigado pela nossa amizade e por, depois de todos os tremores, continuares comigo para me motivares, para me ajudares e para libertar todos os dramas que este ano ofereceu. À Ana, obrigado por toda a ajuda nas “cenas lá dos bioquímicos” e pelos chocolates que nos trazias! Ao Sampaio e ao André, obrigado por deixarem nunca haver um momento aborrecido naquele laboratório, e ao André especialmente pela ajuda e pela confiança de me ter como “mini-boss”.

Ao Jorge, cinco anos depois ainda conseguimos acabar no mesmo laboratório. Não há ironia suficiente para descrever o quão “gémeos” nós fomos durante todo este percurso, por isso resta-me agradecer a tua amizade e tirar conforto em saber que o lodo teve sempre espaço para dois. Ao Pedro, porque #elesfalammasdãolike, por teres sido o melhor colega de estágio, e por seres bronze no LOL, mas challenger como amigo. À Iolanda, obrigado por teres estado sempre comigo ao longo destes anos, mesmo quando nos isolamos do mundo, sabes que não tenho palavras para ti. Aos três, obrigado por serem os melhores irmãos que podia pedir e porque nem aqui deixamos de deprimir e rir em conjunto.

À Cláudia, muito obrigado. Obrigado por seres das pessoas mais importantes que do nada me apareceu e com quem sempre pude contar este ano. Acima de tudo, obrigado por sempre acreditares em mim e na minha força, mesmo quando eu não o conseguia. À Sara, obrigado por tudo! Por todas as gordices, dramas, motivações e séries, foste das melhores pessoas que estes últimos tempos me deu e porque sem ti, não teria muita da motivação que me permitiu chegar aqui. À Catarina, por todos os lanches, por todos os gatos e por me mostrar sempre que nunca estamos velhos demais

enquanto se tem amigos. Às três, obrigado por serem a melhor “poli” que podia pedir e eu estarei cá a retribuir o favor quando for a vossa vez.

Ao Micael e ao Pedro, obrigado por todos os caminhos a pé, por todas as idas à pizza e ao Mac e por estarem sempre comigo ao longo deste ano e por serem sempre uma força positiva quando me afogava em trabalho.

À minha família, obrigado por todo o apoio e por tudo o que fizeram por mim, mesmo quando não é fácil.

A todos que aqui agradei, obrigado por tudo o resto que não mencionei, este sentimentalismo não é de todo o meu forte, mas sabem que sem vocês não teria chegado a este ponto. Muito obrigado.

Resumo

Um problema ambiental que recentemente tem ganho notoriedade é a contaminação de águas superficiais e subterrâneas com fármacos. O diclofenac (DCF) é um dos fármacos mais comumente encontrados nestas águas devido à sua alta taxa de utilização e também à fraca eficácia de remoção nos processos de tratamentos de águas residuais. Neste trabalho, foram usados tomateiros para verificar como uma espécie agronomicamente importante reage a este contaminante, sendo focados os mecanismos internos despoletados por esta exposição e especialmente no papel das enzimas relacionadas com o metabolismo da glutathione (GSH), uma vez que a conjugação GSH-DCF é um fenómeno de destoxificação já descrito em vários mamíferos e algumas plantas. Os resultados obtidos apontam para uma diminuição a nível biométrico da parte aérea das plantas tratadas com concentrações muito elevadas, mas não foi detetado atraso a nível da maturação das plantas, uma vez que atingiram a fase de fruto ao mesmo tempo e com rendimento semelhante. Estes resultados, em conjugação à falta de DCF quantificável nos frutos mostra que no atual contexto ambiental, a espécie vegetal utilizada é candidata viável ao cultivo em zonas contaminadas sem efeitos negativos notórios a nível de rendimento ou de saúde, sendo que a sua presença parece ainda auxiliar na remoção do DCF no meio circundante. Acerca do stresse induzido nas plantas pelo DCF, os resultados mostram que estas sofreram stresse oxidativo devido à acumulação de espécies reativas de oxigénio que em níveis elevados levaram à ocorrência de peroxidação lipídica e danos na integridade membranar das células na raiz. Estes efeitos negativos levaram a planta a focar-se nos efeitos protetores da prolina e da rede redox mediada por grupos tióis, enquanto que através da análise de enzimas antioxidantes foi detetada uma inibição da resposta enzimática, consistindo numa diminuição significativa da atividade da catalase e da peroxidase do ascorbato. A resposta a este contaminante parece ter sido sistémica, mas na generalidade os resultados apontam para que a destoxificação seja um processo na sua maioria confinado à raiz da planta. Para além disto, a hipótese da destoxificação mediada pela GSH parece ter sido corroborada pelos resultados deste trabalho, uma vez que a atividade da glutathione-S-transferase (GST) associada a menores níveis totais de GSH indicam uma conjugação desta ao DCF através da ação da GST. Foi também avaliada a importância da classe tau das GSTs neste processo, mas um maior foco foi dado à análise de genes da classe phi (GSTF), mostrando que *GSTF4* e *GSTF5* são os genes principalmente responsáveis por esta destoxificação.

Abstract

One emerging environmental problem that recently has become a vastly acknowledged topic of concern is surface and groundwater pollution from pharmaceuticals. Diclofenac (DCF) is one of the most common pharmaceuticals found in these waters due to its high utilization rate and low removal in wastewater treatment processes. In this research, tomato plants were used to unravel how DCF contamination can affect an agronomically important crop, focusing on the internal mechanisms triggered by this exposure and especially on the role of glutathione (GSH)-related enzymes, as GSH conjugation to DCF is a well reported detoxification mechanism in mammals and in some plants. Results obtained here point towards a loss of shoot performance when plants were exposed to very high DCF concentrations, but with no delay in their growth, as treated plants presented fruits at the same time period and in similar quantity. These results, along with the lack of DCF quantified in the fruits indicate that, in the current environmental context, tomato plants are applicable to be cultivated in contaminated soils without noticeable negative effects, while also participating in the removal of DCF from the surrounding environment. Regarding DCF-induced stress, results show that a state of oxidative stress due to high reactive oxygen species accumulation was associated with this contamination, with very high DCF levels leading to the rise of lipid peroxidation and subsequent loss of membrane integrity in roots of treated plants. These negative effects triggered the plant to focus on the protective effects of proline and the thiol-based redox network, while the analysis of antioxidant enzymes showed an inhibition of the enzymatic response, as ascorbate peroxidase and catalase had their activities significantly reduced. Although a systemic response seems to be present in response to this contaminant, the results show that detoxification of DCF was mostly a root-specific process. Furthermore, the hypothesis of GSH-mediated DCF detoxification was corroborated by the obtained results, as glutathione-S-transferase (GST) activity associated with lower levels of free GSH point towards a GST-mediated GSH conjugation. Here, the importance of the tau class of GSTs was accessed, but a major focus was given to genes of the phi (GSTF) class, showing that *GSTF4* and *GSTF5* were the main players in the conjugation of this contaminant.

Keywords

Pharmaceuticals; NSAID; glutathione metabolism; glutathione-S-transferase; xenobiotic detoxification; reactive oxygen species; oxidative stress; tomato plants.

Table of Contents

Agradecimentos.....	II
Resumo	IV
Abstract	V
Keywords.....	VI
Table of Contents	VI
Figure Index.....	IX
Table Index.....	XII
Abbreviations and Acronyms	XIII
1. Introduction.....	1
1.1. Pharmaceuticals in the environment – Occurrence, fate and risks	1
1.2. Diclofenac – Occurrence, fate and risks.....	2
1.3. Xenobiotic detoxification	4
1.4. Diclofenac metabolism.....	7
1.5. Oxidative stress and plant antioxidant defense	7
1.5.1. Reactive oxygen species (ROS)	8
1.5.2. Antioxidant mechanism.....	11
1.6. Glutathione	15
1.7. Glutathione-S-Transferase.....	16
1.8. <i>Solanum lycopersicum</i> L. cv. Micro-Tom	17
1.9. Objectives.....	18
2. Material and Methods	20
2.1. Diclofenac.....	20
2.2. <i>Solanum lycopersicum</i> L. seeds	20
2.3. Tested concentrations	20
2.4. Germination assay.....	20
2.5. Growth trial	21
2.6. Diclofenac quantification.....	21
2.7. Analysis of biochemical parameters.....	22
2.7.1. Quantification of soluble proteins.....	22
2.7.2. Determination of lipid peroxidation.....	22

2.7.3.	Determination of ROS levels.....	23
2.7.3.1.	Quantification of H ₂ O ₂	23
2.7.3.2.	Quantification of O ₂ ⁻	23
2.7.4.	Quantification of non-enzymatic AOX metabolites	24
2.7.4.1.	Determination of proline levels.....	24
2.7.4.2.	Quantification of reduced and oxidized glutathione	24
2.7.5.	Quantification of total and non-protein thiols	25
2.7.6.	Determination of ROS-scavenging enzymatic activity	25
2.7.6.1.	Extraction	25
2.7.6.2.	Determination of SOD activity.....	26
2.7.6.3.	Determination of APX activity	26
2.7.6.4.	Determination of CAT activity	26
2.7.7.	Determination of glutathione-related enzymes' activities.....	27
2.7.7.1.	Determination of γ-ECS activity	27
2.7.7.2.	Determination of GR activity	27
2.7.7.3.	Determination of GST activity	28
2.7.7.4.	GST activity in a native polyacrylamide gel electrophoresis (PAGE)	28
2.8.	Analysis of molecular parameters	29
2.8.1.	RNA extraction and quantification.....	29
2.8.2.	Reverse transcription (RT) - cDNA synthesis.....	30
2.8.3.	Semi-quantitative polymerase chain reaction (PCR)	31
2.8.4.	Expression of GSTF genes by Real-Time (q) PCR.....	32
2.9.	Statistical analysis	33
3.	Results	34
3.1.	Effects of increasing diclofenac concentrations on plants' biometry	34
3.1.1.	Effects of increasing diclofenac concentrations on germination and seedlings' biometry	34
3.1.2.	Effects of increasing diclofenac concentrations on the biometrical parameters of exposed plants.....	35
3.2.	Quantification of diclofenac in fruits and in the nutritive medium	37
3.3.	Effects of increasing diclofenac concentrations on several stress biomarkers of <i>S. lycopersicum</i> plants.....	38

3.3.1.	Soluble protein content.....	38
3.3.2.	Diclofenac-induced oxidative stress.....	38
3.3.3.	Effects of diclofenac on the non-enzymatic components of <i>S. lycopersicum</i> plants' antioxidant system	40
3.3.4.	Effects of diclofenac on the enzymatic components of <i>S. lycopersicum</i> plants' antioxidant system	42
3.3.5.	Effects of diclofenac on the GSH-related enzymes' activities.....	44
3.4.	Effects of increasing diclofenac concentrations on the transcript accumulation of several AOX enzymes.....	46
3.4.1.	Effects of increasing diclofenac concentrations on the transcript accumulation of GRcyt, γ -ECS and GSTU genes	46
3.4.2.	Effects of increasing diclofenac concentrations on the transcript accumulation of <i>SIGSTs</i>	48
4.	Discussion	50
4.1.	Diclofenac and plants' growth and development.....	50
4.2.	Diclofenac-induced oxidative stress.....	52
4.3.	Uprising of antioxidant defenses against Diclofenac-induced stress	54
4.4.	Inhibition of ROS-scavenging enzymes after DCF exposure.....	56
4.5.	Glutathione metabolism in response to Diclofenac exposure	58
4.6.	Role of specific GSTs in the response of tomato plants to Diclofenac....	60
4.7.	<i>S. lycopersicum</i> plants in DCF-contaminated soils	62
5.	Concluding Remarks	64
6.	Future Perspectives.....	65
7.	Bibliography.....	66

Figure Index

Figure 1. Fate of pharmaceuticals in the environment (Khetan and Collins, 2007).2	
Figure 2. Equilibrium between AOX and ROS and its unbalance, leading to oxidative stress (Gill and Tuteja, 2010).....	8
Figure 3. Reactive oxygen species (ROS) and oxidative damage to lipids, proteins, and DNA (Sharma et al., 2012).....	11
Figure 4. Antioxidant resources in the different organelles of plant cells. Adapted from Ahmad et al. (2010).....	12
Figure 5. Ascorbate-Glutathione cycle.....	14
Figure 6. <i>Solanum lycopersicum</i> cv. Micro-Tom (left) bearing fruits and a standard tomato fruit (right) (Source: http://www.kazusa.or.jp/jsol/microtom/project.html)	18
Figure 7. Germination rate (A), total biomass (B) and shoot (C) and root (D) length of <i>S. lycopersicum</i> seedlings grown in nutrient medium supplemented with increasing diclofenac concentrations. Values presented are mean \pm SD. * above bars represent significant differences from the control at * $p \leq 0.05$, ** $p \leq 0.01$, *** $p \leq 0.001$, **** $p \leq 0.0001$	34
Figure 8. Effect of different concentrations of diclofenac on tomato plants' morphology. Plants were grown for 6 weeks in a growth chamber (16 h light/8 h dark; 25 °C) and on the last 5 weeks were treated with Hoagland solution supplemented with 0 mg L ⁻¹ (control), 0.5 mg L ⁻¹ and 5 mg L ⁻¹ diclofenac.	35
Figure 9. Root and shoot length (A) and biomass (B) of <i>S. lycopersicum</i> plants grown in nutrient medium supplemented with increasing concentrations of diclofenac. (C) represents the ratio between root and shoot biomass. (D) Water content in the same treated plants. Values presented are mean \pm SD. * above bars represent significant differences from the control at * $p \leq 0.05$, ** $p \leq 0.01$, *** $p \leq 0.001$, **** $p \leq 0.0001$	36
Figure 10. Over-time removal of diclofenac by tomato plants. The brown line represents a “no-plants” situation, which was irrigated with 5 mg L ⁻¹ on day 0 and diclofenac levels were measured over the following three days. The green line represents the “with-plants” situation, which was irrigated with the same concentration on day 0, day 2 and day 4. Values presented are mean \pm SD and values below the limit of quantification are represented as 0.....	37
Figure 11. Soluble protein content of <i>S. lycopersicum</i> plants grown in nutrient medium supplemented with increasing concentrations of diclofenac. Values presented are mean \pm SD. * above bars represent significant differences from the control at * $p \leq 0.05$, ** $p \leq 0.01$, *** $p \leq 0.001$, **** $p \leq 0.0001$	38

Figure 12. Total thiol levels in roots and shoots of *S. lycopersicum* plants grown in nutrient medium supplemented with increasing concentrations of diclofenac. Values presented are mean ± SD. * above bars represent significant differences from the control at * $p \leq 0.05$, ** $p \leq 0.01$, *** $p \leq 0.001$, **** $p \leq 0.0001$ 39

Figure 13. Free proline levels in roots and shoots of *S. lycopersicum* plants grown in nutrient medium supplemented with increasing concentrations of diclofenac. Values presented are mean ± SD. * above bars represent significant differences from the control at * $p \leq 0.05$, ** $p \leq 0.01$, *** $p \leq 0.001$, **** $p \leq 0.0001$ 41

Figure 14. SOD activity levels (left) and function (right) in plants treated with increasing diclofenac concentrations. Values presented are mean ± SD. * above bars represent significant differences from the control at * $p \leq 0.05$, ** $p \leq 0.01$, *** $p \leq 0.001$, **** $p \leq 0.0001$ 42

Figure 15. APX activity levels (left) and function (right) in plants treated with increasing diclofenac concentrations. Values presented are mean ± SD. * above bars represent significant differences from the control at * $p \leq 0.05$, ** $p \leq 0.01$, *** $p \leq 0.001$, **** $p \leq 0.0001$ 43

Figure 16. CAT activity levels (left) and function (right) in plants treated with increasing diclofenac concentrations. Values presented are mean ± SD. * above bars represent significant differences from the control at * $p \leq 0.05$, ** $p \leq 0.01$, *** $p \leq 0.001$, **** $p \leq 0.0001$ 43

Figure 17. γ-ECS activity levels (left) and function (right) in plants treated with increasing diclofenac concentrations. Values presented are mean ± SD. * above bars represent significant differences from the control at * $p \leq 0.05$, ** $p \leq 0.01$, *** $p \leq 0.001$, **** $p \leq 0.0001$ 44

Figure 18. GR activity levels (left) and function (right) in plants treated with increasing diclofenac concentrations. Values presented are mean ± SD. * above bars represent significant differences from the control at * $p \leq 0.05$, ** $p \leq 0.01$, *** $p \leq 0.001$, **** $p \leq 0.0001$ 45

Figure 19. GST activity levels (left) and function (right) in plants treated with increasing diclofenac concentrations. Values presented are mean ± SD. * above bars represent significant differences from the control at * $p \leq 0.05$, ** $p \leq 0.01$, *** $p \leq 0.001$, **** $p \leq 0.0001$ 45

Figure 20. Typical results of a native polyacrylamide gel electrophoresis analysis of tomato GST, disclosing GST activity in plants treated with increasing diclofenac concentrations (40 µg of soluble proteins were loaded for each lane). 46

Figure 21. 0.8% (w/v) agarose gel analysis of the total RNA extracted from *S. lycopersicum* plants treated with increasing diclofenac concentrations. 1. 28 S rRNA; 2. 18 S rRNA; 3. 5 S + tRNAs..... 47

Figure 22. Typical results for GRcyt, γ -ECS and GSTU RT-PCR analysis by 1% (w/v) agarose gel electrophoresis in *S. lycopersicum* plants treated with increasing diclofenac concentrations..... 47

Figure 23. Transcript levels of selected tomato *GSTF* genes in roots (A) and shoots (B) of tomato plants subjected to increasing diclofenac concentrations. Data were normalized using the tomato actin and ubiquitin gene as internal control and the relative transcript level in the control samples was arbitrarily considered as one for each gene. *above bars represent significant statistical differences from the control at $p \leq 0.05$ 49

Table Index

Table 1. Nomenclature and physicochemical properties of diclofenac (Source: www.pubchem.ncbi.nlm.nih.gov).	3
Table 2. Constitution of the native polyacrylamide gel performed for visual determination of GST activity. Volumes presented are the necessary for one gel.	29
Table 3. Gene-specific primers and PCR programs for the RT-PCR reactions carried out. (') minutes; (") seconds.	31
Table 4. Gene-specific primers for the performed qPCR assay, respective melting temperature (T _m) and amplicon sizes.	32
Table 5. MDA, O ₂ ⁻ and H ₂ O ₂ levels in plants treated with increasing diclofenac concentrations. Values presented are mean ± SD. * represent significant differences from the control at * p ≤ 0.05, ** p ≤ 0.01, *** p ≤ 0.001, **** p ≤ 0.0001.....	39
Table 6. Non-protein and protein-bound thiol levels and percentages in plants treated with increasing diclofenac concentrations. Values presented are mean ± SD. * represent significant differences from the control at * p ≤ 0.05, ** p ≤ 0.01, *** p ≤ 0.001, **** p ≤ 0.0001.....	40
Table 7. Glutathione levels in roots and shoots of <i>S. lycopersicum</i> plants grown in nutrient medium supplemented with increasing concentrations of diclofenac. Values presented are mean ± SD. * represent significant differences from the control at * p ≤ 0.05, ** p ≤ 0.01, *** p ≤ 0.001, **** p ≤ 0.0001.	42

Abbreviations and Acronyms

·OH – hydroxyl radical	GSSG – oxidized glutathione
¹O₂ – singlet oxygen	GST – glutathione-S-transferase
ACT – actin	GSTF – glutathione-S-transferase phi class
AOX – antioxidant	GSTL – glutathione-S-transferase lambda class
APS – ammonium persulfate	GSTT – glutathione-S-transferase theta class
APX – ascorbate peroxidase	GSTU – glutathione-S-transferase tau class
AsA – ascorbate	GSTZ – glutathione-S-transferase zeta class
BSA – bovine serum albumin	H₂O₂ – hydrogen peroxide
CAT – catalase	HO₂[·] - hydroperoxyl radical
cDNA – complementary DNA	HPLC – high-performance liquid chromatography
CDNB - 1-chloro-2,4-dinitrobenzene	LPO – lipid peroxidation
C_t – threshold cycle	MDA – malondialdehyde
Cu/Zn – copper/zinc	MDHA - monodehydroascorbate
DAD – diode array detector	MDHAR – monodehydroascorbate reductase
DCF – diclofenac	Mn – manganese
DHA - dehydroascorbate	NADPH – nicotinamide adenine dinucleotide phosphate
DHAR – dehydroascorbate reductase	NBT – nitroblue tetrazolium
DTNB - 5,5'-dithiobis(2-nitrobenzoic acid)	NO[·] - nitric oxide
DTT – dithiothreitol	NSAID – non-steroidal anti-inflammatory drug
EDTA - ethylenediaminetetraacetic acid	O₂ – molecular oxygen
ESI – electrospray ionization	O₂^{·-} - superoxide anion
ETC – electron transport chain	P5C - Δ ¹ -pyrroline-5-carboxylate
Fe – iron	
fw – fresh weight	
GPOX – glutathione peroxidase	
GR – glutathione reductase	
GRchl – plastidial glutathione reductase	
GRcyt – cytosolic glutathione reductase	
Grx - glutaredoxin	
GSH – glutathione	
GSS – glutathione synthetase	

PAGE – polyacrylamide gel

electrophoresis

PCR – polymerase chain reaction

PhAC – pharmaceutically active compound

PMS – phenazine methosulphate

PMSF – phenylmethylsulphonyl fluoride

PPCPs – pharmaceuticals and personal care products

PS – photosystem

PVPP – polyvinylpolypyrrolidone

qPCR – real-time polymerase chain reaction

ROS – reactive oxygen species

RT – reverse transcription

SD – standard deviation

SIM – selected ion monitoring

SIGSTF – *Solanum lycopersicum*

glutathione-s-transferase phi class

SN – supernatant

SOD – superoxide dismutase

TBA – thiobarbituric acid

TCA – trichloroacetic acid

TEMED – tetramethylethylenediamine

Tm – melting temperature

Trx – thioredoxin

γ-EC – γ-glutamylcysteine

γ-ECS – γ-glutamyl-cysteinyl synthetase

1. Introduction

1.1. Pharmaceuticals in the environment – Occurrence, fate and risks

An emerging environmental problem that has recently become a widely acknowledged topic of concern is surface and groundwater pollution from pharmaceuticals and personal care products (PPCPs) (Khetan and Collins, 2007). Pharmaceutical industry is a very large and leading industry around the globe, whose products can be utilized in a vast array of situations, such as in medical, agricultural and biotechnological cases, and averaging a consumption rate of 50 to 150 g per capita per year in industrialized regions (Lonappan et al., 2016). These pharmaceutically active compounds (PhACs) are a category that comprises a vast variety of prescription drugs, over the counter medication, and drugs utilized in hospital or veterinary treatments (Ebele et al., 2017). They can enter the environment (Figure 1) through the disposal of unused medication, but mostly due to incomplete elimination from the organism, as they are excreted in an insignificantly or even non-transformed form. Additionally, these contaminants can be conjugated to polar molecules, with these conjugates suffering cleavage during sewage treatment, discharging the original PhACs in the aquatic environment (Heberer, 2002; Lonappan et al., 2016).

Some of these compounds have already been detected in drinking water throughout the world, utilizing methods that are sensible to ng L^{-1} concentrations, assuring that conventional water treatment processes are not enough to efficiently remove PPCPs and avoid the prospective dangers to aquatic environments and surrounding organisms (Snyder, 2008; Ebele et al., 2017). To add to this, any degradation or removal of some compounds is easily compensated by constant and increasing release in the environment, thus being considered as pseudo-persistent contaminants (Grassi et al., 2013) and danger ensues, as these products are designed to cause deep effects in low concentrations (Fent et al., 2006). PPCPs can then reach plants mostly by the utilization of wastewater for irrigation, as well as the application of treated sewage sludge (i.e. biosolids) for soil fertilization and as the percentage of use of these methods in soil irrigation increases, so does the amount of these compounds in agricultural systems (Bartrons and Peñuelas, 2017). Consequently, as plants are primary producers, pharmaceutical uptake by these organisms can cause problems in those pertaining to higher trophic levels, posing a threat along the entire food chain, through ingestion (Mohapatra et al., 2016). Regarding these problems, most studies up to date utilize

aquatic environments and have shown that exposure to some of these compounds can cause several reactions, affecting per example, mobility, fecundity, embryonic endpoints and cognitive functions, as well as downregulating genes involved in osmoregulation, skeletal development, respiration and immune mechanisms in various species of fish (Jeffries et al., 2015; Overturf et al., 2015; Ford and Fong, 2016).

In plants, and although this knowledge is severely lackluster when compared to different beings, or other compounds in plants (e.g. heavy metals), it is reported that the first and more noticeable effects of toxicity in plants comprise germination inhibition, as well as diminishing root growth, with higher concentrations of contaminants also being reported to damage the photosynthetic apparatus and in the most severe cases, can even cause death (Michelini et al., 2012; Gonzalez-Naranjo et al., 2015; Pino et al., 2016; Bartrons and Peñuelas, 2017).

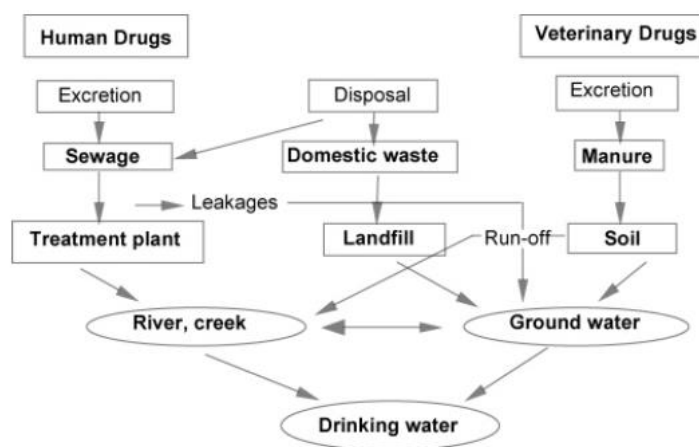
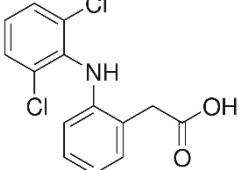


Figure 1. Fate of pharmaceuticals in the environment (Khetan and Collins, 2007).

1.2. Diclofenac – Occurrence, fate and risks

Within PhACs, non-steroidal anti-inflammatory drugs (NSAIDs) comprise some of the most detected types of pharmaceutical products in the environment, as concentrations spreading between ng L^{-1} and mg L^{-1} have been observed throughout the world (Lonappan et al., 2016). This class englobes several known products, with the most utilized worldwide being diclofenac (DCF), ibuprofen, mefenamic acid and naproxen, but the first is highlighted as the most popular NSAID, since it has a usage share almost as large as the latter three products combined (McGettigan and Henry, 2013). DCF (Table 1) is employed to diminish inflammation and pain, also possibly working as a antiuricosuric and is normally administered either through direct contact with the skin or through ingestion (Lonappan et al., 2016).

Table 1. Nomenclature and physicochemical properties of diclofenac (Source: www.pubchem.ncbi.nlm.nih.gov).

 <p>Chemical Structure</p>	IUPAC: 2-(2-(2,6-dichlorophenylamino)phenyl)acetic acid
	Chemical Formula: C ₁₄ H ₁₁ Cl ₂ NO ₂
	CAS: 15307-86-5
	Molecular Weight: 296.147 g mol ⁻¹

Since DCF is an over the counter drug that can be utilized not only in humans, but also for veterinary purposes and can be marketed throughout the world with distinct brand names, there is a lack of precise values regarding its worldwide consumption but reports based on IMS health data show that on average global consumption of DCF for human use reaches about 1450 tons per year, with Europe alone representing 28.7% of this utilization (Acuña et al., 2015).

This compound can enter the environment through deconjugation of the excreted metabolites and other mechanisms described above, while a low removal rate ensures that the amount of DCF present in surface and wastewaters continues to increase, with concentrations of ng L⁻¹ and µg L⁻¹, respectively, being found throughout the globe (Ternes, 1998; Heberer, 2002; Ashton et al., 2004; Han et al., 2006; Kim et al., 2007; Lopez-Serna et al., 2010; Gracia-Lor et al., 2012). This includes Portugal, with Salgado et al. (2010) and Pereira et al. (2017) reporting DCF as one of the most abundant PhACs, based on Portuguese surface and wastewaters analysis. Adding to an ever-increasing amount of this compound in the environment, there have been studies that prove that DCF can harm the surrounding lifeforms, mostly in laboratory-controlled situations but can also cause severe damage in the wild.

The most notorious case portraying the nefarious effects of this pharmaceutical in the environment was described by Oaks et al. (2004), where a direct correlation between the visceral gout that caused a >95% population decrease of the Oriental white-backed vulture, in India and exposure to diclofenac residues was established. This report showed that consumption of DCF via DCF-treated preys was the only common possible cause, as residues of this compound were detected in every tested vulture that died due to the result of renal failure, leading to visceral gout. The amount of diclofenac found in the kidneys of the test subjects was in the range of the high ng g⁻¹ to the low µg g⁻¹, showing that low concentrations of this pharmaceutical are sufficient to cause detrimental effects in wildlife. Besides, and although most studies regarding the effects of DCF exposure in aquatic environments are performed in controlled conditions, several reports have been published that show that even in environmentally relevant concentrations, DCF can cause various effects in fish, such as oxidative stress, tissue damage or

biochemical alterations, with cytological modifications being caused by an accumulation of this compound in the liver, kidney, gills and muscle tissues (Schwaiger et al., 2004; Mehinto et al., 2010; Guiloski et al., 2017; McRae et al., 2018).

Phytotoxicity of this compound is still a relatively understudied topic, but a common occurrence in various reports is the presence of oxidative stress (Bartha et al., 2014; Christou et al., 2016; Pierattini et al., 2018), accompanied by a clear increase in the antioxidant defense mechanism of the treated plants, but can also affect other parameters in a plant-specific way, since exposure to the same concentration of DCF enhanced cotyledon opening in *Lactuca sativa* L. but suppressed it in *Raphanus sativus* L. (Schmidt and Redshaw, 2015). Also, and in parallel to what was described above for other pharmaceuticals, DCF exposure has also been shown to negatively affect biometric and photosynthetic parameters in treated plants (Kummerova et al., 2016; Pierattini et al., 2018).

Therefore, since DCF is considered persistent in the environment and exposure to this contaminant can be hazardous towards surrounding lifeforms, the European Commission has acted by placing DCF in the first-watch list of priority substances in the EU Water Framework Directive in order to collect monitoring data to better determinate a way to respond to the problems emerging from the environmental contamination by DCF (EU, 2015).

1.3. Xenobiotic detoxification

Since conventional water treatments are insufficient in removing these compounds from the environment, it is important to research new and green alternatives. A concept that can possibly help address this problem is the process of phytoremediation (i.e. the use of plants to remove, degrade or contain several types of organic and inorganic pollutants) (Susarla et al., 2002), with published work showing that some pharmaceuticals can effectively be removed from the environment by utilizing this plant-based method (Dordio et al., 2009; Kotyza et al., 2010; Dordio et al., 2011; Matamoros et al., 2012a; Matamoros et al., 2012b). These contaminants can enter the roots and shoots of exposed plants, with diffusion of dissolved compounds being the main mechanisms behind root uptake, while root translocation to shoots is the main pathway towards shoot accumulation of PPCPs (Trapp and Legind, 2011; Bartrons and Peñuelas, 2017). From here, the main factors defining their fate are the physicochemical characteristics of the compound, since roots mostly retain hydrophobic compounds that can partition into lipids, while hydrophilic substances in equilibrium with water should be directed to the xylem. Then, the negatively charged cell walls will repel ionic substances,

possibly trapping them in the phloem and being accumulated in the fruit, while nonionic substances are transported mainly through the transpiration stream and accumulated in leaves (Trapp and Legind, 2011; Dodgen et al., 2015; Bartrons and Peñuelas, 2017).

In the specific case of DCF, several crops show potential to efficiently remove this contaminant from the environment, such as lettuce and poplar, with the same potential being detected in *in vitro* cultures of horseradish (Kotyza et al., 2010; González García et al., 2018; Pierattini et al., 2018). However, for the same concentrations utilized in the horseradish report, three other plants presented low uptake and suffered high toxicity, with yellowing and desiccation of shoots being observed (Kotyza et al., 2010). In all mentioned studies, most or all accumulated DCF was found in the roots of treated plants, with severely minor amounts being observed in the aerial portion.

In this sense, it is important to understand how different plants uptake different compounds in a way to better optimize this process to be a more cost-effective alternative (e.g. utilizing economically important species), with fewer downsides, such as possible health risks by consuming such plants if the compound is only absorbed and accumulated, but not degraded. Other concern associated with this process is that the contaminant of interest can cause phytotoxicity and compromise crop viability. To counter this and since they are incapable or escaping from unfavorable environments, plants have developed ways to metabolize toxic compounds to a non-toxic form in a similar way to metabolic processes described in animals but with a distinct factor, which is the lack of an excretory pathway and therefore a need to store these final metabolites within vacuoles and cell walls. Due to similarities with to animal metabolism, this concept was defined by Sandermann (1994) as a “green liver”, consisting of three different phases, first described by Shimabukuro (1976).

Phase I – Transformation

The first phase in xenobiotic detoxification is a preparation for the following phases. Here, these compounds are activated via oxidation, hydrolysis or reduction, allowing for subsequent transformations, with the first two being the most common form of activation, and are catalyzed by esterases and amidases (in hydrolytic reactions) or by the cytochrome P450 system, in oxidative reactions. The aforementioned processes consist in the addition of functional groups or exposure of already existing ones that are suitable for the next phase, resulting in derivatives that are normally more active in a biological and chemical point of view. However, this activation does not always grant less toxicity, and sometimes the resulting metabolite is even more toxic than the original compound. (Coleman et al., 1997; Komives and Gullner, 2005).

Phase II – Conjugation

After transformation, derivatives are deactivated via conjugation to an endogenous hydrophilic molecule, resulting in a water-soluble compound. The conjugated molecule is dependent of the original properties of the xenobiotic, since amino, carboxyl, sulfhydryl and hydroxyl groups tend to be mostly linked to glucose, through glucosyl-transferases (EC 2.4.-.-), while those with electrophilic sites tend to suffer conjugation to glutathione (GSH), through the action of glutathione-S-transferase (GST, EC 2.5.1.18). Another possible phase II reaction is conjugation with amino acids, mostly glutamate and aspartate, but this mostly occurs when metabolizing herbicides, fungicides and acidic insecticides (Davidonis et al., 1978; Eyer et al., 2016). The main characteristic of this phase as a detoxification mechanism is that the resulting metabolites of the described conjugation are either non-toxic or significantly less toxic than the original xenobiotic (Coleman et al., 1997).

Phase III – Compartmentation

Here, the inactive and less toxic metabolites derived from the previous phase are removed from vulnerable portions of the cytoplasm and are exported to regions where they cannot affect cellular metabolism. Metabolites with soluble properties (e.g. sugar or peptide conjugates) are recognized by ATP-dependent carriers and are transported to the vacuole (Sandermann, 1992; Coleman et al., 1997), while insoluble residues (e.g. xenobiotics with aromatic or heterocyclic rings) can be incorporated in the pectin, lignin, hemicellulose and cellulose portions of the cell wall (Sandermann, 1992; Schröder and Collins, 2002). For some conjugates, the vacuole is considered to be merely an intermediate storage site, to compensate for slower metabolic processes that follow this compartmentalization, in comparison to the fast conjugation rates in phase II. From here, these metabolites can be cleaved and form stable end products or can suffer further metabolic reactions, ending as substrate for different enzymes (Schröder and Collins, 2002). Some of these metabolites can end in the apoplast, in the rhizosphere, and can even suffer volatilization through methyl transferases (Lamoureux et al., 1993).

These reactions are exclusive to plants because the lack of an excretory system drives the need to restrain the xenobiotic within the plant (if impossible to be fully metabolized) and the resulting products of this metabolic cascade do not portray any phytotoxic menace (Wink, 1997).

1.4. Diclofenac metabolism

DCF metabolism in mammals has already been well documented, with 4'-OH DCF and 5'-OH DCF being described as the main phase I metabolites after DCF hydroxylation via P450. Afterwards, these hydroxylated metabolites can either be conjugated with sulphate or glucuronide and then excreted from the body or experience supplementary oxidation, producing a highly toxic and reactive benzoquinone metabolite, whose conjugation with glutathione results in the production of 4'-OH DCF glutathione and 5'-OH DCF glutathione, two nontoxic metabolites that can then be further degraded and eliminated from the body (Bartha et al., 2014). GSH conjugation can also be involved in a different metabolic pathway, with an acyl glucuronidation of DCF causing the resulting metabolite to transacylate GSH, forming a DCF-S-acyl-glutathione thioester, which is then excreted to the bile, highlighting the importance of glutathione in different ways of DCF metabolism, in mammals (Grillo et al., 2003).

In plants, this knowledge is not as deep and there is still much more to unravel, but from what is reported, DCF in these beings experiences fast metabolism in a similar way to mammals, as expected by the “green liver” concept. From phase I, the main metabolites described are the hydroxylated 4-OH-DCF and 5-OH-DCF, while the main phase II products seem to be the glycoside and glutathione conjugates, accompanied by an increased glycosyltransferase and GST activities (Huber et al., 2012; Schröder et al., 2013; Bartha et al., 2014).

1.5. Oxidative stress and plant antioxidant defense

Normal processes associated with aerobic metabolism, like photosynthesis and respiration, in plants and other organisms, can cause the production of reactive oxygen species (ROS) by the activation or reduction of molecular oxygen (O_2). However, and even though in normal conditions, these molecules are scavenged by intrinsic antioxidant (AOX) mechanisms, maintaining the normal redox state of the cell, an overproduction of ROS can be a result of different environmental changes to which the plant was exposed, such as abiotic or biotic stresses. When this occurs, normal plant defenses might not be enough to balance the production and detoxification of these molecules, leading to oxidative stress (Gill and Tuteja, 2010; Tripathy and Oelmüller, 2012) (Figure 2). In fact, and as mentioned, exposure to DCF and other pharmaceuticals has been shown to trigger an increase in ROS content and consequent oxidative stress in plants (Christou et al., 2016; Sun et al., 2017; Pierattini et al., 2018).

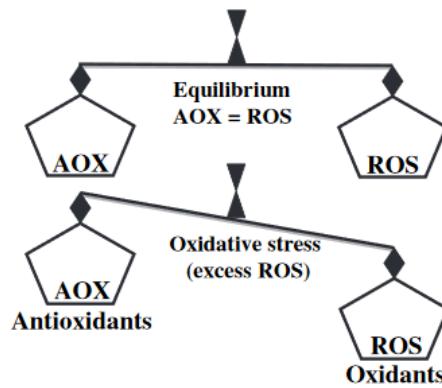


Figure 2. Equilibrium between AOX and ROS and its unbalance, leading to oxidative stress (Gill and Tuteja, 2010).

1.5.1. Reactive oxygen species (ROS)

Dioxygen, the most common allotrope of elemental oxygen, is a fairly non-reactive molecule, but activation or reduction of this form leads to the formation of several reactive species, with the most common being the superoxide anion ($O_2^{\cdot-}$), hydrogen peroxide (H_2O_2), hydroxyl radical ($\cdot OH$) and singlet oxygen (1O_2) species (Tripathy and Oelmüller, 2012). About 1% of the oxygen consumed by plants is utilized in ROS production, taking place in several subcellular regions with high oxidizing metabolic activity or with a large rate of electron flow (e.g. chloroplasts, mitochondria and peroxisomes) (Sharma et al., 2012; Tripathy and Oelmüller, 2012). Depending on the concentration in which they occur, a dual role is recognized to these molecules, which means that in low or moderate concentrations they can be detected by the plant as a signaling mechanism and a proper response is formulated, mediating processes such as stomatal closure, gravitropism, programmed cell death and tolerance to different stresses, but when these ROS occur in a large enough concentration to surpass the equilibrium between production and scavenging, they can severely harm the plant by causing lipid peroxidation (LPO), damage to nucleic acids and other organic molecules, inhibition of enzymes and possibly leading to cellular death (Sharma et al., 2012).

O_2 contains two unpaired electrons with the same spin quantum number, restricting this molecule to only being able to transfer one electron at a time, with the single electron reduction of O_2 generating the superoxide anion (Tripathy and Oelmüller, 2012). $O_2^{\cdot-}$ is usually the first ROS to be generated and is moderately reactive, with a short half-life determined by superoxide dismutase- (SOD, EC 1.15.1.1) catalyzed conversion to H_2O_2 (Jajic et al., 2015). In plants, $O_2^{\cdot-}$ is mostly produced in chloroplasts and mitochondria, with photosystem (PS) I and II being the main producing sites in the thylakoid membrane (Asada, 2006), while complex I and III are the main production sites in the mitochondria (Sharma et al., 2012). However, $O_2^{\cdot-}$ can also be formed in other organelles, such as the peroxisomes, where this ROS can be produced in the peroxisomal matrix, via xanthine

oxidase (EC 1.1.3.22) or by electron transport chain (ETC) in the peroxisomal membrane (Jajic et al., 2015). $O_2^{\cdot-}$ can also be a result of oxygen reduction via an ETC formed by nicotinamide adenine dinucleotide phosphate (NADPH) oxidases (EC 1.6.3.1), or through the action of oxalate oxidase (EC 1.2.3.4) and amine oxidases (EC 1.4.3.21) (Tripathy and Oelmüller, 2012). Lastly, this ROS can be generated in the cytosol as well, by xanthine dehydrogenase (EC 1.17.1.4) and aldehyde oxidase (EC 1.2.3.1) (Jajic et al., 2015).

Since $O_2^{\cdot-}$ has low mobility and is incapable of passing through biological membranes as a result of its negative charge, $O_2^{\cdot-}$ toxicity is usually due to its oxidizing and reducing prowess. In this sense, this ROS can reduce Fe^{3+} , originating Fe^{2+} , which in turn reduces the H_2O_2 (formed by the mentioned SOD-catalyzed $O_2^{\cdot-}$ dismutation) to $\cdot OH$, considered to be central to oxidative damage, as one of the most toxic oxygen species (Demidchik, 2015). This process is known as the Haber-Weiss reaction, with the last step, which forms $\cdot OH$, being called Fenton reaction (Gill and Tuteja, 2010). $O_2^{\cdot-}$ can also react with H^+ , which results in the hydroperoxyl radical ($HO_2^{\cdot-}$), a more reactive, stable and permeable molecule, with the $O_2^{\cdot-}/HO_2^{\cdot-}$ pair possibly reacting with nitric oxide (NO^{\cdot}), forming highly reactive molecules that can decompose to $\cdot OH$ (Demidchik, 2015). This ROS has also been shown to reduce cytochrome c and oxidize enzymes that contain the [4Fe-4S] clusters (Sharma et al., 2012).

H_2O_2 is the most studied and understood ROS within the scientific community, due to its perceived importance in both signaling and toxicity mechanisms (Lopez-Serna et al., 2010). Unlike other ROS, whose half-life is about 2-4 μs (Quan et al., 2008), H_2O_2 has a significantly longer half-life, about 1 ms, which added to other inherent characteristics, such as its small size and lack of unpaired electrons, allows it to pass through membranes, enabling its signaling importance (Lopez-Serna et al., 2010). Consequently, these characteristics also allow that in high concentrations, this ROS can generate oxidative damage in regions distant from its production site (Sharma et al., 2012). The main mechanism regulating H_2O_2 generation is the two-step reduction of oxygen, resulting in the formation of $O_2^{\cdot-}$ and its consequent dismutation, with several metabolic processes also taking part in the formation of this ROS, such as electron transport in the chloroplast, mitochondria, plasma membrane and endoplasmic reticulum, as well as the β -oxidation of fatty acids and photorespiration in the peroxisomes (Lopez-Serna et al., 2010; Sharma et al., 2012). The signaling function of this molecule orchestrates different tolerance (e.g. reinforcement of cell walls, production of phytoalexins and pathogen and direct or indirect toxicity towards pathogens) and metabolic (e.g. regulation of plant cell cycle, senescence and stomatal movement)

processes, while a production/scavenging equilibrium is possible (Quan et al., 2008; Gill and Tuteja, 2010). However, when this equilibrium is not possible and H_2O_2 levels become too much for the plant to withstand, it can portray significant oxidative damage. In this sense, H_2O_2 can oxidize cysteine or methionine residues, oxidize thiol groups of SOD and enzymes of the Calvin cycle, leading to their inhibition (Sharma et al., 2012).

$\cdot\text{OH}$ is considered to be the most toxic and reactive ROS and is generated via the Fe-catalyzed Fenton reaction. Due to its strong ability to be involved in addition and abstraction of hydrogen and electron transfer reactions, this molecule has a very short lifetime (around 1 ns) (Sutherland, 1991; Sies, 1993). For this reason, $\cdot\text{OH}$ can act non-selectively on any biological molecule but only near its production site (Sutherland, 1991). Since plants lack a specific enzymatic $\cdot\text{OH}$ scavenging mechanism, its overproduction can severely harm proteins, nucleic acids and lipids, causing lipid peroxidation, blocking elongation and activation of K^+ efflux channels, resulting in the loss of K^+ and leading to cell death through K^+ -dependent proteases and endonucleases (Demidchik, 2015).

Lastly, $^1\text{O}_2$ is an idiosyncratic and uncommon ROS because it is not caused by electron transfer to O_2 . Instead, inadequate dissipation of energy during photosynthesis leads to production of a chlorophyll triplet state, which reacts with $^3\text{O}_2$ and forms the highly reactive singlet oxygen (Gill and Tuteja, 2010). This molecule can be scavenged shortly after its production by β -carotene, tocopherol, flavonoids or reduced plastoquinone (Demidchik, 2015). Also, different environmental stresses can induce stomatal movement and consequent loss of CO_2 availability, facilitating the production of this ROS (Sharma et al., 2012). Although a short lifespan is associated with $^1\text{O}_2$, an ability to diffuse over large distances from the production site has been reported, as well as an ability to react with most biological molecules, serving as oxidizing agent towards several biomolecules, and being the main cause behind PSII light-induced damages and consequent possible cell death (Gill and Tuteja, 2010; Sharma et al., 2012).

After production of these molecules, a quick response must be formulated to avoid toxic levels of ROS. If the formation/scavenging of ROS equilibrium is disturbed, severe damage can be caused to lipids, DNA and proteins, consequently leading to cell death (Sharma et al., 2012) (Figure 3). One of the most severe results of oxidative stress is LPO and is therefore considered to be an important indicator of ROS damage to cells (Demidchik, 2015). This process is usually triggered by $\cdot\text{OH}$, which can abstract H^+ of polyunsaturated fatty acids and form lipid peroxy radicals and hydroperoxides, who then suffer reductive cleavage and produce reactive species, such as lipid alkoxy radicals, malondialdehyde (MDA) and alcohols (Gill and Tuteja, 2010; Sharma et al., 2012). In

severe conditions, LPO will disturb membrane integrity, affecting its fluidity and permitting the passage of substances that are usually unable to cross it, damaging proteins, receptors, enzymes and ionic channels (Gill and Tuteja, 2010; Demidchik, 2015). Reactive molecules, mainly $\cdot\text{OH}$ can also affect the plant genome, as it can cause base deletions and modifications (e.g. alkylation and oxidation), strand breaks or pyrimidine dimers, resulting in the inhibition of protein synthesis, destruction of cell membrane and affecting the development of the plant (Gill and Tuteja, 2010). Oxidation of proteins is also an undesirable effect of ROS accumulation and are usually irreversible, apart from some with sulfur-containing amino acids (Demidchik, 2015). The most common oxidation process in proteins is the insertion of a carbonyl group (carbonylation), resulting in a modification of their activities and leading to their ubiquitination, which turns them into targets for proteolysis (Gill and Tuteja, 2010; Sharma et al., 2012; Demidchik, 2015).

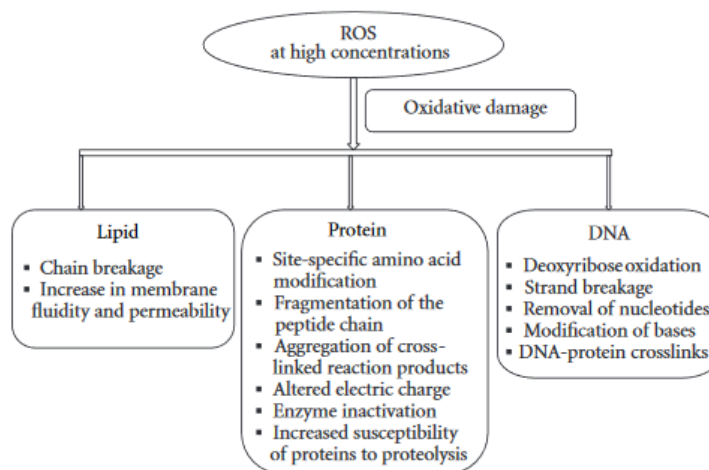


Figure 3. Reactive oxygen species (ROS) and oxidative damage to lipids, proteins, and DNA (Sharma et al., 2012).

1.5.2. Antioxidant mechanism

As mentioned before, it is crucial that plants can maintain the equilibrium between the production and scavenging of ROS, and since plants are characterized by a sessile nature they were forced to develop different mechanisms for compensating the stress-induced overproduction of ROS by utilizing enzymatic and non-enzymatic antioxidants, present in different cellular compartments (Figure 4), to maintain the natural redox state of the plant (Ahmad et al., 2010).

Regarding the enzymatic system, plants utilize different enzymes to eliminate ROS, such as SOD, catalase (CAT, EC 1.11.1.6), GST, glutathione reductase (GR, EC 1.6.4.2), monodehydroascorbate reductase (MDHAR, EC 1.6.5.6), dehydroascorbate reductase (DHAR, EC 1.8.5.1) and ascorbate peroxidase (APX, EC 1.1.11.1) (Gill and Tuteja, 2010).

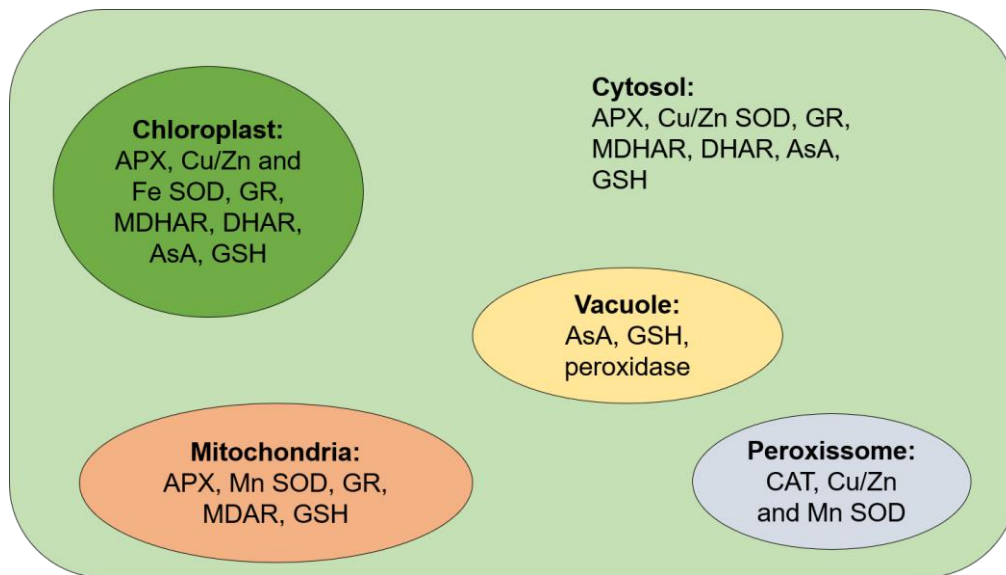


Figure 4. Antioxidant resources in the different organelles of plant cells. Adapted from Ahmad et al. (2010).

SOD is considered to be the primary line of defense from plant cells against high levels of ROS, as it catalyzes the dismutation of the first formed ROS ($O_2^{\cdot-}$) to H_2O_2 (Alscher et al., 2002) and prevents the consequent formation of $\cdot OH$ by Haber-Weiss reaction (Gill and Tuteja, 2010). The importance of this defense is highlighted by the presence of three different forms of SOD, defined by their metal cofactor [iron (Fe) manganese (Mn) or copper and zinc (Cu/Zn)], as evolutionary pressure was very intense and most SOD-lacking organisms could not resist the environmental transition brought by the genesis of oxygenic photosynthesis (Gill and Tuteja, 2010; Miller, 2012). This is a ubiquitous metalloenzyme in most organelles capable of forming the superoxide radical, since this molecule is unable to pass through biological membranes and is confined to the production site (Alscher et al., 2002). The different forms of SOD are all encoded in the nucleus, but are located in different sites due to the presence of a terminal amino acid targeting tag, with Fe SOD being found in the chloroplasts, Mn SOD in the mitochondria and peroxisomes and Cu/Zn SOD being the most abundant forms in plants and contained in the cytosol, chloroplasts, peroxisomes and apoplast (Gill and Tuteja, 2010). The abundance of the metallic ion is considered to be the main factor in the evolution of the three SOD, with a decrease in Fe (II) availability and increase in toxicity driving the evolution of Mn SOD from an ancestral Fe form (Miller, 2012). These two forms share structural similarities, due to similar electric properties of both metals, but do not possess the ability of functioning with the other form's metal as a cofactor. The same cannot be said about Cu/Zn SOD, as the different properties of these metals required major alterations in protein structure after Cu availability rose and started being utilized as a cofactor (Alscher et al., 2002). Various types of environmental stress have been shown to lead to an increase in the activity of this enzyme as a response

mechanism and consequently some studies have focused on the overproduction of SOD, with results showing enhanced tolerance in transgenic lines to the imposed oxidative stress, highlighting the protecting importance of SOD (Gupta et al., 1993; Sharma et al., 2012; Xu et al., 2013).

CAT is a very important AOX enzyme in the elimination of H_2O_2 from the cell and acts by catalyzing the decomposition of two H_2O_2 molecules into H_2O and O_2 (Mhamdi et al., 2010). Along with SOD, CAT plays a major role in avoiding the formation of $\cdot OH$ and preventing the consequent severe damages imposed. This enzyme stands out from other peroxide-metabolizing enzymes by not needing a reductant and by possessing a very high and fast turnover rate, since one CAT molecule can dismutate around 6 million H_2O_2 molecules in only one minute (Gill and Tuteja, 2010). However, the high turnover rate and specificity to H_2O_2 is compensated by its weak affinity to this ROS, meaning that CAT is not as relevant as other H_2O_2 scavengers when concentrations of this peroxide are not very high (Sharma et al., 2012). This enzyme has its presence documented in the cytosol and in different organelles, such as chloroplasts and mitochondria but information on significant activity in these sites are scarce, in contrast to that of peroxisomes. This organelle is the primary action site of CAT, as it is the main producer of the targeted ROS (Gill and Tuteja, 2010). Three classes of CAT have been detected and classified in plants, differing on their expression profiles, with CAT I being light-dependent, involved in dismutating photorespiration-produced H_2O_2 and expressed mostly in leaves, CAT II mostly act in vascular tissues and lastly, CAT III are highly expressed in seeds and young seedlings and are responsible for the detoxification of H_2O_2 formed in the glyoxysomes (Dat et al., 2000). Several forms of stress seem to impact CAT activity, but the nature of this impact (enhancement or inhibition) is very dependent on intensity, duration and type of stress, as well as plant species, as even when exposed to the same conditions, some plants seem to utilize CAT as a defense mechanism, while others present its inhibition (Sharma et al., 2012).

Contrasting with CAT's low affinity to H_2O_2 , APX presents high relevance even in low concentrations of this ROS, suggesting that while CAT might be more involved in ROS-induced damage tolerance, APX might be more adept in signaling processes (Mittler, 2002). This peroxidase comprises five different isoenzymes differing in a chemical and enzymatic context, as well as presence in different cell sites: cytosolic, mitochondrial, stromal, thylakoidal and peroxisomal APX forms (Sharma et al., 2012). APX utilizes two molecules of ascorbate (AsA) as substrate in order to reduce H_2O_2 to water, with adjuvant production of two monodehydroascorbate (MDHA) molecules. In this sense, it is important to maintain the levels of reduced AsA to allow a consequent

oxidation by APX and H_2O_2 dismutation. The MDHA radical produced due to APX is not stable for long periods of time and can either be quickly reduced to AsA by MDHAR, via oxidation of NADPH or can non-enzymatically react with another MDHA molecule, forming one molecule of AsA and one molecule of dehydroascorbate (DHA). The latter is then reduced by DHAR, making use of GSH as the reducing substrate, regenerating the reduced form of AsA and oxidized GSH (GSSG). From here, the reduced/oxidized AsA homeostasis is maintained but an imbalance of the GSH/GSSG ratio is created. Then a NADPH-dependent reaction of disulfide bond of GSSG is quickly enforced by GR, ensuring the regeneration of GSH (Ahmad et al., 2010; Gill and Tuteja, 2010; Do et al., 2016). The latter enzyme pertains to the NADPH-dependent oxidoreductase family and while it can also be found in the cytosol and mitochondria, most (>80%) of GR activity in photosynthetic tissues is associated with the chloroplast (Gill et al., 2013).

This cycle of H_2O_2 detoxification consisting of consecutive oxidations and reductions of AsA and GSH is named AsA-GSH or Halltwell-Asada cycle (Figure 5) (Dąbrowska et al., 2007).

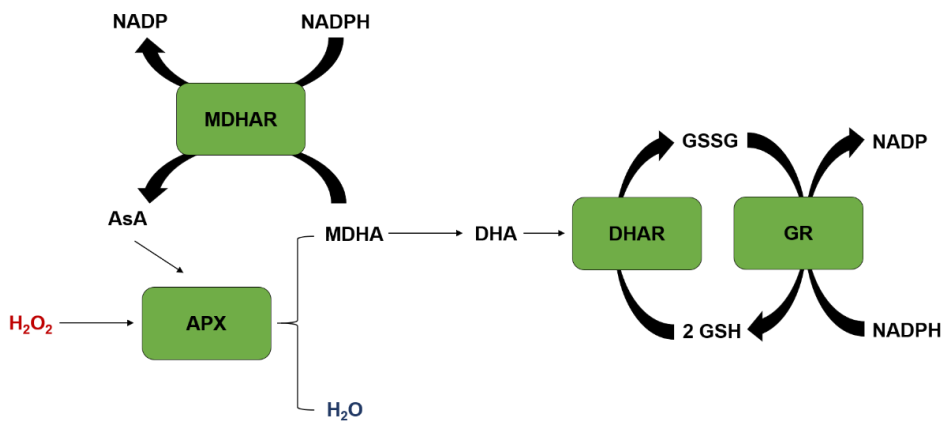


Figure 5. Ascorbate-Glutathione cycle.

The non-enzymatic system comprises the amino acid proline, low molecular weight cellular compounds, such as carotenoids, flavonoids and phenolic acids, as well as the cellular redox buffers GSH and AsA. These compounds can directly detoxify the plant from ROS or act indirectly by reducing substrates for the enzymatic system (Kasote et al., 2015; Caverzan et al., 2016). Alongside the described role in the Asa-GSH cycle, AsA can also partake a vital role on the AOX defense without enzymatic action, as it can directly react with H_2O_2 and $O_2^{\cdot-}$, assuring the integrity of plant membranes (Sharma et al., 2012). Proline is commonly reported as an osmolyte involved in the protection of cellular structures from osmotic stress, but recently this amino acid is showing positive influence in other stress-related processes (Kaur and Asthir, 2015). Currently, proline is being described as an important amino acid in osmoprotection, protein stabilization, lipid

peroxidation inhibition and $\cdot\text{OH}$ and $^1\text{O}_2$ scavenging (Gill and Tuteja, 2010). Not only that, but proline levels seem to be related with the ratio of $\text{NADP}^+/\text{NADPH}$, necessary for the maintenance of the important reduced state of both AsA and GSH (Hare and Cress, 1997), since proline biosynthesis from glutamate, via Δ^1 -pyrroline-5-carboxylate (P5C) is associated with oxidation of NADPH to NADP^+ , with subsequent induction of the pentose phosphate pathway and reduction to NADPH (Liang et al., 2013).

1.6. Glutathione

As a low molecular weight tripeptide, formed by a γ -L-glutamyl-L-cysteinyl-L-glycine sequence, GSH is considered one of the most important metabolites in several physiological processes of plants (Gill and Tuteja, 2010).

GSH is generated by the subsequent action of two enzymes: γ -glutamyl-cysteinyl synthetase (γ -ECS, EC 6.3.2.2) and glutathione synthetase (GSS, EC 6.3.2.3). In the first step γ -ECS potentiates the bond of Cys with Glu, forming γ -glutamylcysteine (γ -EC) in the presence of ATP, whereas, in the second step, GSS catalyzes an ATP-dependent linkage between γ -EC and Gly, forming the final GSH product (Noctor et al., 1998; Rouhier et al., 2008). This thiol-containing molecule is nearly ubiquitous and can be found in most cellular sites in either the original reduced form with a free thiol group or as GSSG, an oxidized form constituted by two GSH molecules linked by a disulfide bond (Gill and Tuteja, 2010; Gill et al., 2013). Two main differences between GSH and other thiol groups correlate with the high concentration of this metabolite but also with its major reduced status (Noctor et al., 2012). This occurs due to GR, as this enzyme utilizes NADPH as an electron donor in order to reduce the glutathione oxidized during a stress response to its original state (Gill et al., 2013).

GSH is a major water-soluble redox buffer in the cell partaking in plant defense against oxidative stress in different ways. In this sense, glutathione can act directly in ROS scavenging by reacting with $\text{O}_2^{\cdot-}$, H_2O_2 or $\cdot\text{OH}$, yielding GSSG, as well as forming adducts with reactive electrophiles, protecting other biomolecules, such as DNA, proteins and lipids. Indirectly, GSH can also act in the protection against ROS by facilitating the regeneration of reduced AsA by the AsA-GSH cycle (Rouhier et al., 2008; Hasanuzzaman et al., 2017). Another important process where GSH functions as a key player is the detoxification of xenobiotics, via a GST-mediated conjugation (Gill and Tuteja, 2010). In summary, GSH is a crucial thiol-containing compound for normal plant development, with several other functions being added to the ones described above, such as cell differentiation and death, regulation of sulfate transport, heavy metal detoxification, senescence, enzymatic regulation, pathogen resistance and also in

glutathionylation reactions in response to stress (Rouhier et al., 2008; Noctor et al., 2012).

1.7. Glutathione-S-Transferase

Glutathione transferases (or GSTs) are a heterogeneous superfamily of cell detoxifying enzymes, being major players in the plant xenome (i.e. xenobiotic detoxification mechanism) (Labrou et al., 2015), and although other functions are associated with this transferase, the main GST-catalyzed reaction is the GSH conjugation to electrophilic sites of several phytotoxic compounds (Sasan et al., 2011).

Three families constitute the plant GSTome (i.e. the collective presence and function of all GSTs in the respective organism), with mitochondrial and microsomal families being evolutionarily very distinct to the cytosolic family and are not thought as partaking in cell detoxification. Despite the most prevailing cytosolic GSTs in plants pertaining to the GSTF (ϕ) and GSTU (τ) classes, eight other classes are present in these organisms: GSTL (λ), DHAR, GSTT (θ), GSTZ (ζ), TCHQD, EF1BG, hemerythrin and Iota, but solely GSTF, GSTU, GSTL and DHAR are plant-specific (Labrou et al., 2015). A great divergence is associated with the different classes of GST but strong similarities are found in the three-dimensional structure, a trait shared with other GSH-dependent proteins (Dixon et al., 2002; Öztetik, 2008). Structurally, these enzymes are generally homo or hetero-dimers, consisting of two domains linked by a variable region. The first domain (G-site) is a thioredoxin-like fold and presents a GSH-specific binding site, while the second domain (H-site) is formed by a variable amount of α -helices and a binding site specific to the hydrophobic substrate (Sasan et al., 2011).

As mentioned, GSTs play a very important role in the detoxification mechanisms of plants against external compounds, potentiating the conjugation reaction of GSH to the electrophilic site of several phytotoxic substances, such as PhACs and herbicides, forming S-glutathionylated conjugates in the cytosol, which are then sent towards the vacuole through the action of ABC transporters (Öztetik, 2008). This process is usually associated with GSTF and GSTU (Csiszar et al., 2014) and recently overexpression of GSTs pertaining to these classes has been successfully employed to improve herbicide tolerance (Benekos et al., 2010; Cummins et al., 2013). Furthermore, GSTs can also be involved in the response and tolerance towards oxidative stress by functioning as glutathione peroxidases (GPOX, EC 1.11.1.9). In this case, GST-GPOX will reduce peroxides, utilizing GSH as a substrate and yielding GSSH (Dixon et al., 2002; Öztetik, 2008). This is highlighted by several studies showing that overexpression of some GST is related with a higher tolerance to oxidative stress (Yu et al., 2003; Sharma et al., 2014),

with a tomato GSTU suppressing the ROS-induced apoptosis caused by the Bax protein in yeast (Kampranis et al., 2000). Taking in mind these protective functions, it comes as no surprise that GST is becoming an interesting biomarker in plant stress studies and a better understanding of how this enzyme works, as well as what classes are involved with each process is an important tool in allowing its use to induce higher tolerance to different forms of abiotic and biotic stresses (Labrou et al., 2015).

1.8. *Solanum lycopersicum* L. cv. Micro-Tom

Tomato (*S. lycopersicum*) originated in South America and was later brought to the European continent and maintains its status as one of the most relevant crops worldwide. As a member of the Solanaceae family, tomato shares the trait of economic importance with other Solanaceae plants, like potato, eggplant, petunias, peppers and tobacco (Gerszberg et al., 2015). However, the importance of this crop extends beyond economics and consumption, reaching scientific importance as a model system for basic and applied research. This importance correlates with several characteristics inherent to this plant, such as an ability to grow under different conditions, lack of gene duplication and a small and fully sequenced genome, with high efficiency transformation protocols already established. While these characteristics are not unique to *S. lycopersicum*, it distinguishes itself from other biologic models, such as *Arabidopsis thaliana* L., due to its associated photoperiod-independent sympodial flowering, compound leaves and production of fleshy fruits highly consumed by humans and also for the ability to be utilized in the research of agronomically important interactions (Kimura and Sinha, 2008; Campos et al., 2010; Gerszberg et al., 2015). The main disadvantage concerning the use of tomato as a plant model is the normal size of this crop, requiring large growing sites and high maintenance, as well as a four-month generation period. Because of this, the “laboratory tomato” (Meissner et al., 1997), which is the dwarf cultivar Micro-Tom (Figure 6), has gained attention as the most convenient model, since it can grow in smaller spaces and takes only around ten weeks to bear fruits (Campos et al., 2010). Besides, and a very important characteristic, is that this cultivar only differs in two major genes from the standard tomato, meaning that research performed in the dwarf cultivar can be easily transferred to an environmental context (Meissner et al., 1997).



Figure 6. *Solanum lycopersicum* cv. Micro-Tom (left) bearing fruits and a standard tomato fruit (right) (Source: <http://www.kazusa.or.jp/jsol/microtom/project.html>).

1.9. Objectives

This research work aimed to better understand how an economically important species (*S. lycopersicum*) responds to being exposed to an emerging contaminant that has been detected in water and soils, possibly damaging cultivation perspectives throughout the world. In this sense, and at a macroscopic scale, it is important to verify if the cultivation of this species in contaminated soils can lead to morphologic alterations that can compromise crop yield or even be detrimental to human health, while understanding the plants' internal mechanisms that are being triggered during this process.

As the main purpose of this work, the GSH metabolism was in the spotlight, as this metabolite has been considered instrumental in both antioxidant and detoxification processes. For this, enzymatic activity and transcript accumulation of different GSH-related enzymes was analyzed to investigate how exposure to DCF affected synthesis, utilization and regulation of the redox ratio of this molecule. Additionally, as claimed by various reports, the conjugation of GSH to DCF with an adjuvant increase in GST activity is a common occurrence, similarly to what happens in mammals. Taking this in consideration, five different GST genes pertaining to the phi class were evaluated regarding their mRNA accumulation to understand the role taken by specific gene members in the detoxification of this contaminant, as up to date there is no information besides the global spectrum of GST activity and conjugate detection.

Also, it is important to understand if the plant can cope with a long-term exposure to DCF on an external and internal level. For this, seedlings and plants were evaluated biometrically, and the edible fruits tested for the presence of DCF to unveil if any toxicity may be passed through the food chain in this scenario. It is also pertinent to assess the intrinsic defenses triggered to combat a possible DCF-induced stress and therefore the antioxidant mechanisms of treated plants were also evaluated.

Hopefully, this research will proportionate new and important information about the underlying mechanisms regarding the detoxification of DCF and defense against subsequent damages, serving as a precedent for further research aimed at better improving and understanding these processes.

2. Material and Methods

2.1. Diclofenac

Diclofenac was purchased from Sigma-Aldrich® (Steinheim, Germany) as a sodium salt (D6899).

2.2. *Solanum lycopersicum* L. seeds

Solanum lycopersicum L. cv. Micro-Tom (Tomato Genetics Resource Center; germplasm LA3911) certified seeds were surface-disinfected with a 10-minute immersion in 70% ethanol before being washed, in constant agitation, for 5 minutes, with a solution containing 20% commercial bleach and 0.02% tween-20. Following these steps, the seeds were then repeatedly washed with double-distilled sterile water.

2.3. Tested concentrations

Even though not every utilized dosage was maintained for the consequent assays, some concentrations had to be chosen for preliminary studies to select the final ones. In this sense, two current environmentally relevant concentrations ($15 \mu\text{g L}^{-1}$ and $30 \mu\text{g L}^{-1}$) were used alongside two higher concentrations, one that has been utilized in other assays utilizing diclofenac and plants (1 mg L^{-1}) and a higher concentration unlikely to be found in the environment (10 mg L^{-1}) (if this latter concentration does not provoke harmful effects, then no danger should be associated with the presence of these plants in contact with this contaminant in the environment). A control situation was used under the same conditions, but without the addition of diclofenac.

2.4. Germination assay

Following disinfection, seeds were distributed in sterile Petri dishes (10 cm diameter) containing a solidified medium consisting of 1X Hoagland solution (Taiz and Zeiger, 2010) supplemented with the respective diclofenac concentrations ($0 \mu\text{g L}^{-1}$, $15 \mu\text{g L}^{-1}$, $30 \mu\text{g L}^{-1}$, 1 mg L^{-1} and 10 mg L^{-1}) and 0.625% (w/v) agar. Subsequently, these Petri dishes were stored at $4 \text{ }^\circ\text{C}$ during 48h to break seed dormancy and synchronize germination, and afterwards they were placed in a growth chamber with controlled optimized conditions (16 h light/8 h dark; $25 \text{ }^\circ\text{C}$) and $60 \mu\text{mol m}^{-2} \text{ s}^{-1}$ photosynthetically active radiation for 10 days. Following this period, the germination rate in each Petri dish was registered and the grown plantlets were evaluated regarding their shoot and root size, as well as total fresh weight.

2.5. Growth trial

After selecting the final concentrations to be exploited in the posterior assays, seeds were grown under the same conditions described for the germination assay but without the addition of diclofenac to any Petri dish. After 10 days in the growth chamber, seedlings were transferred to individual pots filled with a 2:1 mixture of expanded vermiculite and perlite and separated amongst the different experimental conditions. The trays containing these pots were then moved to the growth chamber and left to grow in the aforementioned conditions. For the first week, in order to acclimatize plantlets to the new conditions, every tray was irrigated only with 1X Hoagland solution, while for the following 5 weeks each tray was being supplied a different diclofenac concentration (0 mg L⁻¹, 0.5 mg L⁻¹ and 5 mg L⁻¹) diluted in Hoagland solution. The DCF-containing nutritive medium was renewed when necessary.

When the treatment period was completed, the grown plants were removed from the pots, their roots washed with tap and then deionized water, with biometrical analysis ensuing. Here, shoots and roots were separated and the length and fresh weight of both portions of the plant were determined. Afterwards, plants were divided in two groups: the first group was left to dry at 65 °C in an oven for the posterior determination of the hydric content, while the second group was frozen and pulverized in liquid N₂, with aliquots being stored at -80 °C until used for biochemical and molecular assays.

2.6. Diclofenac quantification

The quantification of diclofenac was performed on both the growth medium and mature fruits. To quantify diclofenac on the solution supplied to the plants, samples of this medium were retrieved some minutes after irrigation and new samples were collected day(s) later to determine how and if diclofenac was absorbed/degraded over-time. The same procedure was done on a no-plant situation to test if diclofenac disappearance was a natural process or if it could be attributed mostly to plant action. In this situation, pots were filled with the same artificial substrate, maintaining every condition, apart from the presence of plants in the vermiculite:perlite mixture. These samples were kept at -20 °C before being filtered and injected. Additional plants were grown until reaching the stage of mature fruits, with fruits being collected to assess if consumption of tomatoes collected from treated plants could possess any hazardous effects for human consumption. Fruits were lyophilized and 0.5 g of dry tissue were subjected to a solid-liquid extraction with 10 mL of 50:50 methanol:H₂O, in ultrasounds for 10 mins, followed by 15 minutes of magnetic agitation. The extracts were then centrifuged and the SN was subjected to another solid-liquid extraction with 5 mL of

50:50 methanol:H₂O₂. These samples were then treated with the same method as the liquid medium samples.

For the chromatographic method, separation was performed on a Supelco Ascentis Express C₁₈ column 2.7 mm x 5 mm x 2.1 mm equipped with a pre-column with the same stationary phase, which was kept at 40 °C during the analysis process. The mobile phase, in isocratic mode, was acetonitrile:0.1% formic acid (45:55 v/v). The utilized flow was of 0.4 mL min⁻¹ and the used wavelengths were of 280 nm (excitation) and 365 nm (emission). This method was performed on an UltiMate™ 3000 HPLC and UHPLC Systems with an UltiMate™ 3000 Fluorescence Detector (Thermo Fisher Scientific, USA), injecting 5 mL of filtered samples. Data was then acquired and treated via Chromeleon® Dionex v 7.2 software and results were expressed in mg L⁻¹ for the liquid samples and mg g⁻¹ for the fruit samples.

2.7. Analysis of biochemical parameters

2.7.1. Quantification of soluble proteins

To quantify soluble proteins, aliquots of 300 mg of frozen tissue were grounded on ice, with the aid of some quartz sand, using 2 mL of a potassium phosphate buffer (100 mM, pH 7.3) with the addition of 1 mM Ethylenediaminetetraacetic acid (EDTA), 1 mM Phenylmethylsulphonyl fluoride (PMSF), 5 mM L-ascorbic acid, 8% glycerol and 1% (w/v) Polyvinylpolypyrrolidone (PVPP). The homogenates were then centrifuged at 4 °C for 25 mins at 16,000 *g* and the supernatants (SNs) were collected for soluble protein quantification by an adapted Bradford method (Bradford, 1976). A 1:100 dilution of each SN was prepared and 75 µL of this dilution were mixed with 750 µL of Bradford solution. Afterwards, this mixture was left to incubate in the dark at room temperature for 15 minutes and absorbances were read at 595 nm. A standard curve utilizing known doses of bovine serum albumin (BSA) was determined, as a way to establish a link between obtained absorbances and protein content. Final results were expressed in mg g⁻¹ of fresh weight (fw).

2.7.2. Determination of lipid peroxidation

Lipid peroxidation was evaluated in accordance to Heath and Packer (1968), via quantification of MDA levels, as it is an end product formed from polyunsaturated fatty acids peroxidation in the cells, permitting an evaluation of diclofenac-induced membrane damage. Aliquots of 200 mg were homogenized in 0.1% (w/v) trichloroacetic acid (TCA) (1 mL for shoot samples and 0.8 mL for root samples) and some quartz sand, and centrifuged during 5 minutes at 10,000 *g*. Two hundred and fifty µL of recovered SN were

then added to 1 mL of 0.5% (w/v) thiobarbituric acid (TBA) in 20% (w/v) TCA. Homogenization solution was utilized instead of SN for the blank measurement. Tubes containing this mixture were then heated at 95 °C for 30 minutes, followed by incubation on ice for 15 minutes. Following an 8-minute centrifugation at 10,000 g, the absorbance values of each sample were read at both 532 and 600 nm. The latter result was subtracted to the first to avoid the effects of non-specific turbidity and by utilizing the extinction coefficient of 155 mM⁻¹ cm⁻¹, MDA content was expressed as nmol g⁻¹fw.

2.7.3. Determination of ROS levels

2.7.3.1. Quantification of H₂O₂

H₂O₂ levels in tomato plants were quantified in accordance to de Sousa et al. (2013), with frozen aliquots of 200 mg that were grounded, under ice-cold conditions, using 1.2 mL of potassium phosphate buffer (50 mM, pH 6.5). Afterwards, the homogenates were centrifuged at 6,000 g for 25 minutes at 4 °C and the SNs were collected to new tubes. After mixing 500 µL of SN to 500 µL of 0.1% (w/v) TiSO₄ in 20% (w/v) H₂SO₄, these tubes were vortexed for 15 seconds. A blank tube was prepared using homogenization solution instead of SN. Then, each sample was centrifuged at 4 °C during 15 minutes at 6,000 g and absorbances were read at 410 nm. Final results were expressed in nmol g⁻¹fw, using 0.28 µM⁻¹ cm⁻¹ as extinction coefficient.

2.7.3.2. Quantification of O₂⁻

For the quantification of O₂⁻, fresh samples of roots and shoots were utilized and the assay was based on the reduction of nitroblue tetrazolium (NBT), as described by Gajewska and Skłodowska (2007). With a scalpel, tissue samples were finely cut in equal pieces, amounting to a total of around 200 mg and immersed in a reaction solution consisting of 10 mM NaN₃ and 0.05% (w/v) NBT in sodium phosphate buffer (0.01 M, pH 7.8) (3 mL for shoots and 2 mL for roots) and left in the dark, with constant agitation for one hour. Then, 1.5 mL of this mixture were incubated for 15 minutes at 85 °C, with a brief cooling on ice afterwards. Parallel to this incubation, 1.5 mL of reaction solution were subjected to the same conditions, as a blank. The tubes were then vortexed and centrifuged at maximum speed for 15 seconds and absorbance of each SN was read at 580 nm, with final O₂⁻ content being expressed as Abs_{580 nm} h⁻¹ g⁻¹fw.

2.7.4. Quantification of non-enzymatic AOX metabolites

2.7.4.1. Determination of proline levels

The quantification of proline levels was performed as described by Bates et al. (1973). Three percent (w/v) sulfosalicylic acid was employed to homogenize frozen samples of 200 mg (1.5 mL for shoots and 1 mL for roots) in mortars containing some quartz sand and the resulting homogenates were centrifuged at 500 g for 10 minutes. This step was followed by mixing 200 μ L of SN with 200 μ L of glacial acetic acid and 200 μ L of acid ninhydrin, with a subsequent incubation at 96 °C during one hour. After briefly cooling on ice, 1 mL of toluene was supplied to each sample and the mixture was vortexed for 15 seconds to separate a red upper phase from a whiteish lower phase. The upper one was recovered, and its respective absorbance was read at 520 nm. Proline concentration and absorbance were connected via a standard curve designed with increasing known proline concentrations and results were expressed as mg g⁻¹fw. In this assay, toluene was applied as blank.

2.7.4.2. Quantification of reduced and oxidized glutathione

To quantify both glutathione states in tomato tissues, 1.5 mL of 3% (w/v) metaphosphoric acid were used to homogenize 300 mg frozen samples, at 4 °C. The resulting extracts were then subjected to a 15-minute centrifugation (19,000 g, 4 °C) and SNs were recovered and filtered through a 0.45 μ m nylon filter.

Both GSSG and GSH content were determined via High-Performance Liquid Chromatography (HPLC, Thermo Electron Corporation, Waltham, MA) consisting of a low-pressure quaternary pump with autosampler and diode array detector (DAD) coupled with an ion-trap mass spectrometer. Analysis were performed on a Phenomenex (Torrance, CA) Gemini-NX reverse C₁₈ column (150 mm x 4.6 mm; 3 μ m) and a guard column (4 mm x 3 mm), utilizing a 0.4 mL min⁻¹ flow rate and 25 μ L of injected filtered sample, with a linear gradient program from solvent A (methanol) to solvent B (0.1% aqueous formic acid): from 0 to 10 minutes, 10% of A; from 10 to 15 minutes, increase to 50% of A, with these conditions being maintained for 5 minutes and then over the course of 3 minutes returning to the original conditions and maintained for 5 minutes before the following injection. A quadrupole ion-trap mass spectrometer (Finnigan LCQ Deca XP Plus, San Jose, CA) linked with an electrospray ionization (ESI) source was operated to acquire and process data, with the following interface conditions: 275 °C capillary temperature, 4 kV source voltage, 31 V capillary voltage, 10 V tube lens voltage, sheath gas (N₂) flow at 60 arbitrary units and auxiliary gas (N₂) flow at 23 arbitrary units. Selected ion monitoring (SIM) mode was exploited for data acquisition by selecting m/z

308 for GSH and m/z 613 for GSSG and analysis were carried out in positive ion mode. The diode array detection was conducted by scanning between 200 and 750 nm. Both GSH and GSSG content was estimated with the aid of calibration curves determined from standard solutions based on the peak obtained for increasing concentrations of GSH and GSSG. Through data processing in Xcalibur software version 2.1.0 (Finnigan), peaks were measured, and glutathione levels were expressed in $\mu\text{mol g}^{-1}\text{fw}$.

2.7.5. Quantification of total and non-protein thiols

To determine the thiol content in plants, a method described by Zhang et al. (2009) was used. For this assay, frozen aliquots of 300 mg were homogenized in ice-cold conditions utilizing quartz sand and an extraction solution of 20 mM EDTA and 20 mM AsA (1.9 mL for shoots and 1.5 mL for roots). Afterwards, the homogenates were centrifuged at 12,000 g for 20 mins (4 °C). The SNs were then recovered and utilized for two different purposes.

To determine total thiol content, 100 μL of SN were mixed with 480 μL of Tris-HCl (200 mM, pH 8.2) and 20 μL of 5,5'-dithiobis(2-nitrobenzoic acid) (DTNB, 10 mM) and the resulting solution was incubated at room temperature during 15 minutes. Total thiols were expressed in $\text{mol g}^{-1}\text{fw}$, using 13,600 $\text{M}^{-1} \text{cm}^{-1}$ as molar extinction coefficient, after absorbances were read at 412 nm.

For the quantification of non-protein thiols, 250 μL of SN were added to 250 μL of 10% (w/v) sulfosalicylic acid and then incubated at room temperature for 15 minutes, followed by a 15-minute centrifugation (3,000 g, 4 °C). This was performed in duplicates for each sample and both SNs from each sample were recovered and mixed together. Two hundred and fifty μL of this SN were then mixed with 237.5 μL of Tris-HCl (400 nM, pH 8.9) and 12.5 μL of 10 mM DNTB and left at room temperature to develop color for 5 minutes. Lastly, non-protein thiol content was calculated applying the same molar extinction coefficient, wavelength and units as before. Protein-bound thiol levels were then determined by subtracting the non-protein thiols to the total thiol content.

2.7.6. Determination of ROS-scavenging enzymatic activity

2.7.6.1. Extraction

To determine the activity of three AOX enzymes (SOD, CAT and APX), frozen samples of 300 mg were grounded on ice with some quartz sand and 2 mL of extraction buffer, consisting of 8% glycerol, 1 mM PMSF, 1 mM EDTA, 5 mM L-ascorbic acid and 1% (w/v) PVPP in a potassium phosphate buffer (100 mM, pH 7.3). The resulting homogenates were then centrifuged for 25 minutes (16,000 g, 4 °C) and SNs were

recovered and aliquoted to be used in protein quantification (Bradford, 1976) and enzymatic activity determination. SNs meant to be used for SOD assays were mixed with a final concentration of 10 mM NaN_3 .

2.7.6.2. Determination of SOD activity

The method for determining SOD activity consisted on measuring the inhibition of photochemical reduction of NBT and was carried out as described by Donahue et al. (1997). From the SN aliquot, 35 μg of protein were mixed in 2.8 mL of a solution consisting of 0.1 mM EDTA, 13 mM L-methionine and 75 μM NBT in potassium phosphate buffer (50 mM, pH 7.8). The same potassium phosphate buffer was added in the necessary amount to achieve a final volume of 2.970 mL. To start the reaction, 30 μL of 200 μM riboflavin were added to the tubes, which were then immediately stored under 6 fluorescent 8 W lamps for 10 minutes, with constant rotation. A blank was prepared utilizing potassium phosphate buffer (50 mM, pH 7.8) instead of protein extract. To determine the enzymatic activity, the absorbance of each mixture was read at 580 nm and final results were expressed as units of SOD mg^{-1} of protein, with one unit of SOD being defined as the amount of enzyme required to cause 50% inhibition of the NBT photoreduction rate (Beauchamp and Fridovich, 1971).

2.7.6.3. Determination of APX activity

Determination of APX activity was carried out spectrophotometrically in a UV-microplate, following the method described by (Murshed et al., 2008). To accomplish this, 20 μL of SN were mixed with 170 μL of potassium phosphate buffer (50 mM, pH 7.0), containing 0.6 mM AsA. Before measurement, 10 μL of H_2O_2 (254 mM) were added to each well. Various blank wells were prepared utilizing homogenization buffer instead of SN. After a brief shake of the microplate (5 seconds), APX-mediated AsA oxidation was followed at 290 nm each 5 seconds, during 2 minutes. Utilizing AsA molar extinction coefficient ($0.49 \text{ mM}^{-1} \text{ cm}^{-1}$), final activity values were expressed as $\mu\text{mol DHA min}^{-1} \text{ mg}^{-1}$ of protein.

2.7.6.4. Determination of CAT activity

To determine CAT activity, the temporal catalase-mediated degradation of H_2O_2 was measured spectrophotometrically via an adaptation of the protocol described by Aebi (1984). In a UV-microplate, 20 μL of SN were mixed with 160 μL of potassium phosphate buffer (50 mM, pH 7.0). Immediately before spectrophotometric measure, 20 μL of 100 mM H_2O_2 were added to each microplate well to start the reaction. Blanks were prepared similarly to the APX assay. The microplate was briefly shaken (5 seconds) and H_2O_2

decomposition was monitored at 240 nm each 5 seconds, during 2 minutes. Final activity values were determined utilizing H_2O_2 molar extinction coefficient ($39.4 \text{ mM}^{-1} \text{ cm}^{-1}$) and expressed as $\mu\text{mol H}_2\text{O}_2 \text{ min}^{-1} \text{ mg}^{-1}$ of protein.

2.7.7. Determination of glutathione-related enzymes' activities

2.7.7.1. Determination of γ -ECS activity

The activity of γ -ECS was determined under the conditions described by Sengupta et al. (2012). Here, frozen tissues were homogenized, on ice, with quartz sand and an extraction buffer containing 10 mM MgCl_2 and 1 mM EDTA in Tris-HCl (100 mM, pH 8.0) and 1% (w/v) PVPP. In this assay, samples of around 300 mg were used, using a relation of 2.5 (shoots) or 2 (roots) mL of extraction buffer per 1 g of sample. The extracts were then centrifuged for 15 minutes (10,000 g, 4 °C) and part of the SN was used for protein quantification (Bradford, 1976) and the remainder for the activity assay.

To start the reaction, 140 μL of SN were mixed with 10 μL of pyruvate kinase (475 U/mL) and 350 μL of a reaction mixture consisting of 71.43 mM MgCl_2 , 28.57 mM L-glutamate, 1.43 mM L-cysteine, 7.14 mM phosphoenolpyruvate and 7.14 mM DTT in HEPES buffer (143 mM, pH 8.0). The resulting mixture was left at 37 °C for 45 minutes and the reaction was then stopped by the addition of 100 μL of 50% (w/v) TCA, followed by a vigorous mix. Phosphate content was then evaluated by the phosphomolybdate method (De Groeve et al., 2010) to determine enzymatic activity after centrifuging the mixture for 15 minutes (10,000 g, 4 °C). Fifty μL of this solution were mixed with 75 μL of 12% (w/v) L-ascorbic acid in 1 M HCl and 75 μL of 2% (w/v) ammonium molybdate tetrahydrate and then incubated at room temperature for 20 minutes. Afterwards, 1 mL of stop solution [2% acetic acid, 2% (w/v) sodium citrate tribasic dihydrate] was added to each tube and absorbances were read at 655 nm. A standard curve was established, utilizing known concentrations of KH_2PO_4 , with 0 mM KH_2PO_4 serving as the spectrophotometric blank. The value obtained from the blank tubes (utilizing extraction buffer in place of SN) was subtracted from the one in each sample to determine the amount of ATP used by γ -ECS during the reaction. Final activity values were expressed as $\text{nmol min}^{-1} \text{ mg}^{-1}$ of protein.

2.7.7.2. Determination of GR activity

Determination of GR activity was based on the temporal oxidation of NADPH and carried out by following the method performed by Yannarelli et al. (2007). Frozen aliquots were grounded, under ice-cold conditions, using 1 mM EDTA, 1 mM PMSF and 10 mM dithiothreitol (DTT) in potassium phosphate buffer (100 mM, pH 7.5) as extraction

solution, adding 1% (w/v) PVPP to the mortar, containing some quartz sand, before homogenization. Samples used in this assay weighed around 300 mg and a proportion of 3 mL of buffer per g was utilized. After extraction, the homogenates were centrifuged for 30 minutes at 20,000 *g* (4 °C) and the SNs were recovered to be used in protein (Bradford, 1976) and enzymatic activity quantification.

For the spectrophotometric quantification, 50 μ L of protein extract were mixed in a quartz cuvette already containing 500 μ L of 200 mM potassium phosphate buffer (pH 7.8), 100 μ L of 20 mM EDTA, 100 μ L of 2 mM NADPH, 100 μ L of 5 mM GSSG and 150 μ L of H₂O. Δ Abs_{340 nm} per minute reflected the oxidation of NADPH and utilizing its molar extinction coefficient (6.22 mM⁻¹ cm⁻¹), the final GR activity values were expressed as μ kat mg⁻¹ of protein, with 1 kat representing 60 mol min⁻¹.

2.7.7.3. Determination of GST activity

A standard spectrophotometric assay, measuring the temporal GST-mediated conjugation of GSH to a substrate was utilized to quantify enzymatic activity, as described in Teixeira et al. (2011). Frozen tissue samples of around 300 mg were homogenized, on ice, utilizing some quartz sand, 1% (w/v) PVPP and a 1 g to 2.5 mL proportion of extraction buffer, consisting of 1 mM EDTA, 1 mM PMSF and 1 mM DTT in Tris-HCl (50 mM, pH 7.5). The extracts were then centrifuged for 25 minutes (20,000 *g*, 6 °C) and the SNs were recovered to be used to estimate protein content (Bradford, 1976) and enzymatic activity.

In a quartz cuvette, 100 μ L of SN were mixed with 700 μ L of potassium phosphate buffer (71.43 mM, pH 7.5) and 100 μ L of a 10 mM substrate solution. For this assay, 1-chloro-2,4-dinitrobenzene (CDNB, $\epsilon_{340 nm} = 9.6$ mM⁻¹ cm⁻¹) was employed as a substrate for GSH conjugation. To start the reaction, 100 μ L of 10 mM GSH were pipetted to the cuvette and Δ Abs_{340 nm} min⁻¹ was measured, over the course of 2 minutes. Real activity values were expressed in μ kat mg⁻¹ of protein and were determined by subtracting the obtained value by the one obtained in a reading where SN was replaced by 100 μ L of H₂O, correspondent to the non-enzymatic conjugation of GSH to CDNB.

2.7.7.4. GST activity in a native polyacrylamide gel electrophoresis (PAGE)

For a visual representation of GST activity, a native PAGE was performed by loading the volume corresponding to 40 μ g of protein extract in a 10% (resolving) and 4% (stacking) polyacrylamide gel (Table 2), using a running buffer consisting of 25 mM Tris and 192 mM L-glycine and the run performed at 15 mA per gel (4 °C). Afterwards, each gel was incubated in the dark, with constant agitation and at room temperature for 10 minutes in 15 mL of a solution containing 4.5 mM GSH, 1 mM CDNB and 1 mM NBT in

potassium phosphate buffer (100 mM, pH 7.5). Utilizing deionized water, the gels were then washed twice and left for 5 minutes at room temperature, with constant agitation in the dark in 15 mL of 3 mM phenazine methosulphate (PMS) in Tris-HCl (100 mM, pH 9.6). Imaging of the gels was performed with a ChemiDoc™ XRS+ System (Bio-Rad, Hercules, CA), allowing a better visualization of achromatic bands in a blue background. This is a consequence of formation of blue formazan, due to the fast reduction of NBT in the presence of PMS and GSH. Since GST acts by conjugating GSH to CDNB, inhibiting the use of GSH for the reduction of NBT, the achromatic bands are a direct representation of GST activity, with higher intensity being a repercussion of higher enzymatic activity (Ricci et al., 1984).

Table 2. Constitution of the native polyacrylamide gel performed for visual determination of GST activity. Volumes presented are the necessary for one gel.

	10% polyacrylamide resolving gel	4% polyacrylamide stacking gel
Acrylamide 30%	3.33 mL	0.33 mL
1.5 M / 0.25 M Tris-HCl pH 8.8 / 6.8	1.25 mL	0.625 mL
Glycerol 87%	1.15 mL	0.285 mL
H ₂ O	4.2 mL	1.241 mL
Ammonium persulfate (APS) 10% (w/v)	0.075 mL	0.00625 mL
Tetramethylethylenediamine (TEMED)	0.005 mL	0.0125 mL
Final Volume (per gel)	10 mL	2.5 mL

2.8. Analysis of molecular parameters

2.8.1. RNA extraction and quantification

RNA from plant tissues was extracted via the NZYol (NZytech®, Portugal) method, in accordance to the supplied instructions. Frozen 50-100 mg samples of roots and shoots were homogenized in 1 mL of NZYol and were then centrifuged for 10 minutes (12,000 g, 4 °C). The cleared homogenates were transferred and after a 5-minute room temperature incubation, they were mixed with 0.2 mL of chloroform. Afterwards, tubes were briefly shaken and incubated at room temperature for 3 minutes, followed by another centrifugation at 12,000 g (15 minutes, 4 °C). This process induces a phase separation, with a lower pale green, phenol-chloroform phase, an interphase and a transparent upper phase, which contains the RNA. Carefully, the latter was recovered without disturbance of the interphase and 0.5 mL of cold isopropanol were added to the

SN. This mixture was left for 10 minutes at room temperature and centrifuged for 10 minutes (12,000 *g*, 4 °C), allowing the RNA to precipitate. The resulting SN was discarded, and the pellet was washed with 80% ethanol, followed by quick vortex and a 5-minute centrifugation (7,500 *g*, 4 °C). The pellet was then air-dried and after ethanol evaporation it was re-suspended in nuclease-free water.

RNA quantification was spectrophotometrically performed in a μ Drop plate (Thermo Fisher Scientific) and a Multiskan GO microplate spectrophotometer (Thermo Fisher Scientific) at 260 nm, with a ratio of 1.0 $Abs_{260\text{ nm}}$ corresponding to a 1 mg mL⁻¹ RNA concentration. Since unlike nucleic acids, proteins have a maximum UV absorption at 280 nm, the ratio between $Abs_{260/280\text{ nm}}$ is a good indicator of protein and phenolic contamination. This parameter was also evaluated, and samples were selected if they presented values ranging from 1.8 to 2.0, since lower results indicate the presence of protein contamination. To estimate polysaccharide contamination, the ratio of $Abs_{260/230\text{ nm}}$ was also measured and samples were considered valid if the measured value was around 2 (Farrell, 2010).

RNA integrity was assessed by analyzing 300 ng of RNA by a 0.8% (w/v) agarose gel electrophoresis in 1X sodium boric acid (SB) buffer, at 250 V and non-limiting amperage, and using Xpert Green DNA Stain (GRiSP, Portugal) to stain the nucleic acids. Until further use, samples considered acceptable in all evaluated parameters were stored at -80 °C.

2.8.2. Reverse transcription (RT) - cDNA synthesis

To generate complementary DNA (cDNA) from the previously extracted mRNA, RT reactions were carried out utilizing SuperScript™ IV VILO™ Master Mix kit, following the supplied instructions (Invitrogen, USA). First, a tube was prepared by mixing 1 μ L of 10X ezDNase buffer, 1 μ L of ezDNase enzyme, 2.5 μ g of template RNA and nuclease-free water to a final volume of 10 μ L. This enzyme is a novel double-strand specific thermolabile DNase utilized for removing genomic DNA contamination from the RNA sample before the RT reaction. After a quick mix, the prepared tubes were incubated for 2 minutes at 37 °C, briefly centrifuged and placed on ice. Then, 4 μ L of SuperScript™ IV VILO™ Master Mix and 6 μ L of nuclease-free water were added to the tubes containing the 10 μ L reaction mix. Primers were annealed with a gentle mix and 10-minute incubation at 25 °C and the RT reaction occurred in a 20-minute incubation at 50 °C. To heat-inactivate the enzyme, these tubes were incubated at 85 °C during 5 minutes and then stored at -20 °C until further use.

2.8.3. Semi-quantitative polymerase chain reaction (PCR)

To estimate differences in the accumulation of the mRNAs coding for different enzymes (plastidial and cytosolic GR, γ -ECS and GSTU) after the treatments with DCF, semi-quantitative reverse-transcriptase PCR (RT-PCR) was performed. Reactions were prepared in a MJ Mini™ Thermal Cycler (Bio-Rad®, Portugal) under the conditions reported in Table 3, with the respective tubes containing: 1x Taq Master Mix (Bioron, Germany), 0.4 μ M of forward and reverse primers (Table 3), 0.4 μ L cDNA and sterile distilled water to bring the total volume to 10 μ L.

Table 3. Gene-specific primers and PCR programs for the RT-PCR reactions carried out. (') minutes; (") seconds.

Primer identifier	Primer sequence	Amplicon size (bp)	Thermocycler program
GRchl_FW	5' GAGTTTGAGGAGAGTTGTGG 3'	581	Lid 110 °C 94 °C – 2 ' 30 cycles of: 94 °C – 30 ", 54 °C – 30 ", 72 °C – 45 " 72 °C – 5 '
GRchl_RV	5' GAGAAACCTTCAACTGTTCC 3'		
GRcyt_FW	5' AAAGACCGAGGAGATTGTACG 3'	322	Lid 110 °C 94 °C – 2 ' 30 cycles of: 94 °C – 10 ", 57 °C – 20 ", 72 °C – 45 " 72 °C – 2 '
GRcyt_RV	5' CATTCTCGCCATATAGAAGC 3'		
γ-ECS_FW	5' GAAACAGGGAAAGCAAAGC 3'	725	Lid 110 °C 94 °C – 2 ' 30 cycles of: 94 °C – 20 ", 51 °C – 30 ", 72 °C – 45 " 72 °C – 2 '
γ-ECS_RV	5' CATCAGCACCTCTCATTTC 3'		
TAU_FW	5' GGGAAACCAATTTGTGAATC 3'	568	Lid 110 °C 94 °C – 5 ' 30 cycles of: 94 °C – 30 ", 51 °C – 30 ", 72 °C – 90 " 72 °C – 10 '
TAU_RV	5' GCGTTGGCTCTTTCATAAGG 3'		
ACT_FW	5' GAAATAGCATAAGATGGCAGACG 3'	159	Lid 110 °C 95 °C – 5 ' 30 cycles of: 95 °C – 30 ", 58 °C – 20 ", 72 °C – 20 " 72 °C – 5 '
ACT_RV	5' ATACCCACCATCACACCAGTAT 3'		

To visualize differences, the amplicons were loaded on a 1% (w/v) agarose (1X SB buffer) gels, running at 250 V and non-limiting amperage, and using Xpert Green DNA Stain to stain the nucleic acids. To guarantee that different band intensities were directly correlated with different transcript accumulation levels and not with different quantities of loaded cDNA, the constitutive actin (ACT) gene was utilized as an internal control. In this sense, actin amplicons were loaded and the volumes which resulted in similar bands for

each treatment were utilized in the subsequent comparative quantifications. GeneRuler 50 bp DNA Ladder (Thermo Fisher Scientific) was used to verify the size of the amplified fragments. The gels were then imaged in a GenoSmart 2 (VWR, USA) and treated with the respective imaging software.

2.8.4. Expression of GSTF genes by Real-Time (q) PCR

The transcript levels of five *S. lycopersicum* GSTF (*SIGSTF*) genes in shoots and roots of untreated and treated plants were monitored via quantitative real-time PCR (qPCR) carried out in a CFX96 Real-Time Detection System (Bio-Rad®, Portugal). PowerUp™ SYBR® Green Master Mix (Applied Biosystems, CA) was used for this assay and each reaction was performed in triplicate. The qPCR reaction consisted in the addition of 1 µL of 1:10 diluted cDNA to a reaction mixture of 1X PowerUp™ SYBR® Green Master Mix, 0.4 µM of forward and reverse primers and water to a final volume of 20 µL per well. qPCR cycling conditions were as follows: 50 °C for 2 minutes, 95 °C for 2 minutes and 40 cycles of 95 °C for 3 seconds and 60 °C for 30 seconds. Melting curve analysis was performed with a 60 – 95 °C increment at 0.5 °C intervals to verify primer specificity, revealing a single peak for each gene. The results were then resolved using CFX Maestro™ 1.0 Software (Bio-Rad®, Portugal) and expressed as C_t (threshold cycle).

Primer information is described in table 4, with gene-specific primers for *SIGSTF4* and *SIGSTF5* being previously designed and reported by Csiszar et al. (2014), while primers for *SIGSTF1*, *SIGSTF2* and *SIGSTF3* were designed and optimized in unpublished work from the same laboratory where this work was conducted (Pinto, 2017).

Table 4. Gene-specific primers for the performed qPCR assay, respective melting temperature (T_m) and amplicon sizes.

Gene name	Accession number	Primer sequence	T _m (°C)	Amplicon size (bp)
<i>SIGSTF1</i>	Solyc02g081340	5' TTACAGCCATTTGGACAGGTTCC 3' 5' GTCGTTCCGGTTAGTTTCTTTCCC 3'	57.5 / 57.8	125
<i>SIGSTF2</i>	Solyc06g009020	5' GTCTGTATGGATGGAAGTAG 3' 5' GAAGTTTCCCAGTTTCTC 3'	49.4 / 50.6	143
<i>SIGSTF3</i>	Solyc06g009040	5' ACATGGTGACTGATGATGCAATC 3' 5' GCGTGGTTCAAATCAGCTAGGG 3'	57.6 / 58.4	136
<i>SIGSTF4</i>	Solyc09g074850	5' CGTGTGAGTGTATGGTGTGCT 3' 5' CATCTTCTCCAACCCCTCA 3'	57.3 / 54.3	66
<i>SIGSTF5</i>	Solyc12g094430	5' CCGATCTCTCTCACCTTCCA 3' 5' TGCTCTGTGTGCCGTTCC 3'	55.7 / 57	56

2.9. Statistical analysis

Every parameter, either biometric, molecular or biochemical, was performed in at least three biological replicates ($n \geq 3$), with at least three technical replicates per assay and results were expressed as mean \pm standard deviation (SD). Values for the control situation were compared with the treated samples and significant differences were monitored via one-way ANOVA, in conjunction with a Dunnet post-hoc test. The robustness and strong analysis associated with ANOVA allows its use in place of nonparametric statistical tests (Zar, 1996). These analyses were carried out using Prism[®] 7 (GraphPad Software Inc., USA), considering significant the differences at $p \leq 0.05$.

Regarding the RT-qPCR assay, the resulting data was normalized by the $2^{(-\Delta\Delta C_t)}$ formula of Livak and Schmittgen (2001), using ACT and ubiquitin as reference genes (Løvdaal and Lillo, 2009). In this sense, the relative normalized expression ($\Delta\Delta C_t$) accurately conveys the differences in transcript levels between treated and untreated situations, eliminating differences based on different cDNA amount loaded.

3. Results

3.1. Effects of increasing diclofenac concentrations on plants' biometry

3.1.1. Effects of increasing diclofenac concentrations on germination and seedlings' biometry

After ten days of growth, subjected to increasing DCF concentrations, seedlings were collected, and their biometry analyzed. Germination was not affected, as Petri dishes containing plantlets grown in different treatments presented a similar seed germination rate (Figure 7A). Regarding total fresh weight (Figure 7B) and shoot length (Figure 7C), the presence of DCF did not seem to provoke negative effects, as these parameters did not present any statistical differences compared to untreated seedlings. Statistical significance only takes place when analyzing root length (Figure 7D), as seedlings grown exposed to 10 mg L⁻¹ presented a 1.43-fold reduction in size.

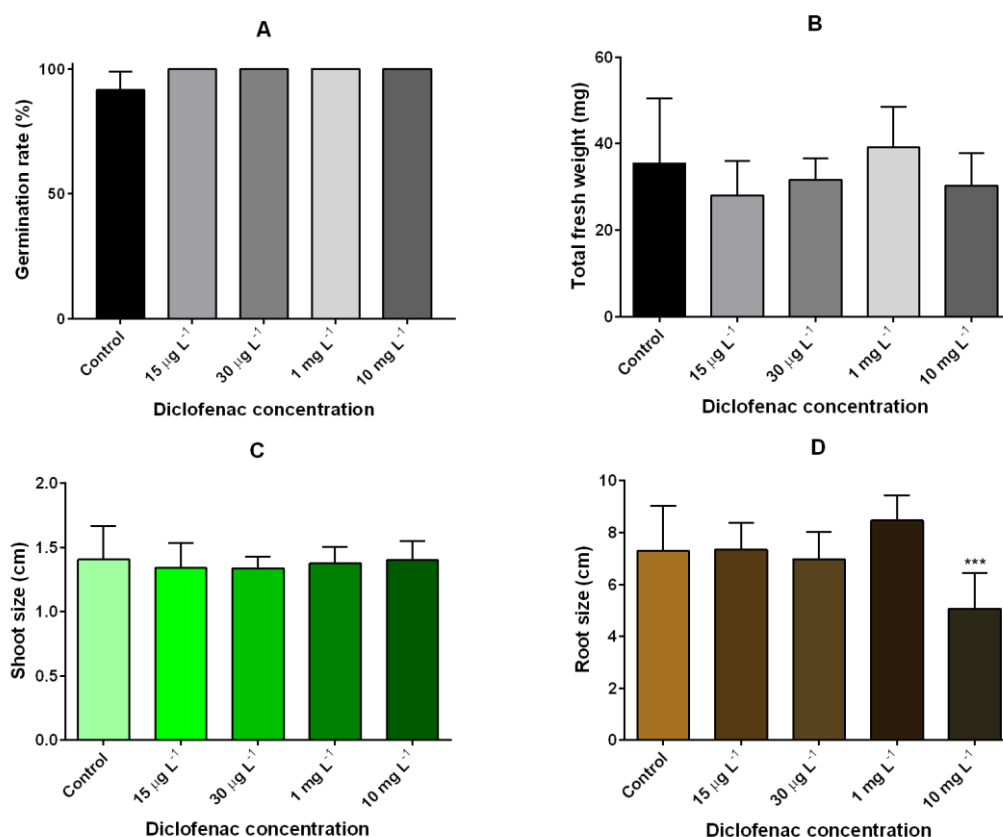


Figure 7. Germination rate (A), total biomass (B) and shoot (C) and root (D) length of *S. lycopersicum* seedlings grown in nutrient medium supplemented with increasing diclofenac concentrations. Values presented are mean ± SD. * above bars represent significant differences from the control at * $p \leq 0.05$, ** $p \leq 0.01$, *** $p \leq 0.001$, **** $p \leq 0.0001$.

From these results, it was possible to select the concentrations to be used in the following studies. As the highest concentration (10 mg L^{-1}) presented visible negative effects in the grown seedling and the second highest (1 mg L^{-1}) presented a slight tendency to enhance the studied parameters, these were the selected situations. However, several reports using different types of contaminants have shown that even in high and usually toxic concentrations, germination and early growth parameters can possibly remain unaffected due to a protective effect of the seed coat and nutrients released from the cotyledons and endosperm (An et al., 2009; Akinci and Akinci, 2010; Chen et al., 2011). In this sense, as some effects have already been shown in the seedlings and to avoid nefarious effects and therefore lack of biomass, while also approximating to the current environment context, the final concentrations were reduced to half, with the subsequent studies being performed with 0.5 mg L^{-1} and 5 mg L^{-1} of DCF.

3.1.2. Effects of increasing diclofenac concentrations on the biometrical parameters of exposed plants

As observed in Figure 8, no morphological differences could be detected after the visual analysis of the plants from the different treatments.



Figure 8. Effect of different concentrations of diclofenac on tomato plants' morphology. Plants were grown for 6 weeks in a growth chamber (16 h light/8 h dark; 25 °C) and on the last 5 weeks were treated with Hoagland solution supplemented with 0 mg L^{-1} (control), 0.5 mg L^{-1} and 5 mg L^{-1} diclofenac.

Following biometrical measurements, no significant effects were detected in roots from any concentration, but the same pattern did not occur in the aerial portion of the plants. In shoots it is possible to observe that exposure to 5 mg L^{-1} DCF negatively influenced both length (Figure 9A) and fresh weight (Figure 9B), leading to a reduction of 1.29- and 1.72-fold, respectively. In accordance, it was also noticeable that the ratio between root and shoot biomass was increased, as a result of the maintenance of root

biomass levels, with a decrease in shoots in the highest DCF concentration (Figure 9C). Lastly, to infer if DCF could affect water retention in tomato plants, water content was evaluated (Figure 9D) and while most data remained similar to the control, a subtle but significant decrease of 1.04-fold was detected for the roots in the most concentrated solution.

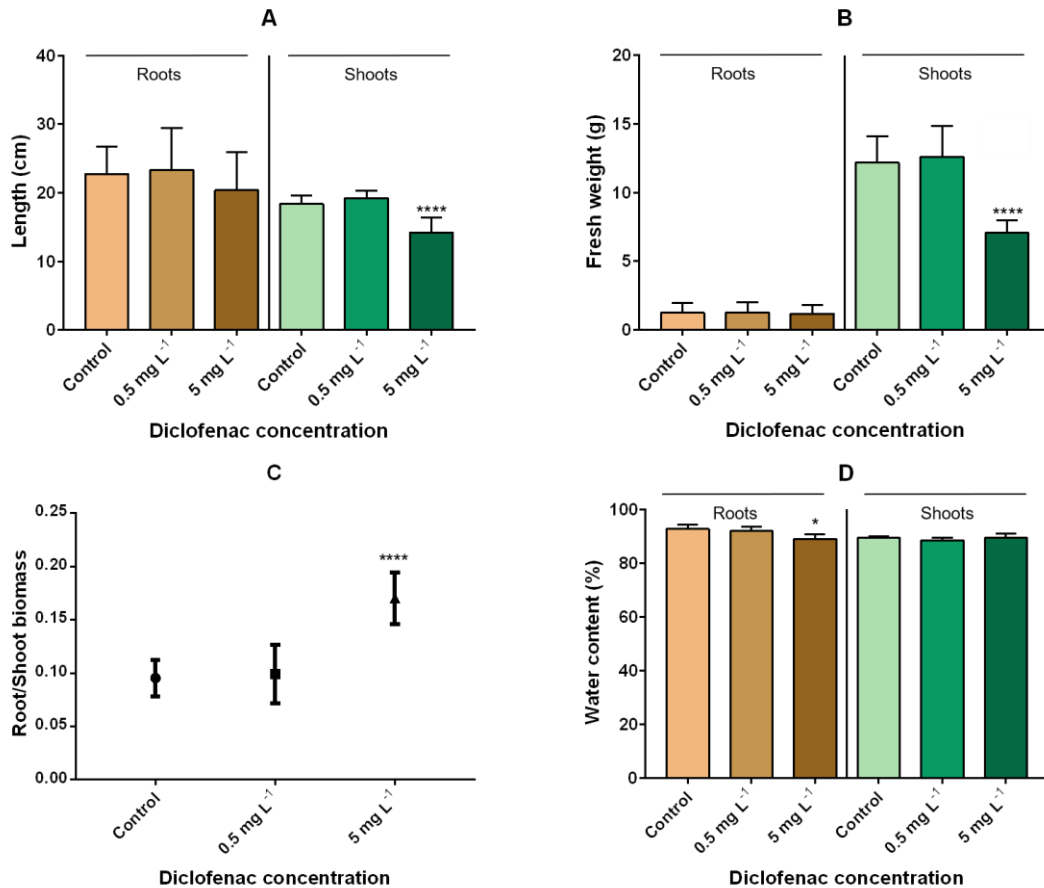


Figure 9. Root and shoot length (A) and biomass (B) of *S. lycopersicum* plants grown in nutrient medium supplemented with increasing concentrations of diclofenac. (C) represents the ratio between root and shoot biomass. (D) Water content in the same treated plants. Values presented are mean \pm SD. * above bars represent significant differences from the control at * $p \leq 0.05$, ** $p \leq 0.01$, *** $p \leq 0.001$, **** $p \leq 0.0001$.

Additionally, it was possible to realize that diclofenac exposure did not affect the tomato plants' life cycle, as all plants from all growth situations reached the flowering stage at the same time and with the same flower intensity. This pattern was also observed for fruits, as the plants who were kept for DCF quantification also produced fruits at around the same time, with similar intensity and morphology as the control plants.

3.2. Quantification of diclofenac in fruits and in the nutritive medium

After supplying the trays with Hoagland solution containing 5 mg L⁻¹ DCF, it was possible to observe that plants rapidly decreased the amount of DCF in liquid solution to levels below the limit of quantification (0.1 mg L⁻¹), even after new medium was added to replenish its levels in the tray at the second and fourth day (Figure 10). Such decrease was so rapid that no DCF could ever be detected for the 0.5 mg L⁻¹-growth condition. Contrarily, it was possible to verify that the material used for root support had initially a high affinity for DCF, as practically no DCF was detected in the day it was added, but then would gradually release it to the nutrient medium along time, as observed for the “no-plants” condition, thus indicating that no non-plant degradation of DCF occurred. Moreover, the DCF levels were always lower in the “with-plants” condition than in the “no-plants” condition.

Regarding the fruits, DCF content was quantified and it was possible to determine that no fruit presented DCF levels above the limit of quantification (3 µg g⁻¹), independent of the supplied DCF dosage.

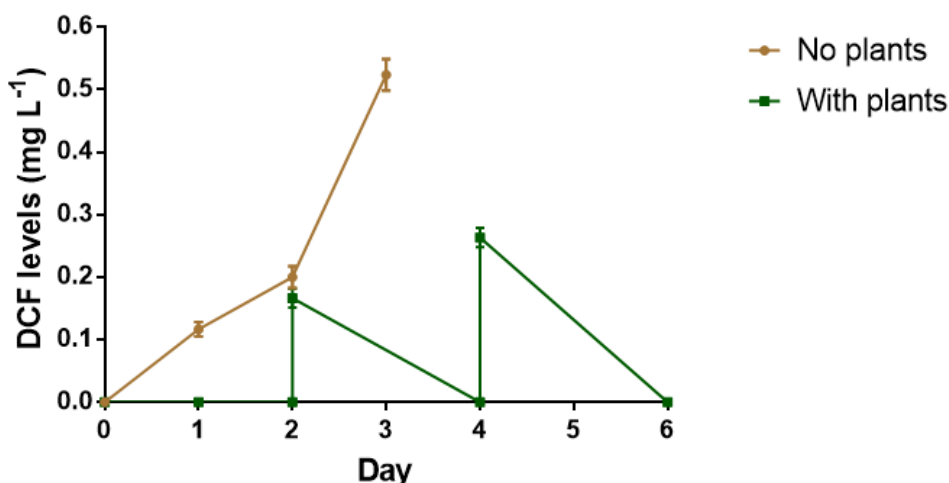


Figure 10. Over-time removal of diclofenac by tomato plants. The brown line represents a “no-plants” situation, which was irrigated with 5 mg L⁻¹ on day 0 and diclofenac levels were measured over the following three days. The green line represents the “with-plants” situation, which was irrigated with the same concentration on day 0, day 2 and day 4. Values presented are mean ± SD and values below the limit of quantification are represented as 0.

3.3. Effects of increasing diclofenac concentrations on several stress biomarkers of *S. lycopersicum* plants

3.3.1. Soluble protein content

Exposure to DCF had a positive effect regarding this parameter (Figure 11), as increased contents were found for the roots from both concentrations (1.92- and 2.16-fold increase) and for the shoots from the treatment with 0.5 mg L⁻¹ of DCF (1.40-fold increase). For the remaining treatment, a significant reduction of 1.24-fold was detected.

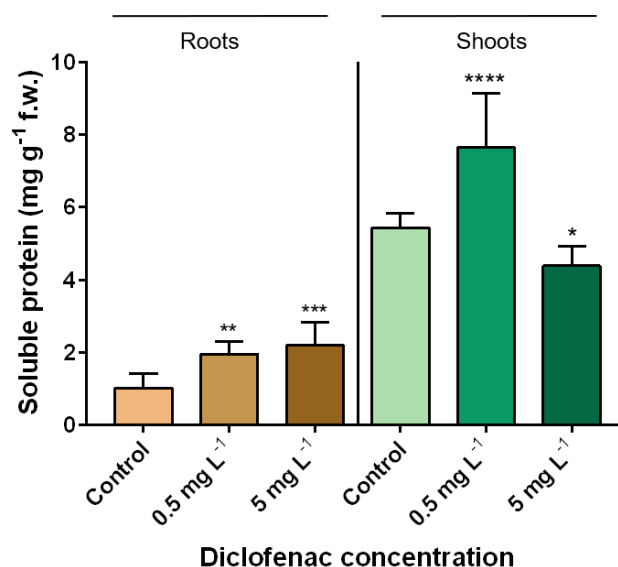


Figure 11. Soluble protein content of *S. lycopersicum* plants grown in nutrient medium supplemented with increasing concentrations of diclofenac. Values presented are mean \pm SD. * above bars represent significant differences from the control at * $p \leq 0.05$, ** $p \leq 0.01$, *** $p \leq 0.001$, **** $p \leq 0.0001$.

3.3.2. Diclofenac-induced oxidative stress

MDA levels were utilized as a marker for LPO, as it is a possible consequence of diclofenac-induced oxidative stress. No effects were detected in shoots from either treatment, but it is possible to notice that exposure to 5 mg L⁻¹ of DCF enhanced LPO in roots, with a 1.80-fold increase in MDA content being detected (Table 5).

The oxidative state of these plants was also studied by determining O₂⁻ and H₂O₂ levels, with no significance being attributed to the former in both conditions and organs. It is however possible to encounter a significantly higher amount of H₂O₂ for both treatments in roots, with the lowest concentration presenting a 1.32-fold increase and the highest showing an even larger increase of 1.85-fold. In shoots, only the highest concentration caused a significant effect, as H₂O₂ content increased 1.25-fold.

Table 5. MDA, O₂⁻ and H₂O₂ levels in plants treated with increasing diclofenac concentrations. Values presented are mean ± SD. * represent significant differences from the control at * p ≤ 0.05, ** p ≤ 0.01, *** p ≤ 0.001, **** p ≤ 0.0001.

Situation	[MDA] (nmol g ⁻¹ fw)		[O ₂ ⁻] (Abs _{580 nm} h ⁻¹ g ⁻¹ fw)		[H ₂ O ₂] (nmol g ⁻¹ fw)	
	Roots	Shoots	Roots	Shoots	Roots	Shoots
Control	3.01 ± 0.56	30.59 ± 2.80	1.14 ± 0.12	0.56 ± 0.15	337.37 ± 44.29	558.01 ± 27.31
0.5 mg L ⁻¹	3.80 ± 0.51	30.42 ± 0.82	0.82 ± 0.33	0.44 ± 0.15	447.26 ± 52.07 *	602.82 ± 50.66
5 mg L ⁻¹	5.43 ± 0.84 ***	27.53 ± 1.81	0.91 ± 0.06	0.46 ± 0.17	626.05 ± 69.15 ****	678.01 ± 85.33 *

Another stress biomarker evaluated to understand the effects triggered by diclofenac exposure was the quantification of total thiols (Figure 12), as well as the proportion of non-protein and protein-bound thiols (Table 6) in exposed plants. In shoots, no significant differences were detected regarding total thiol levels, but a slight tendency to increase was observed, with a higher thiol content being associated to a higher DCF concentration. In roots, this tendency portrays statistical significance, with increasing DCF concentrations leading to 2.57- and 2.35-fold increases, respectively, in total thiol levels.

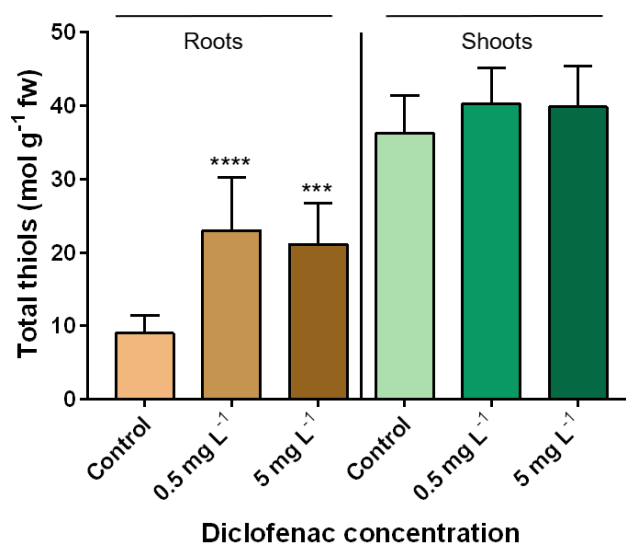


Figure 12. Total thiol levels in roots and shoots of *S. lycopersicum* plants grown in nutrient medium supplemented with increasing concentrations of diclofenac. Values presented are mean ± SD. * above bars represent significant differences from the control at * p ≤ 0.05, ** p ≤ 0.01, *** p ≤ 0.001, **** p ≤ 0.0001.

This increase was mostly due to an increase in protein-bound thiols, as this class presented noticeably higher levels in every situation and organ, which accompanied the

increase in total thiol content, while the same cannot be held for the other thiol class. For increasing DCF concentrations, the levels of protein-bound thiols in roots were 3.28- and 2.97-fold superior, respectively, while in shoots this parameter showed values 1.23- and 1.25-fold above the ones quantified in the untreated plants. Even in the only situation where non-protein thiols presented a small increase (roots – 5 mg L⁻¹; 1.75-fold), it was still minimal when compared to the increase in protein-bound thiols, as better perceived by the increase in the percentage of the latter class in the total thiol levels depicted in Table 6.

Table 6. Non-protein and protein-bound thiol levels and percentages in plants treated with increasing diclofenac concentrations. Values presented are mean ± SD. * represent significant differences from the control at * p ≤ 0.05, ** p ≤ 0.01, *** p ≤ 0.001, **** p ≤ 0.0001

Situation	Roots		Shoots	
	Non-protein thiols (mol g ⁻¹ fw)	Protein-bound thiols (mol g ⁻¹ fw)	Non-protein thiols (mol g ⁻¹ fw)	Protein-bound thiols (mol g ⁻¹ fw)
Control	3.19 ± 0.92 (36%)	5.76 ± 1.56 (64%)	15.03 ± 3.43 (41%)	21.25 ± 2.70 (59%)
0.5 mg L⁻¹	2.99 ± 0.74 (15%)	18.90 ± 4.84 **** (85%)	13.57 ± 1.10 (35%)	26.13 ± 4.24 * (65%)
5 mg L⁻¹	5.57 ± 0.85 **** (24%)	17.09 ± 4.90 **** (76%)	13.24 ± 1.00 (33%)	26.62 ± 4.20 * (67%)

3.3.3. Effects of diclofenac on the non-enzymatic components of *S. lycopersicum* plants' antioxidant system

As figure 13 illustrates, proline levels in tomato plants were affected by the long-term exposure to DCF, but while this parameter only increased significantly with the highest concentration in roots, the aerial portion of the plant presented a higher proline content for both tested conditions, with higher values being detected along with the increasing concentration of DCF supplied, amounting to 1.60- and 1.73-fold increases. Nonetheless, the most noticeable effect occurred in the roots, as exposure to 5 mg L⁻¹ of DCF led to a 1.88-fold increase in proline levels.

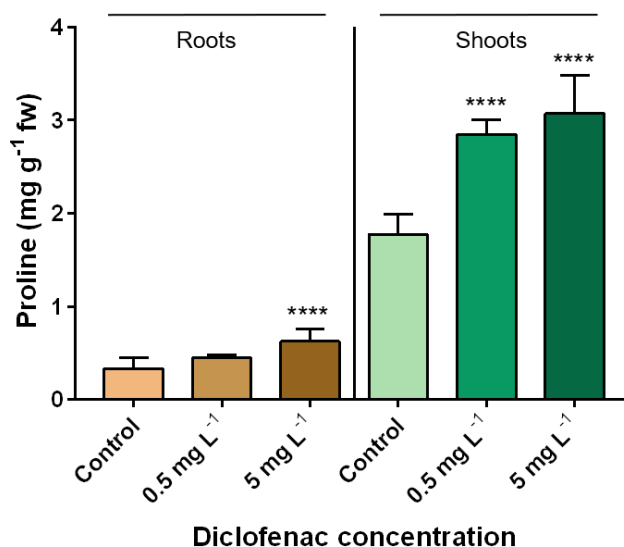


Figure 13. Free proline levels in roots and shoots of *S. lycopersicum* plants grown in nutrient medium supplemented with increasing concentrations of diclofenac. Values presented are mean \pm SD. * above bars represent significant differences from the control at * $p \leq 0.05$, ** $p \leq 0.01$, *** $p \leq 0.001$, **** $p \leq 0.0001$.

Regarding GSH (Table 7), it is possible to observe a significant decrease in roots and shoots of *S. lycopersicum* plants treated with 0.5 mg L⁻¹ DCF. This decrease was of 1.89- and 1.86-fold, respectively. Although total shoot GSH for the 5 mg L⁻¹ situation was very similar to that of untreated shoots, a smaller amount was observed for the roots of the same plants, but with no statistical significance. The redox state of GSH was evaluated by the GSH/GSSG ratio and once again plants treated with 0.5 mg L⁻¹ were the most different regarding this parameter. Here, and even if statistically insignificant, a clear tendency was observed for these plants to present a more reduced GSH state than their counterparts. It was also shown that this tendency to favor GSH was mostly due to lower GSSG levels, as the content in oxidized GSH was 6.54- and 2.39-fold inferior in roots and shoots of plants treated with 0.5 mg L⁻¹ DCF.

Also, it was possible to detect a difference in the GSH redox state between roots and shoots of treated and untreated plants, as most GSH in roots was present in the reduced form, whereas in shoots it was more common in the oxidized form.

Table 7. Glutathione levels in roots and shoots of *S. lycopersicum* plants grown in nutrient medium supplemented with increasing concentrations of diclofenac. Values presented are mean ± SD. * represent significant differences from the control at * p ≤ 0.05, ** p ≤ 0.01, *** p ≤ 0.001, **** p ≤ 0.0001.

Situation	Roots				Shoots			
	GSH (µmol g ⁻¹ fw)	GSSG (µmol g ⁻¹ fw)	Total GSH (µmol g ⁻¹ fw)	GSH/GSSG	GSH (µmol g ⁻¹ fw)	GSSG (µmol g ⁻¹ fw)	Total GSH (µmol g ⁻¹ fw)	GSH/GSSG
Control	2.81 ± 0.19	2.29 ± 0.44	5.23 ± 0.17	1.43 ± 0.22	3.42 ± 0.20	8.10 ± 0.78	11.52 ± 1.55	0.42 ± 0.14
0.5 mg L ⁻¹	2.40 ± 0.16	0.35 ± 0.28*	2.76 ± 0.45*	2.38 ± 3.07	2.67 ± 0.36	3.39 ± 0.39**	6.20 ± 0.77*	0.83 ± 0.02
5 mg L ⁻¹	2.66 ± 0.27	1.07 ± 0.64	3.74 ± 0.83	1.97 ± 0.41	3.62 ± 1.07	8.01 ± 0.80	11.64 ± 0.28	0.46 ± 0.17

3.3.4. Effects of diclofenac on the enzymatic components of *S. lycopersicum* plants' antioxidant system

As described in the figures below (14-16), several ROS scavenging enzymes were analyzed following a 5-week exposure to diclofenac to better understand the mechanisms behind the enzymatic response of tomato plants to the reactive oxygen species produced as a consequence of this exposure. SOD (Figure 14) did not present significant differences for either treatment in roots, but this pattern did not transfer to the aerial portion, as exposure to 0.5 mg L⁻¹ decreased its activity levels by 1.34-fold, contrasting with the exposure to 5 mg L⁻¹, which led to a 1.39-fold increase.

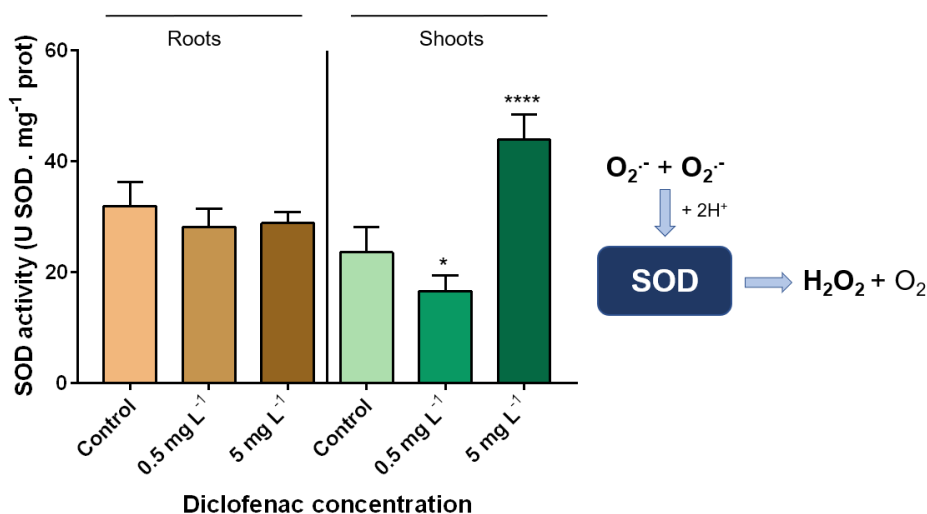


Figure 14. SOD activity levels (left) and function (right) in plants treated with increasing diclofenac concentrations. Values presented are mean ± SD. * above bars represent significant differences from the control at * p ≤ 0.05, ** p ≤ 0.01, *** p ≤ 0.001, **** p ≤ 0.0001.

APX activity significantly decreased in both organs and tested concentrations (Figure 15). In roots, this reduction was very similar between the two tested situations, as the lower DCF concentration presented a 1.97-fold decrease and the highest a 2.05-fold reduction. In shoots, a dose-dependent reduction was observed with the increase of DCF concentration resulting in a 1.63- and 3.00-fold decrease in APX activity.

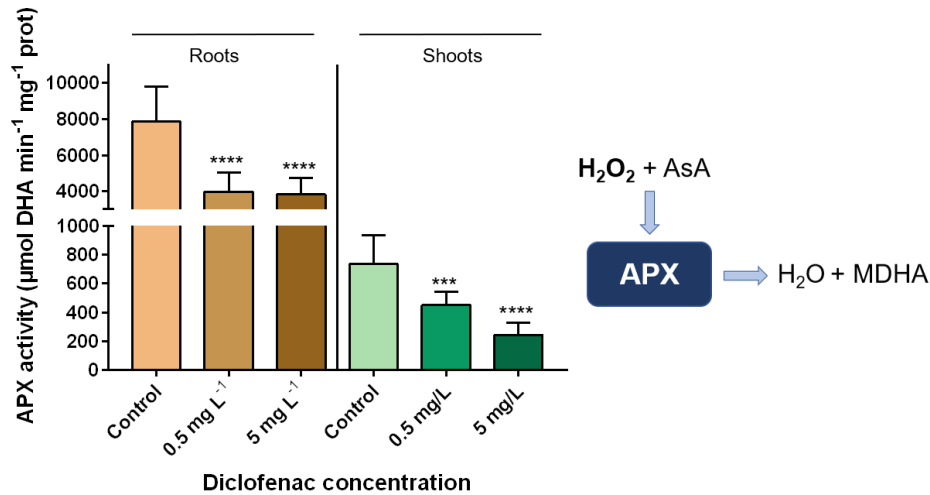


Figure 15. APX activity levels (left) and function (right) in plants treated with increasing diclofenac concentrations. Values presented are mean ± SD. * above bars represent significant differences from the control at * $p \leq 0.05$, ** $p \leq 0.01$, *** $p \leq 0.001$, **** $p \leq 0.0001$.

Similarly to APX, CAT activity (Figure 16) also decreased in both organs after the prolonged exposure to DCF. In roots, a reduction of 1.64-fold was detected in the first situation, while the second treatment reduced CAT activity by 1.39-fold. In shoots, this decrease was of 1.26-fold for the lowest concentration and 1.27-fold for the highest DCF dosage.

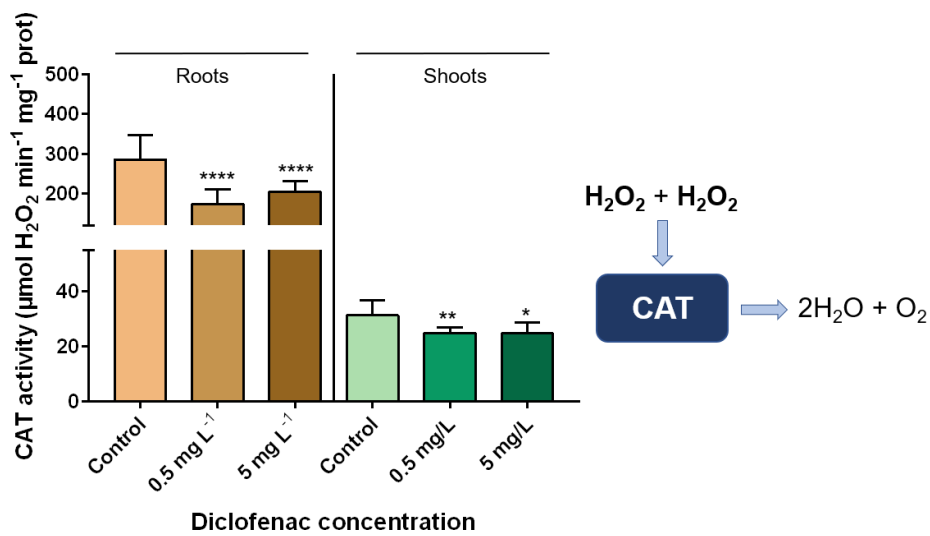


Figure 16. CAT activity levels (left) and function (right) in plants treated with increasing diclofenac concentrations. Values presented are mean ± SD. * above bars represent significant differences from the control at * $p \leq 0.05$, ** $p \leq 0.01$, *** $p \leq 0.001$, **** $p \leq 0.0001$.

3.3.5. Effects of diclofenac on the GSH-related enzymes' activities

Because GSH is one of the most important molecules in several physiological processes, mainly in ROS scavenging mechanisms and xenobiotic detoxification, both relevant upon the exposure to DCF, three enzymes related to its metabolism were studied.

As shown by Figure 17, long-term exposure to DCF did not affect the activity of γ -ECS as for both treatments and organs, this enzyme presented similar levels of activity to those registered for the untreated plants.

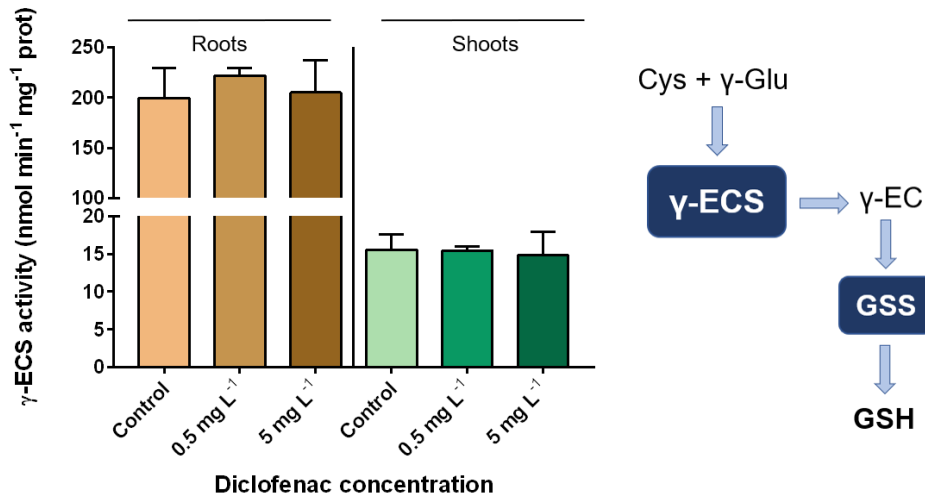


Figure 17. γ -ECS activity levels (left) and function (right) in plants treated with increasing diclofenac concentrations. Values presented are mean \pm SD. * above bars represent significant differences from the control at * $p \leq 0.05$, ** $p \leq 0.01$, *** $p \leq 0.001$, **** $p \leq 0.0001$.

GR activity suffered a dose-dependent increase in the roots with the exposure to DCF (Figure 18), as a dosage of 0.5 mg L^{-1} increased its activity levels by 1.3-fold, while the exposure to a concentration ten times higher caused an increase of 1.95-fold. Comparing both situations, it was also possible to see a 1.5-fold increase in GR activity in the most concentrated situation. In shoots, only with the 0.5 mg L^{-1} situation it was possible to detect a significant 1.87-fold rise in GR activity.

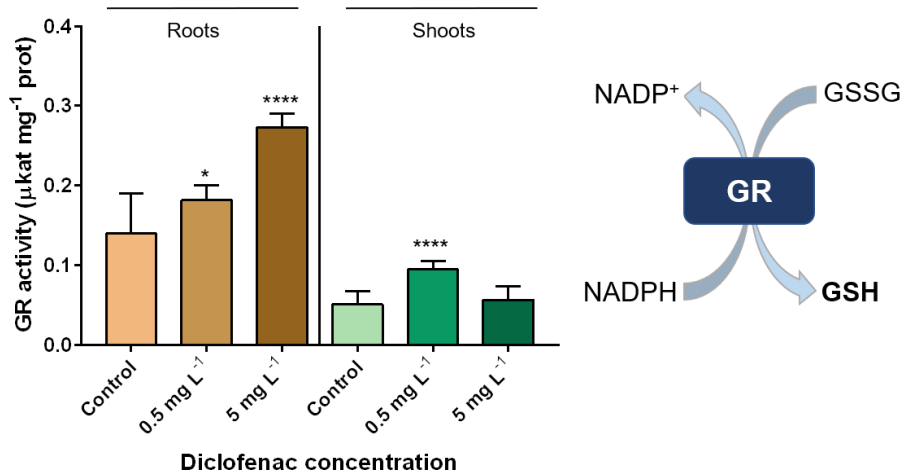


Figure 18. GR activity levels (left) and function (right) in plants treated with increasing diclofenac concentrations. Values presented are mean ± SD. * above bars represent significant differences from the control at * p ≤ 0.05, ** p ≤ 0.01, *** p ≤ 0.001, **** p ≤ 0.0001.

Lastly, GST activity (Figure 19) was not severely affected in the aerial portion, registering only a slight decrease (1.42-fold) with the lower DCF concentration, but in roots, the first contact point of the plant with DCF, a different pattern emerged. Here, GST activity increased with the increase in concentration supplied, showing 1.35- and 2.5-fold increases with the increasing dosage. Between both situations it was possible to see a 1.85-fold rise of GST activity levels with the most concentrated treatment.

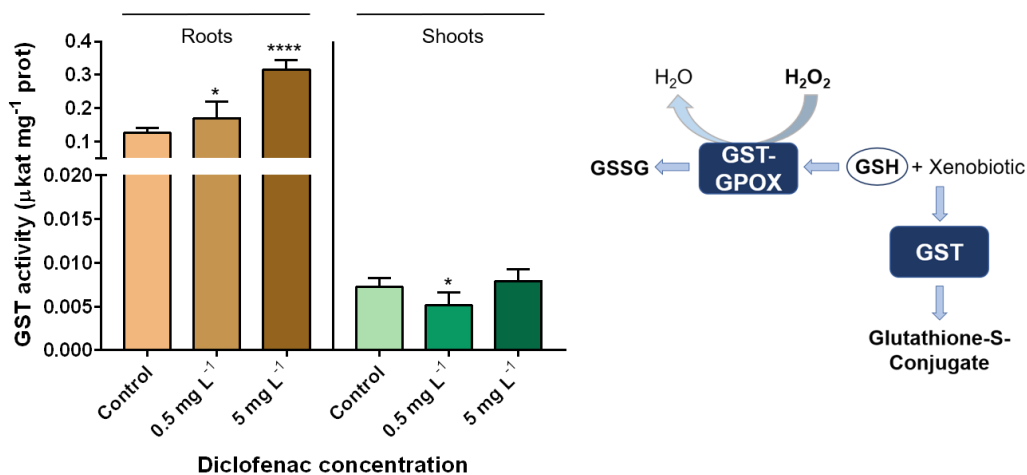


Figure 19. GST activity levels (left) and function (right) in plants treated with increasing diclofenac concentrations. Values presented are mean ± SD. * above bars represent significant differences from the control at * p ≤ 0.05, ** p ≤ 0.01, *** p ≤ 0.001, **** p ≤ 0.0001.

To better interpret these differences in GST activity, a native polyacrylamide gel electrophoresis analysis was carried out (Figure 20), by loading 40 µg of soluble proteins in each well to guarantee that any differences observed in the gel were not a result of different amounts of protein being loaded in the different lanes. The results obtained fall in accordance to the ones observed by the spectrophotometric assay, with a very

noticeable increase in intensity being observed in the lane corresponding to the 5 mg L⁻¹ condition in the roots, accompanied by new bands that were not detected in the untreated and the 0.5 mg L⁻¹ lanes. Curiously, the same pattern occurs in the shoots of these plants, as very similar intensities are observed between the untreated plants and those treated with 0.5 mg L⁻¹ DCF, while bands in the last lane appear to be more intense than the previous ones, even when no different activity levels were detected spectrophotometrically, although a slight tendency for this enzyme's activity to increase could be noticed (Figure 19).

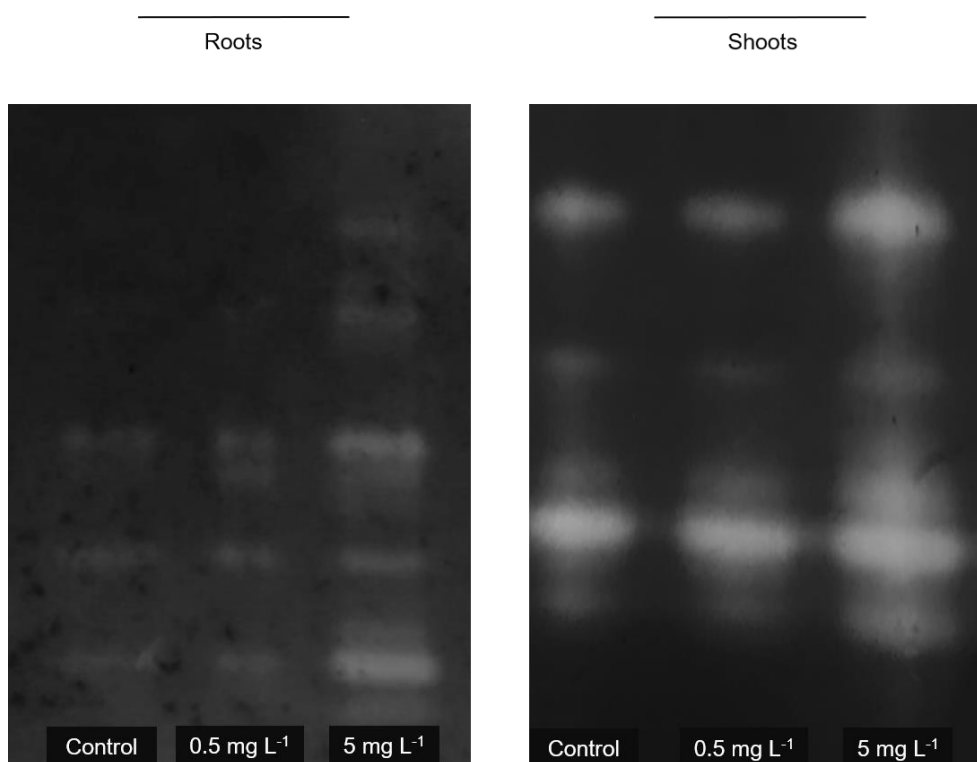


Figure 20. Typical results of a native polyacrylamide gel electrophoresis analysis of tomato GST, disclosing GST activity in plants treated with increasing diclofenac concentrations (40 µg of soluble proteins were loaded in each lane).

3.4. Effects of increasing diclofenac concentrations on the transcript accumulation of several AOX enzymes

3.4.1. Effects of increasing diclofenac concentrations on the transcript accumulation of GRcyt, γ-ECS and GSTU genes

After quantification and quality assessment (Figure 21) of the extracted RNA, a semi-quantitative RT-PCR analysis (Figure 22) permitted a general understanding of how DCF interfered with transcript accumulation of some genes related to the enzymes described before. The RNA preparations used for RT-PCR from shoots and roots of the tomato plants used revealed to be in good quality, considering the high definition of the

rRNA bands, with no smears related to its degradation being detected along the lanes and with no visible contamination by genomic DNA (Figure 21).

Cytosolic GR (GR_{cyt}) mRNA suffered no changes in its accumulation as a result of DCF exposure in either situation and organ analyzed (Figure 22). DCF treatment induced a differential γ -ECS transcript accumulation, as a slight increase was observed for this mRNA in roots treated with 5 mg L⁻¹, but in shoots of these plants, there was a constant expression pattern independently of the increasing concentrations used. Lastly, both DCF doses induced the accumulation of GSTU transcripts in the aerial portion of the plant, but a possible hormesis was seen in the roots of these plants, as an induction was observed for the lowest dosage, but similar-to-control levels were found after treatment with 5 mg L⁻¹ DCF.

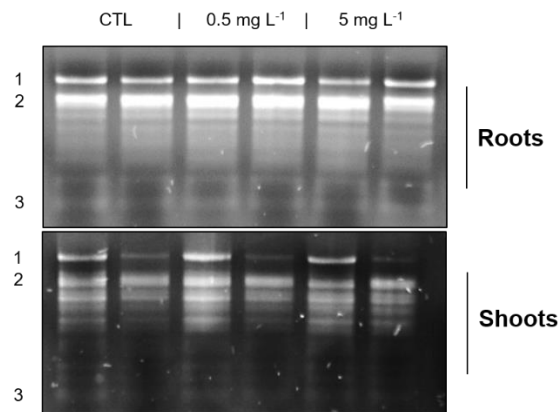


Figure 21. 0.8% (w/v) agarose gel analysis of the total RNA extracted from *S. lycopersicum* plants treated with increasing diclofenac concentrations. 1. 28S rRNA; 2. 18S rRNA; 3. 5S + tRNAs.

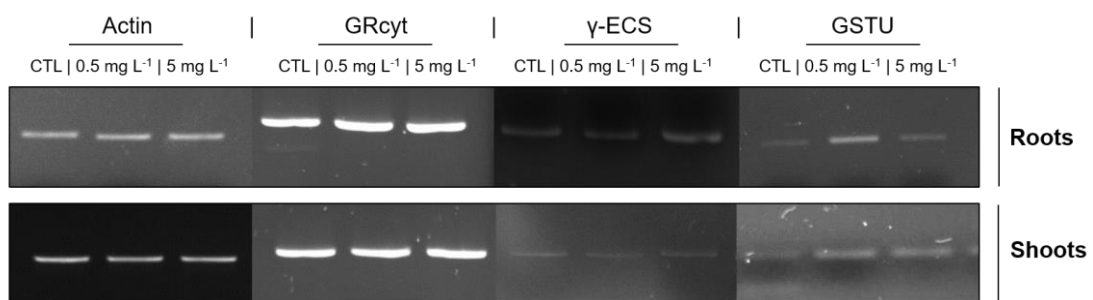


Figure 22. Typical results for GR_{cyt}, γ -ECS and GSTU semi-quantitative RT-PCR analysis by 1% (w/v) agarose gel electrophoresis in *S. lycopersicum* plants treated with increasing diclofenac concentrations.

Regarding the plastidial GR (GR_{chl}), several optimizations from the presented methodology were performed, either within the PCR program, or cDNA template and respective amount but at the moment, no valid amplicons were detected.

3.4.2. Effects of increasing diclofenac concentrations on the transcript accumulation of *SIGSTs*

For the RT-qPCR analysis of different *SIGSTs* after exposure to DCF, the relative transcript level for the untreated situation for each gene was considered as 1, allowing to associate an x-fold increase or decrease in transcript accumulation after the treatment (Figure 23).

For plants treated with 0.5 mg L⁻¹ DCF, it was possible to verify a slight increase in the transcript levels of *GSTF5* in roots, although no significant induction for any *GSTF* gene was detected. Also, roots in this treatment condition presented a 1.67-fold reduction in transcript accumulation for *GSTF3*. In shoots, while *GSTF3*, *GSTF4* and *GSTF5* presented constant mRNA levels, a 3.7-fold decrease in the transcripts of *GSTF1* and a 1.5-fold increase regarding *GSTF2* were recorded. For the other treatment, there was a sharp up-regulation of *GSTF4* and *GSTF5*, with this increment amounting to 4.4- and 4.8-fold in roots and 2- and 1.35-fold in shoots, respectively. Additionally, a 2-fold reduction was observed regarding transcript levels of *GSTF2* in shoots in this situation, while down-regulations of 10-, 2.5- and 1.67-fold were detected for *GSTF1*, *GSTF2* and *GSTF3* in the roots.

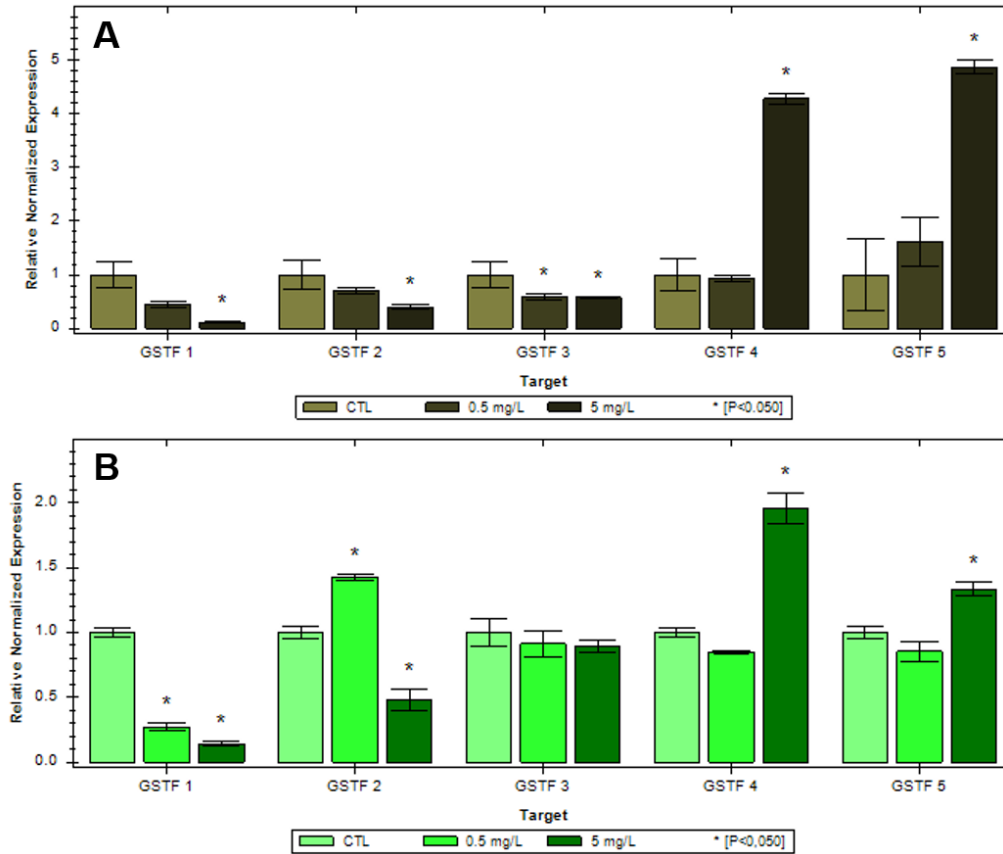


Figure 23. Transcript levels of tomato *GSTF* genes in roots (A) and shoots (B) of tomato plants subjected to increasing diclofenac concentrations. Data were normalized using the tomato actin and ubiquitin gene as internal control and the relative transcript level in the control samples was arbitrarily considered as one for each gene. * above bars represent significant differences from the control at $p \leq 0.05$.

4. Discussion

4.1. Diclofenac and plants' growth and development

As the amount of DCF in both aquatic and terrestrial ecosystems increases, a higher possibility of it becoming in contact with plant-based systems materializes. In this sense, it is important to evaluate how plants can be affected in their development and yield throughout every stage of their lifecycle. Regarding the early stages of plant development, there are some parameters that are very commonly used to assess the phytotoxic potential of different compounds, which include the study of seed germination and early seedling growth (Gong et al., 2001).

To evaluate these parameters, tomato seeds were germinated under contaminated conditions and after ten days of growth, the effects of DCF were examined, evidencing that contamination with DCF had no effect in the germination process, as a 100% germination rate was found for every tested concentration. The fresh weight of the entire plantlet was also not affected by DCF exposure, as biomass remained constant between the different growth conditions. Additionally, no negative effect was found in the elongation of the aerial portion, but roots suffered from exposure to this contaminant, as those that contacted with 10 mg L^{-1} were about two-thirds the size of roots of the untreated seedlings. This decrease in root length can be explained by the fact that they present the first line of contact between the plant and the contaminant and should, therefore, be more affected by its respective toxicity. Several other studies document that regarding early development, roots seem to be the most sensitive portion of the plant to different substances, while inhibition of shoot growth is less common and almost always much less severe than that reported for roots (Sresty and Madhava Rao, 1999; An et al., 2009; Pan and Chu, 2016), although Jin et al. (2009) found a higher inhibition in shoots than in roots after exposure to some pharmaceuticals. The lack of sensitivity in early shoot growth presented in this work is therefore an unsurprising result and may be a consequence of the discharge of nutrients from the cotyledons or endosperm counteracting a possible toxic effect (Chen et al., 2011).

A common occurrence through different researches with different types of pollutants (such as other pharmaceuticals or heavy metals) is the absence of germination inhibition, with effects normally being observed after exposure to very high and toxic dosages (Kösesakal and Ünal, 2012; Pan and Chu, 2016; Soares et al., 2016; Bartrons and Peñuelas, 2017). This also falls in line with what was observed in this work, as germination had a total success rate in every situation. Having this in mind, an arising hypothesis is that DCF might be unable to penetrate the seed coat, which can serve as

a barrier protecting the embryogenic tissues (An et al., 2009; Akinci and Akinci, 2010; Pan and Chu, 2016) from its toxicity, and therefore negative effects would only be noticed at a later development stage when this barrier is naturally broken, shown by the inhibition in root growth.

A similar approach was performed with grown plants, where untreated seedlings grew for five weeks in contaminated conditions. In this assay, as the intention was to observe a response and better understand how tomato plants can react to this exposure, the two lowest concentrations were discarded, with the two highest remaining. However, there was a possibility that without the protection supplied by the seed coat and the nutrients released from the cotyledons and endosperm, the highest concentration could be too damaging to the plant, hindering the development of the subsequent assays. In this sense, and also to approximate the other selected situation to the currently increasing environmental levels, both these concentrations were halved and the remainder of this work was performed utilizing 0.5 mg L⁻¹ and 5 mg L⁻¹ DCF concentrations.

Here, the observed pattern contrasted with the germination assay, as the most affected portion of the plants were the shoots, while roots remained mostly unaffected. The root/shoot biomass ratio is an indicator of the overall health of plants, with an increase or decrease possibly signifying differences in the plant health status. Tomato plants treated with 5 mg L⁻¹ DCF had this parameter increased due to the lower biomass of the shoots, while no effect was observed in roots. If the opposite occurred, it could be a sign of a healthier plant, as it would improve the absorption of water and nutrients, but in this case it is possible to infer that the massive change observed is a sign for unhealthy plants. Pierattini et al. (2018) documented similar results in poplar, but an exact opposite result was documented for radish, as Schmidt and Redshaw (2015) reported a decrease in the root/shoot ratio due to a lower root biomass. Both authors utilized the same final DCF concentration (1 mg L⁻¹), indicating that these differences might be dependent on the plant species and not only on the contaminant. Taking in account the results from the germination assay, a possibility to be considered is that in the early exposure of these plantlets to DCF, the roots were the first to suffer, leading to negative effects in their growth, with this hypothesis being reinforced by the fact that, even though not statistically significant, there was a clear tendency for roots in 5 mg L⁻¹ DCF to be smaller than their untreated and less contaminated counterparts. In turn, the plant might have reacted by allocating more resources towards root development at the cost of the length and biomass of their aerial portion, since roots are the main source of nutrient uptake and a healthy root system is key to a healthy plant.

Additionally, for the same condition, treated roots seem to have their water absorption affected, as they present significantly lower water content. Effects of DCF or other PPCPs on the water uptake ability of plants has yet not been documented but it is a common occurrence in plants subjected to heavy metal exposure (Rucińska-Sobkowiak, 2016). Furthermore, in several abiotic stresses, the formation of excess ROS appears to mediate the reduction of hydraulic conductivity in roots, as well as inhibit the normal functions of water channels (Luu and Maurel, 2005), so it is unclear if this reduction in water content is a direct consequence of a DCF interaction or a secondary result of DCF-induced oxidative stress. Regardless, this effect can also have taken a part in the performance reduction of the aerial portion of the plants, as when subjected to water stress conditions, these organisms can allocate a larger amount of photosynthates towards the roots, at the cost of shoot length and biomass. This allows the plant to improve its uptake ability, while reducing water loss with a smaller leaf area (Li et al., 1994).

As exposure to an already high concentration (0.5 mg L^{-1}) did not present any sign of toxicity and exposure to a very high (5 mg L^{-1}) diminished shoot performance but kept the root system relatively efficient and biometrically similar to the untreated roots, while no differences were observed in flower and fruit intensity, the preliminary suggestion taken from the biometrical stage of this research is that *S. lycopersicum* plants should not be affected in terms of yield if cultivated in DCF-contaminated soils, as these do not yet reach the same DCF levels as those used in this work. Nonetheless, to further verify this claim it is necessary to run similar tests in different soil types to verify the influence of some factors associated with different soils, (e.g. pH, temperature, contaminant bioavailability or organic matter) in the obtained results (Walker et al., 1989; Streibig et al., 2006; Karnjanapiboonwong et al., 2011).

4.2. Diclofenac-induced oxidative stress

The presence of higher ROS levels, accompanied by an increased activity of antioxidant defenses, is a common phenomenon in plants exposed to DCF or other PPCPs (Bartha et al., 2014; Christou et al., 2016; Sun et al., 2017; Pierattini et al., 2018) and organic compounds (Teixeira et al., 2011; de Sousa et al., 2013). In this sense, as a way to see if this contaminant can induce similar effects in tomato plants, the oxidative state of these plants was followed by the determination of ROS levels ($\text{O}_2^{\cdot-}$ and H_2O_2), as well as by monitoring LPO, a possible subsequent reaction.

Here, it is observed that the levels of $\text{O}_2^{\cdot-}$ suffered no alteration between different treatment conditions in both tested organs. As this ROS possesses a very short lifetime

and is locally produced, the quantitative determination of $O_2^{\cdot-}$ does not always describe an accurate representation of what is occurring in the plant (Demidchik, 2015), but the noticeable increase in H_2O_2 can be due to a fast dismutation of $O_2^{\cdot-}$, leading to its depletion and therefore lower content. In shoots, the increase in H_2O_2 was accompanied by higher SOD activity, as this enzyme is responsible for $O_2^{\cdot-}$ dismutation to H_2O_2 . In roots, however, the same pattern does not appear, as SOD activity remains constant (in fact, slightly lower, although not statistically significant) after DCF treatment, when H_2O_2 levels increase significantly. While the final concentrations of H_2O_2 are similar in both tissues, its increase, compared to untreated plants, is more pronounced in the roots, which can explain the differential pattern. Since Cu/Zn SOD is considered to be the most abundant SOD type in plants and H_2O_2 is a known inhibitor of both Cu/Zn and Fe SOD (Grune, 2005; Sharma et al., 2012), it is possible that after the SOD-catalyzed dismutation, the content in H_2O_2 surpassed a certain threshold and inhibited the activity of this enzyme, explaining the lower SOD values in roots, while in shoots the increase in peroxide levels was not sufficient for this effect. In fact, overproduction of H_2O_2 , with adjuvant downregulation of SOD activity after exposure to different PhACs, including DCF, has already been documented in roots of *Medicago sativa* L. (Christou et al., 2016).

Overproduction of ROS is usually associated with the occurrence of LPO, affecting several cellular components and disturbing normal physiological processes. LPO consists in several processes leading to the formation of reactive species, such as MDA, which due to its ability to react with TBA and form a colored product, is normally used as a marker for the occurrence of LPO (Gill and Tuteja, 2010). Studies performed in plants subjected to different abiotic stresses, such as metal (Mobin and Khan, 2007) and PhAC (Yan et al., 2016) exposure, as well as salt (Khan and Panda, 2007) and water (Zlatev et al., 2006) stresses, have reported ROS-induced LPO. In this work, it was observed that MDA levels were vastly increased only in roots exposed to 5 mg L^{-1} DCF, which was also the situation that presented the highest increase in ROS content. This correlation indicates that while the amount of overproduced H_2O_2 observed in roots exposed to 0.5 mg L^{-1} and shoots exposed to 5 mg L^{-1} was not sufficient to surpass the antioxidant buffering capacity of tomato plants, the increase occurring in roots subjected to the most concentrated situation was not efficiently dealt with, causing a state of oxidative stress to which the plant was unable to respond properly. Regarding DCF, Christou et al. (2016) has also showed that exposure to this contaminant is related to damages to the membrane integrity of root cells in *M. sativa*, due to an increase in LPO. Curiously, this report also shows increased H_2O_2 levels in the aerial portion but no effect in the MDA content, in accordance with that observed in this work. As roots are the first line of contact

between the plant and the contaminant, it seems that toxicity is slightly confined to this organ, which might also explain the need for the plant to direct resources towards the maintenance of the root system in exchange of shoot performance.

4.3. Uprising of antioxidant defenses against Diclofenac-induced stress

Recently, the role of thiols in a redox network responsible for increasing plant tolerance to several abiotic stresses has become prominent. In this sense, it is accepted that regulation and accumulation of these compounds is heavily correlated with tolerance mechanisms and therefore it has become an important marker for better understanding the tolerance or susceptibility of plants towards different oxidative stress inducers. This group can be divided in two classes: a) protein-bound thiols, such as thioredoxins (Trx) and glutaredoxins (Grx), and b) non-protein thiols, like phytochelatins and GSH (Zagorchev et al., 2013).

Lemna minor L. plants subjected to DCF reacted with the formation of thiol groups (Kummerova et al., 2016), so a similar determination was carried out to understand if a pattern was observable. In the present work, a long-term exposure to DCF was associated with a massive increase in total thiol levels in the roots, while in shoots there was also a slight increase, but it was not deemed as statistically significant. Analyzing the two classes, it is clearly noticed that the vast majority of newly produced thiols, in both organs, relate to the protein-bound group, as the increase was significant for both organs. Within non-protein thiols, GSH is considered a major player in both oxidative stress and xenobiotic detoxification, so the lack of increased GSH content and γ -ECS activity is concordant with the seemingly constant levels of this thiol class in DCF-treated plants. The findings of Soares et al. (2018), after exposing barley plants to a different pharmaceutical (acetaminophen), suggested a similar mechanism of increased thiol contents merely in the roots of treated plants, with protein-bound thiols being the main cause behind that increase.

Per example, Trx and Grx are important components of the protein-bound class, as they are of high significance in the maintenance of a normal redox state and a higher induction is usually associated with increased ROS levels (Grant, 2001; Vieira dos Santos and Rey, 2006). These proteins possess oxidoreductase activity and with the action of Trx-dependent peroxidases (peroxiredoxins) can intervene in the scavenging of H_2O_2 and in other response mechanisms via protein-protein interactions (Zagorchev et al., 2013; Sevilla et al., 2015).

Since H_2O_2 levels significantly increased in every situation, except in shoots of plants exposed to 0.5 mg L^{-1} (and even then, a slight increase was noticed), there might be a correlation between these two parameters. With this in mind, the increase in protein-bound thiols might be due to an investment of these plants in the thiol redox network for H_2O_2 scavenging, which was sufficiently effective for most situations but unable to prevent LPO in roots subjected to the highest DCF concentration.

In general, soluble protein content presented a positive response to DCF, since this parameter was increased in both situations for the roots and with the less concentrated DCF treatment for the aerial portion of the plants, coinciding with the increase in protein-bound thiols. However, for shoots treated with 5 mg L^{-1} DCF, protein levels were lower than those of the control, while the content in protein-bound thiols increased, indicating that some protein degradation might be occurring after exposure to this contaminant. A possibility might be correlated with the increasing ROS levels in this situation, as it is known that high H_2O_2 levels can significantly interact with enzymes of the Calvin Cycle, such as RuBisCO, (He et al., 2004; Zhou et al., 2006; Sharma et al., 2012), which accounts for 30 to 50% of total soluble proteins in C3 leaves (Erb and Zarzycki, 2018) and whose content and activity has been shown to severely decrease after exposure of a Solanaceae to another organic compound, coincident with the increased H_2O_2 levels (Teixeira et al., 2011; de Sousa et al., 2017). Within this research group, a simultaneous investigation studied photosynthetic parameters in the same plants which were grown for the assays developed in this dissertation and resulting unpublished data showed decreased RuBisCO content in plants exposed to 5 mg L^{-1} of DCF, granting more validity towards this hypothesis.

The maintenance of the normal plant status is not on the sole basis of a single process or molecule and several enzymes or metabolites can act directly or indirectly, alone or in an interactive network in order to establish a redox balance in plants subjected to different environmental stresses. One example of this is proline, an amino acid that can act in several ways to protect the plant from stress-induced damage, working as, per example, an osmolyte, a metal chelator, as well as a signaling and antioxidant molecule (Hayat et al., 2012; Liang et al., 2013).

Increased proline levels in response to higher H_2O_2 content is a widely acknowledged phenomenon, caused by increased biosynthesis of this amino acid, as well as H_2O_2 -mediated inhibition of enzymes related to proline degradation (Yang et al., 2009; Rejeb et al., 2015). In this sense, the results obtained here seem coherent, as overproduction of H_2O_2 in roots and shoots of *S. lycopersicum* plants treated with 5 mg L^{-1} DCF was met with a responsive rise in proline content. Also, taking in account that a

described function of proline is the stabilization of membranes (Hayat et al., 2012), it could be expected that when signs of LPO arise, the plant might respond with an increase in proline content (Dhir et al., 2004; de Sousa et al., 2013), which was also observed in the present work, as roots subjected to 5 mg L⁻¹ presented increased MDA content, accompanied by a significant increment in total proline content.

To add to this, the H₂O₂-mediated degradation of Calvin cycle enzymes described above is associated to a reduction of NADP⁺ levels, in turn leading to a more likely production of ¹O₂ (Liang et al., 2013). Since biosynthesis of proline is directly related to the production of NADP⁺, the increase in the amount of this amino acid might also be acting towards compensating a possible H₂O₂-caused NADP⁺ depletion and minimizing future ROS production, acting protectively and preemptively.

Shoots of plants treated with the lowest concentration also show significantly higher levels of proline, even though no overproduction of ROS or presence of LPO were detected. It is however possible that the slightly higher H₂O₂ levels might have been sufficient to induce a preventive proline accumulation. Additionally, roots of these plants presented a significant increase in ROS content, which might have led to a systemic response and consequent proline accumulation in shoots. Regarding these roots, a slight increase in free proline was also detected, but it was not regarded as significant. This pattern was already seen in plants exposed to acetaminophen, since Soares et al. (2018) also documented higher H₂O₂ levels in roots, while no significant accumulation was found in shoots of barley but a significant increase in proline content was reported merely in the shoots, indicating a possible organ-specific differential response to xenobiotics.

Such as Soares et al. (2018), Teixeira et al. (2011) has also reported the importance of proline in plants' defense against organic contaminants but regarding DCF, only Christou et al. (2016) tried to establish a relation between contamination and proline levels in alfalfa, showing a clear decrease in proline after exposure. This discrepancy might be due to a differential response based both on plant species and DCF concentration.

4.4. Inhibition of ROS-scavenging enzymes after DCF exposure

Having covered how *S. lycopersicum* plants focus on a thiol-based redox network and induction of proline levels to counteract the unbalance of their redox status, it is still a reality that H₂O₂ levels remain significantly above the control, except for one situation, where a slight increase is also present. Additionally, the occurrence of LPO in roots exposed to 5 mg L⁻¹ DCF is a clear sign that those defenses are not sufficient to surpass

ROS overproduction and adjuvant damages to the integrity of the plant. Usually high levels of H_2O_2 are efficiently scavenged through CAT action or through the AsA-GSH cycle but it seems that DCF exposure hindered the ability of both these enzymes to properly fulfill their functions.

CAT is an important AOX enzyme, differing from APX for not being dependent on a substrate (such as AsA) to act, but in turn requiring much higher levels of H_2O_2 to be considered efficient (Sharma et al., 2012). To add to this, some authors consider that due to the high relevance of CAT in peroxisomes, and with a very scarce activity in chloroplasts and mitochondria where most $O_2^{\cdot-}$ is produced and converted to H_2O_2 , CAT might not be of utmost importance in dealing with stress-induced overproduction of ROS (Halliwell, 2006). Accordingly, the present work has detected that after exposure to DCF, CAT activity has significantly declined for both treatment conditions in roots and shoots, once again contrasting with the findings of Christou et al. (2016). Curiously, while in this work *S. lycopersicum* upregulated the non-enzymatic AOX proline and downregulated enzymatic AOX, Christou et al. (2016) observed the exact opposite in *M. sativa*, indicating a plant-specific or dose-based differential response mechanism. Using acetaminophen, a NSAID like DCF, both Bartha et al. (2010) and Soares et al. (2018) reported a significant reduction in CAT activity levels in *Brassica juncea* L. and *Hordeum vulgare* L., respectively, further showing how CAT might not be a reliable strategy for ROS scavenging in response to these types of contaminants.

Regarding APX, in contrast to what was observed in this work, roots of both poplar (Pierattini et al., 2018) and *Typha latifolia* L. (Bartha et al., 2014) seem to up-regulate the activity of this enzyme upon immediate contact with DCF, but in poplar roots, APX activity tends to decrease as exposure continues over-time, actually ending lower than that of untreated plants. In this sense, it might be of interest to determine AOX activity in plants right after being subjected to DCF and during the following hours to understand the over-time AOX mechanics of *S. lycopersicum* plants.

A possible scenario to explain the reduction of APX activity in treated roots resides on the basis of the AsA-GSH cycle. By analyzing γ -ECS activity and total GSH values it is possible to notice that the plants were not focusing on GSH biosynthesis and that total GSH levels were slightly decreasing with the increased GST activity. If tomato plants were focused on using GSH for GST-mediated conjugation, they were likely to compensate by inhibiting other GSH-mediated activities, such as the ROS-scavenging cycle. Coincidentally, the over-time inhibition of APX mentioned above in poplar was also overlapped with an over-time induction of GST activity. This pattern was similarly

observed in roots of *B. juncea* exposed to acetaminophen, as APX activity was inhibited, while GST presented higher activity in GSH conjugation (Bartha et al., 2010).

Higher ROS production also occurs in shoots of 5 mg L⁻¹ DCF-treated plants and in this case no overlapping GST activity is presented, so a different mechanism might also be causing APX inhibition, but it seems coherent with results obtained by Pierattini et al. (2018), as stems of poplar presented an initial drastic reduction and an over-time stabilization of APX activity, once again showing the exposure time-based dynamics of the AOX mechanism. Here, it might also be of interest to measure AsA levels in these DCF-exposed plants to determine if the treatment with DCF is interfering with the AsA-GSH cycle or if this inhibition in APX activity is due to other influences, such as a higher focus on other redox mechanisms.

4.5. Glutathione metabolism in response to Diclofenac exposure

The importance of GSH in the normal physiological processes of plants is undeniable, as this molecule is involved in a vast range of processes, but in this work the main properties to be highlighted are GSH's ability to participate in ROS-scavenging mechanisms and in the detoxification of toxic substances. GSH biosynthesis was evaluated by analyzing γ -ECS, as this enzyme is considered to be the limiting player in this process (Hossain et al., 2017) and results show no increased or decreased γ -ECS activity after 0.5 mg L⁻¹ and 5 mg L⁻¹ DCF treatment in both roots and shoots. Since no effect has been shown on the enzymatic synthesis of GSH, it is possible to infer that DCF exposure does not influence the plant in continuously producing more GSH, but this does not mean that GSH is not heavily involved in the plants' response to this treatment, as validated by analyzing other GSH-related parameters.

Regarding total GSH levels, the results demonstrate that after exposure to 0.5 mg L⁻¹ DCF, tomato plants show a lower content in GSH in both organs, while exposure to 5 mg L⁻¹ causes a slight (but not statistically significant) reduction in root GSH but no effect in the aerial portion of these plants. On the basis of the "green liver", one pillar of this research was GSH being behind DCF detoxification and these results do seem to confirm that hypothesis. Decreased total GSH levels for roots of both treatments align with the increased activity of GST observed spectrophotometrically, indicating that the missing GSH might have been conjugated to DCF, as the quantification method only measures free GSH. In this sense, it seems likely that *S. lycopersicum* plants are focused on the GST-mediated GSH-DCF conjugation, with the roots being the core of this detoxification, showing that most of the DCF metabolism mechanism is confined to the

first contact point with the plant. The prominent role of GST in catalyzing the conjugation of GSH to DCF has been similarly documented in both poplar (Pierattini et al., 2018) and *T. latifolia* (Bartha et al., 2014), but those authors also reported increased GST activity in shoots of the treated plants, indicating that while the root system of *S. lycopersicum* is possibly sufficient to quickly metabolize DCF, in other plant systems, some residual DCF might be translocated towards the shoots where the conjugation process also occurs. In fact, both studies report a much lower DCF concentration in the aerial portion of the plant, even reaching levels lower than the limit of detection in poplar, further showing how DCF metabolism is preferentially a root-specific process, where DCF metabolites were detected at higher concentrations. The presence of GSH conjugates has also been reported for acetaminophen (Bartha et al., 2010) but the same did not occur in plants exposed to ibuprofen (He et al., 2017), indicating differential detoxification patterns for different compounds within the NSAID class.

The utilization of other GST substrates (e.g. DCNB or fluorodifen) can influence the observed activity pattern, since different isoenzymes can differ in their affinity to distinct substrates (Schröder et al., 1997), but CDNB is considered to be a general substrate suitable for a broad range of GST isoenzymes, allowing for a valid representation of the general GST behavior.

Additionally, the plants' effort to present higher levels of reduced GSH, in detriment of the oxidized form, is noticeable as decreasing GSSG content in roots of both situations was observed. Since there is a marked decrease in APX activity, it is clear that GR is not acting as a part of the AsA-GSH AOX cycle and the reduced GSH obtained should be meant for other purposes. Coincidentally, GR activity levels in roots also increase in a dose-dependent manner, perfectly aligning with the alterations in GST activity. Therefore, it seems that as the DCF concentration increases, so does the occurrence of conjugates and the need of more reduced GSH. In shoots, GST activity remains constant or even below untreated levels, further indicating how DCF conjugation is mostly happening in the roots of treated plants, while little to no DCF is being metabolized in the aerial portion. The function of some GSTs as GPOX must also be considered as a defense mechanism against increased ROS (Wagner et al., 2002), although the reduced total GSH levels due to decreasing GSSG seem to indicate that most if not all GST activity is related to a conjugation context.

Curiously, GR activity is also increased in shoots treated with 0.5 mg L^{-1} , but no GSH-mediated AOX activity is detected, as well as no observable increase in ROS or membrane damage. Taking in mind that translocation of GSH from shoots to reinforce the root system is a common response of plants exposed to contaminants, such as heavy

metals (Zhang et al., 2016), a similar scenario might be occurring in these plants. Analyzing combined total GSH values for roots and shoots of plants in this treatment, it becomes clear that there is a severely lower GSH content in comparison to the other two situations. It is a possibility that following GST-mediated conjugation, the depletion of root GSH had to be compensated by transporting GSH from the shoots, hence the need of the aerial portion of the plant to reduce GSH. The same pattern does not occur in the roots treated with the highest concentration, but a slight reduction in total GSH levels is observed. As observed for different enzymes in the work developed by Pierattini et al. (2018), it is possible that there is a temporal response to DCF exposure. In this sense, after treating roots with 5 mg L⁻¹, a quicker depletion of GSH might have induced γ -ECS (as suggested by the increase in γ -ECS mRNA accumulation) to produce more GSH and when GSH values were sufficient for subsequent GST-mediated conjugation, enzymatic activity stabilized to control levels, suggesting a possible post-translational regulation of γ -ECS. Nonetheless, the conjunction of activity patterns of the different enzymes with GSH levels seem to indicate that, if possible, tomato plants after being exposed to DCF prefer to invest in the regeneration of existing GSH, rather than focusing on its biosynthesis.

Also, the transcription pattern for the cytosolic GR remains similar between treatment conditions, although different activity levels were detected spectrophotometrically. Unfortunately, no valid transcript accumulation analysis was successfully carried out for the plastidial GR, but a future determination might provide more insight if this plastidial form is the main responsible for different activity levels or if a post-transcriptional regulation of the cytosolic isoform explains a differential pattern between transcript accumulation and enzymatic activity.

4.6. Role of specific GSTs in the response of tomato plants to Diclofenac

GSTs are associated with different protective functions, such as the response to oxidative stress or the conjugation and detoxification of different xenobiotics. The peroxidase property of GST is usually more associated with the GSTT class, while GSTFs and GSTUs are commonly considered in a conjugation context (Edwards and Dixon, 2005). As DCF-GSH conjugates have already been described for other species (Schröder et al., 2013; Bartha et al., 2014), the presented results point to a contaminant-specific detoxification pattern that falls in accordance with the “green liver” concept, highlighting the importance of GST in the response of plants to DCF contamination. However, only general data has been reported regarding the role of this enzyme, with no

relevant information about the specific mechanisms triggered by DCF on different GST isoenzymes.

Csiszar et al. (2014) described some putative *S. lycopersicum* genes encoding GSTs from the phi and tau class, but the characterization of this family still remains an underdeveloped topic. However, utilizing the sequences and primers described by this author, along the work previously developed within the research group (Pinto, 2017), it was possible to evaluate the transcript accumulation pattern of the five different *SIGSTF* genes after exposure to DCF. Although the tau class could also be related to DCF detoxification, a combined total of 56 putative genes have been described, which would not allow for a timely design of specific primers and respective analysis. Therefore, a semi-quantitative RT-PCR was performed to assess general transcript accumulation for this class, with results pointing to a noticeable increase for every situation except in roots treated with 5 mg L⁻¹ DCF.

Regarding the phi class, it is clear that *GSTF4* and *GSTF5* are the main genes responsive to the DCF treatment, as there was a sudden and severe increment in the transcript accumulation of both these genes in response to a 5 mg L⁻¹ treatment. Also, it appears that induction of these genes was correlated with a down-regulation of *GSTF1*, *GSTF2* and *GSTF3*, indicating a compensatory mechanism between different GSTs from the phi class. This increment occurred in both organs, but it is observable that the major response happened in the roots, since the percentage increase in comparison to the untreated situation is much more accentuated in this organ, once again showing how most of the detoxification process was confined to the roots. After treatment with 0.5 mg L⁻¹ DCF, the induction of GSTF transcripts in the roots did not seem to be of major relevance, with only a slight increase being observed in *GSTF5* mRNA, but there is a visible increase in the accumulation for GSTU mRNA, while in roots treated with 5 mg L⁻¹, the inverse occurred, as the increase in the transcripts of the aforementioned GSTFs was not accompanied by more transcripts of GSTUs. In shoots, the induction of GSTUs seems to occur for both treatment situations, whereas the phi class seems to only be up-regulated for the highest DCF concentration. The non-induced activity of GST in the shoots of treated plants, as well as the fact that GSH seems not to be utilized for conjugation purposes in shoots of plants exposed to 5 mg L⁻¹ DCF is not concordant with the increase in transcript accumulation in the aerial portion of the plants. In this sense, it is possible that DCF exposure might result in a systemic response, leading to triggered defenses in tissues distant from the original stress site, as reported by Pierattini et al. (2018) and is common with other types of abiotic stress, as well as pathogen and

wounding stresses, through ROS (in this case, H₂O₂ produced in roots) or calcium signaling, per example (Choi et al., 2014; Zhu, 2016).

Analyzing these results as a whole comes the suggestion that while the presence of DCF is sufficient to stimulate the tau class, GSTFs appear to require a different stimulus. In fact, it is possible that these genes are induced by a state of oxidative stress, rather than the contaminant itself, since higher ROS levels are associated with the plants grown in this concentration of DCF. Even in roots subjected to the lowest concentration, with a less severe increase in ROS it is possible to observe a subtle increase in the transcripts of *GSTF5*, while the same does not occur in the shoots of the same plants, where ROS levels remain constant. Similarly, Csiszar et al. (2014) describes both *GSTF4* and *GSTF5* as orthologues of the *A. thaliana* *GSTF8*, which is known to be induced by high H₂O₂ content (Moons, 2005; Thatcher et al., 2007). The similar-to-control levels of GSTU transcripts in the roots where GSTF genes were significantly over-expressed might indicate that there is no synergistic effect between both classes. In shoots *GSTF* induction was much lower than in the roots, and GSTU presented higher-than-control transcript levels, indicating a possible regulation based on the transcript amount of each class. In this sense, it is possible that early detoxification process in tomato plants after exposure to DCF is regulated by the tau class and if contamination levels reach a threshold where the production of ROS is sufficiently higher, then the plant triggers the action of GSTFs and down-regulates GSTU transcription.

4.7. *S. lycopersicum* plants in DCF-contaminated soils

To define the role of this crop in a contaminated environment, it was pertinent to assess how these plants can influence the degradation of DCF on contaminated soils. A striking characteristic of this study was the fact that little to no DCF was able to be detected shortly after the first irrigation, indicating that the vermiculite:perlite mixture utilized as a root support possessed a high affinity towards this contaminant. This effect was not as notorious in the following irrigations because the artificial substrate was not dry as it was at the moment of the first supply, leading to a lower DCF adsorption. The differential pattern of DCF levels in the “with-plants” and “no-plants” situation is of high importance to verify if the presence of these plants is associated to a quicker elimination of DCF and this becomes clear by observing that when DCF was supplied in a tray containing plants, there was a rapid depletion of this contaminant in the medium, while in the absence of plants, the DCF retained in the artificial substrate is released back into the medium, further empowering the notion that DCF was promptly absorbed by the roots of the tomato plants, as was already described for other species (Bartha et al., 2014;

Pierattini et al., 2018). Nevertheless, a more sensitive method able to measure quantitatively and qualitatively the DCF-related metabolites in the tomato plants' tissues could be of use to better understand this mechanism. Still, taking in account that GSH is being utilized and GSTs associated with xenobiotic conjugation processes are highly expressed in roots, the obtained results do suggest that DCF is indeed being absorbed by the plant, triggering a detoxification mechanism mediated by GSTs.

Additionally, to determine if cultivation of tomato plants in DCF-contaminated soils can be hazardous to other beings, the edible part of these plants was used for DCF contamination, but as the detoxification process seem to be occurring mostly in the roots of treated plants, it seemed unlikely that DCF would be translocated to the aerial portion and much less to the fruits. In fact, and after quantification, no fruit presented DCF levels above the limit of quantification ($3 \mu\text{g g}^{-1}$). As mentioned, it is quite probable that this value is very close to zero (or is in fact zero), but even if one takes in consideration that $3 \mu\text{g}$ are present in a gram of every tomato and that on average a human being consumes 0.83 g kg^{-1} of tomatoes daily (National Center for Environmental Assessments, 2011), the DCF consumption rate would be of about $2.49 \mu\text{g kg}^{-1}$ per day, a value much lower than the maximum acceptable daily intake of $67 \mu\text{g kg}^{-1}$ (Bruce et al., 2010). In this sense, when plants are constantly supplied with DCF every three to four days in a concentration hundreds of times superior to those found in the environment, even accounting for the worst-case scenario (by considering an accumulation of $3 \mu\text{g g}^{-1}$), it is not sufficient to be considered dangerous to human health.

Overall, it was possible to observe that, in the current environmental context, tomato plants are not only capable of being cultivated in DCF-contaminated soils without loss of yield or portraying any danger to human health, but this crop also appears to have positive consequences in these environments, since the presented results point towards a large influence of these plants on a quick depletion of DCF from the soil, associated with a fast detoxification mechanism.

5. Concluding Remarks

At the end of this research, the results obtained are able to fill a large gap in the knowledge about how agronomically important crops are not only able to withstand an emerging problem but might also take part in solving it by removing DCF from their surrounding medium.

Regarding the harmful effects induced by this contaminant, it was observable that exposure to DCF was associated with a higher production of ROS and when in high enough concentrations, this redox imbalance compromised the integrity of plants' membranes due to an increased LPO. To counteract these harmful effects, it was clear that tomato plants invested in the protective role of proline and the thiol-based redox network, while inhibiting the action of enzymatic AOX mechanisms.

To deal with the presence of this contaminant, this work provides results that point to a root-specific detoxification mechanism that is based on the GST-mediated conjugation properties of GSH. Here, this process occurs through an early GSTU-mediated conjugation, whose levels were then down-regulated by the ROS-induced detoxification action of GSTF, indicating a dose-dependent differential detoxification pattern. To date, this was the first research focusing on the role of specific *SIGSTFs* in the response to this contaminant and the results obtained here evidence the importance of *GSTF4* and *GSTF5* in this mechanism, as they were induced for both organs after exposure to high DCF concentrations.

At the current environmental context, DCF contamination does not reach the levels utilized for this work, but it became clear that even in high concentrations this contaminant is not a limiting factor regarding the productivity of tomato plants, even when presenting a lower length and biomass for the aerial portion. Additionally, evaluation of hazardous health prospects and involvement in the DCF elimination shows a clear tendency for the presence of these plants to be associated with a quick depletion of the contaminant, while no dangerous amount of DCF was translocated to the edible fruits even when exposed to very high doses. The overall analysis of these parameters allowed to conclude that in a situation where this crop is exposed to contaminated soils, not only there appears to be no observable negative consequences but may also present positive effects to the surrounding environment.

6. Future Perspectives

While the results obtained within this research offer more insight on the toxicity of DCF in tomato plants, as well as on the response mechanism of this crop in terms of defense and detoxification, there are still some gaps that are expected to be filled in the future of this investigation:

- Utilization of sensitive methods to identify and quantify metabolites resulting from DCF conjugation to further validate the hypothesis discussed in this work;
- Evaluate other forms of AOX defense, such as the non-enzymatic antioxidant AsA (as this molecule could be limiting APX activity or directly acting in ROS scavenging);
- Evaluate the temporal dynamics of plants' defense mechanism, by determining the already studied parameters immediately after DCF exposure and hours after irrigation with DCF-containing medium;
- Analyze specific GSTU genes in DCF detoxification, since this work shows that this family is an early player in this process;
- Silence or overexpression of *SIGSTF4* and/or *SIGSTF5* to highlight the important role of these genes in the defense of tomato plants to DCF.

7. Bibliography

- Acuña V, Ginebreda A, Mor JR, Petrovic M, Sabater S, Sumpter J, Barceló D** (2015) Balancing the health benefits and environmental risks of pharmaceuticals: Diclofenac as an example. *Environ Int* **85**: 327–333
- Aebi H** (1984) Catalase in vitro. *Methods Enzymol* **105**: 121–6
- Ahmad P, Jaleel CA, Salem MA, Nabi G, Sharma S** (2010) Roles of enzymatic and nonenzymatic antioxidants in plants during abiotic stress. *Crit Rev Biotechnol* **30**: 161–175
- Akinci IE, Akinci S** (2010) Effect of chromium toxicity on germination and early seedling growth in melon (*Cucumis melo* L.). *African J Biotechnol* **9**: 4589–4594
- Alscher RG, Erturk N, Heath LS** (2002) Role of superoxide dismutases (SODs) in controlling oxidative stress in plants. *J Exp Bot* **53**: 1331–1341
- An J, Zhou Q, Sun F, Zhang L** (2009) Ecotoxicological effects of paracetamol on seed germination and seedling development of wheat (*Triticum aestivum* L.). *J Hazard Mater* **169**: 751–757
- Asada K** (2006) Production and Scavenging of Reactive Oxygen Species in Chloroplasts and Their Functions. *Plant Physiol* **141**: 391–396
- Ashton D, Hilton M, Thomas K V** (2004) Investigating the environmental transport of human pharmaceuticals to streams in the United Kingdom. *Sci Total Environ* **333**: 167–184
- Bartha B, Huber C, Harpaintner R, Schroder P** (2010) Effects of acetaminophen in *Brassica juncea* L. Czern.: investigation of uptake, translocation, detoxification, and the induced defense pathways. *Environ Sci Pollut Res Int* **17**: 1553–1562
- Bartha B, Huber C, Schroder P** (2014) Uptake and metabolism of diclofenac in *Typha latifolia*--how plants cope with human pharmaceutical pollution. *Plant Sci* **227**: 12–20
- Bartrons M, Peñuelas J** (2017) Pharmaceuticals and Personal-Care Products in Plants. *Trends Plant Sci* **22**: 194–203
- Bates LS, Waldren RP, Teare ID** (1973) Rapid determination of free proline for water-stress studies. *Plant Soil* **39**: 205–207

Beauchamp C, Fridovich I (1971) Superoxide dismutase: improved assays and an assay applicable to acrylamide gels. *Anal Biochem* **44**: 276–87

Benekos K, Kissoudis C, Nianiou-Obeidat I, Labrou N, Madesis P, Kalamaki M, Makris A, Tsaftaris A (2010) Overexpression of a specific soybean GmGSTU4 isoenzyme improves diphenyl ether and chloroacetanilide herbicide tolerance of transgenic tobacco plants. *J Biotechnol* **150**: 195–201

Bradford MM (1976) A rapid and sensitive method for the quantitation of microgram quantities of protein utilizing the principle of protein-dye binding. *Anal Biochem* **72**: 248–254

Bruce GM, Pleus RC, Snyder SA (2010) Toxicological Relevance of Pharmaceuticals in Drinking Water. *Environ Sci Technol* **44**: 5619–5626

Campos ML, Carvalho RF, Benedito VA, Peres LEP (2010) Small and remarkable: The Micro-Tom model system as a tool to discover novel hormonal functions and interactions. *Plant Signal Behav* **5**: 267–70

Caverzan A, Casassola A, Brammer SP (2016) Reactive Oxygen Species and Antioxidant Enzymes Involved in Plant Tolerance to Stress. *Abiotic Biot Stress Plants*. doi: 10.5772/61368

Chen QY, Wu ZH, Liu JL (2011) Ecotoxicity of Chloramphenicol and Hg Acting on the Root Elongation of Crops in North China. *Int J Environ Res* **5**: 909–916

Choi W-G, Toyota M, Kim S-H, Hilleary R, Gilroy S (2014) Salt stress-induced Ca²⁺ waves are associated with rapid, long-distance root-to-shoot signaling in plants. *Proc Natl Acad Sci* **111**: 6497–6502

Christou A, Antoniou C, Christodoulou C, Hapeshi E, Stavrou I, Michael C, Fattakassinos D, Fotopoulos V (2016) Stress-related phenomena and detoxification mechanisms induced by common pharmaceuticals in alfalfa (*Medicago sativa* L.) plants. *Sci Total Environ* **557–558**: 652–664

Coleman J, Blake-Kalff M, Davies E (1997) Detoxification of xenobiotics by plants: chemical modification and vacuolar compartmentation. *Trends Plant Sci* **2**: 144–151

Csiszar J, Horvath E, Vary Z, Galle A, Bela K, Brunner S, Tari I (2014) Glutathione transferase supergene family in tomato: Salt stress-regulated expression of representative genes from distinct GST classes in plants primed with salicylic acid. *Plant Physiol Biochem PPB* **78**: 15–26

Cummins I, Wortley DJ, Sabbadin F, He Z, Coxon CR, Straker HE, Sellars JD, Knight K, Edwards L, Hughes D, et al (2013) Key role for a glutathione transferase in multiple-herbicide resistance in grass weeds. *Proc Natl Acad Sci U S A* **110**: 5812–7

Dąbrowska G, Kata A, Goc A, Szechyńska-Hebda M, Skrzypek E (2007) Characteristics of the plant ascorbate peroxidase family. *Acta Biol Cracoviensia Ser Bot* **49**: 7–17

Dat J, Vandenabeele S, Vranová E, Van Montagu M, Inzé D, Van Breusegem F (2000) Dual action of the active oxygen species during plant stress responses. *Cell Mol Life Sci* **57**: 779–795

Davidonis GH, Hamilton RH, Mumma RO (1978) Metabolism of 2,4-dichlorophenoxyacetic Acid in soybean root callus and differentiated soybean root cultures as a function of concentration and tissue age. *Plant Physiol* **62**: 80–3

Demidchik V (2015) Mechanisms of oxidative stress in plants: From classical chemistry to cell biology. *Environ Exp Bot* **109**: 212–228

Dhir B, Sharmila P, Saradhi PP (2004) Hydrophytes lack potential to exhibit cadmium stress induced enhancement in lipid peroxidation and accumulation of proline. *Aquat Toxicol* **66**: 141–147

Dixon DP, Laphorn A, Edwards R (2002) Plant glutathione transferases. *Genome Biol* **3**: REVIEWS3004

Do H, Kim I-S, Jeon BW, Lee CW, Park AK, Wi AR, Shin SC, Park H, Kim Y-S, Yoon H-S, et al (2016) Structural understanding of the recycling of oxidized ascorbate by dehydroascorbate reductase (OsDHAR) from *Oryza sativa* L. *japonica*. *Sci Rep* **6**: 19498

Dodgen LK, Ueda A, Wu X, Parker DR, Gan J (2015) Effect of transpiration on plant accumulation and translocation of PPCP/EDCs. *Environ Pollut* **198**: 144–153

Donahue JL, Okpodu CM, Cramer CL, Grabau EA, Alscher RG (1997) Responses of Antioxidants to Paraquat in Pea Leaves (Relationships to Resistance). *Plant Physiol* **113**: 249–257

Dordio A, Ferro R, Teixeira D, Palace AJ, Pinto AP, Dias CMB (2011) Study on the use of *Typha* spp. for the phytotreatment of water contaminated with ibuprofen. *Int J Environ Anal Chem* **91**: 654–667

Dordio A V., Duarte C, Barreiros M, Carvalho AJP, Pinto AP, da Costa CT (2009) Toxicity and removal efficiency of pharmaceutical metabolite clofibric acid by *Typha* spp.

– Potential use for phytoremediation? *Bioresour Technol* **100**: 1156–1161

Ebele AJ, Abdallah MA-E, Harrad S (2017) Pharmaceuticals and personal care products (PPCPs) in the freshwater aquatic environment. *Emerg Contam* **3**: 1–16

Edwards R, Dixon DP (2005) Plant Glutathione Transferases. *Methods Enzymol.* pp 169–186

Erb TJ, Zarzycki J (2018) A short history of RubisCO: the rise and fall (?) of Nature's predominant CO₂ fixing enzyme. *Curr Opin Biotechnol* **49**: 100–107

EU (2015) Commission implementing decision (EU) 2015/495 of 20 March 2015. Establishing a watch list of substances for Unionwide monitoring in the field of water policy pursuant to Directive 2008/105/EC of the European Parliament and of the Council. <https://eur-lex.europa.eu/legal-content/EN/TXT/?uri=CELEX:32015D0495>

Eyer L, Vain T, Pařízková B, Oklestkova J, Barbez E, Kozubíková H, Pospíšil T, Wierzbicka R, Kleine-Vehn J, Fránek M, et al (2016) 2,4-D and IAA Amino Acid Conjugates Show Distinct Metabolism in *Arabidopsis*. *PLoS One* **11**: e0159269

Farrell RE (2010) Quality Control for RNA Preparations. *RNA Methodol* 139–154

Fent K, Weston AA, Caminada D (2006) Ecotoxicology of human pharmaceuticals. *Aquat Toxicol* **76**: 122–159

Ford AT, Fong PP (2016) The effects of antidepressants appear to be rapid and at environmentally relevant concentrations. *Environ Toxicol Chem* **35**: 794–798

Gajewska E, Skłodowska M (2007) Effect of nickel on ROS content and antioxidative enzyme activities in wheat leaves. *BioMetals* **20**: 27–36

Gerszberg A, Hnatuszko-Konka K, Kowalczyk T, Kononowicz AK (2015) Tomato (*Solanum lycopersicum* L.) in the service of biotechnology. *Plant Cell, Tissue Organ Cult* **120**: 881–902

Gill SS, Anjum NA, Hasanuzzaman M, Gill R, Trivedi DK, Ahmad I, Pereira E, Tuteja N (2013) Glutathione and glutathione reductase: A boon in disguise for plant abiotic stress defense operations. *Plant Physiol Biochem* **70**: 204–212

Gill SS, Tuteja N (2010) Reactive oxygen species and antioxidant machinery in abiotic stress tolerance in crop plants. *Plant Physiol Biochem PPB* **48**: 909–930

Gong P, Wilke BM, Strozzi E, Fleischmann S (2001) Evaluation and refinement of a continuous seed germination and early seedling growth test for the use in the

ecotoxicological assessment of soils. *Chemosphere* **44**: 491–500

Gonzalez-Naranjo V, Boltes K, de Bustamante I, Palacios-Diaz P (2015) Environmental risk of combined emerging pollutants in terrestrial environments: chlorophyll a fluorescence analysis. *Environ Sci Pollut Res Int* **22**: 6920–6931

González García M, Fernández-López C, Pedrero-Salcedo F, Alarcón JJ (2018) Absorption of carbamazepine and diclofenac in hydroponically cultivated lettuces and human health risk assessment. *Agric Water Manag* **206**: 42–47

Gracia-Lor E, Sancho J V, Serrano R, Hernandez F (2012) Occurrence and removal of pharmaceuticals in wastewater treatment plants at the Spanish Mediterranean area of Valencia. *Chemosphere* **87**: 453–462

Grant CM (2001) Role of the glutathione/glutaredoxin and thioredoxin systems in yeast growth and response to stress conditions. *Mol Microbiol* **39**: 533–41

Grassi M, Rizzo L, Farina A (2013) Endocrine disruptors compounds, pharmaceuticals and personal care products in urban wastewater: implications for agricultural reuse and their removal by adsorption process. *Environ Sci Pollut Res Int* **20**: 3616–3628

Grillo MP, Knutson CG, Sanders PE, Waldon DJ, Hua F, Ware JA (2003) Studies on the chemical reactivity of diclofenac acyl glucuronide with glutathione: identification of diclofenac-S-acyl-glutathione in rat bile. *Drug Metab Dispos* **31**: 1327–1336

De Groeve MRM, Tran GH, Van Hoorebeke A, Stout J, Desmet T, Savvides SN, Soetaert W (2010) Development and application of a screening assay for glycoside phosphorylases. *Anal Biochem* **401**: 162–167

Grune T (2005) Oxidants and antioxidant defense systems. Springer Science & Business Media

Guiloski IC, Stein Pincini LD, Dagostim AC, de Moraes Calado SL, Fávaro LF, Boschen SL, Cestari MM, da Cunha C, Silva de Assis HC (2017) Effects of environmentally relevant concentrations of the anti-inflammatory drug diclofenac in freshwater fish *Rhamdia quelen*. *Ecotoxicol Environ Saf* **139**: 291–300

Gupta AS, Heinen JL, Holaday AS, Burke JJ, Allen RD (1993) Increased resistance to oxidative stress in transgenic plants that overexpress chloroplastic Cu/Zn superoxide dismutase. *Proc Natl Acad Sci U S A* **90**: 1629–1633

Halliwell B (2006) Reactive Species and Antioxidants. Redox Biology Is a Fundamental Theme of Aerobic Life. *Plant Physiol* **141**: 312 LP-322

Han GH, Hur HG, Kim SD (2006) Ecotoxicological risk of pharmaceuticals from wastewater treatment plants in Korea: occurrence and toxicity to *Daphnia magna*. *Environ Toxicol Chem* **25**: 265–271

Hare PD, Cress WA (1997) Metabolic implications of stress-induced proline accumulation in plants. *Plant Growth Regul* **21**: 79–102

Hasanuzzaman M, Nahar K, Anee TI, Fujita M (2017) Glutathione in plants: biosynthesis and physiological role in environmental stress tolerance. *Physiol Mol Biol Plants* **23**: 249–268

Hayat S, Hayat Q, Alyemeni MN, Wani AS, Pichtel J, Ahmad A (2012) Role of proline under changing environments. *Plant Signal Behav* **7**: 1456–1466

He J-M, She X-P, Meng Z-N, Zhao W-M (2004) Reduction of Rubisco amount by UV-B radiation is related to increased H₂O₂ content in leaves of mung bean seedlings. *Zhi Wu Sheng Li Yu Fen Zi Sheng Wu Xue Xue Bao* **30**: 291–6

He Y, Langenhoff AAM, Sutton NB, Rijnaarts HHM, Blokland MH, Chen F, Huber C, Schröder P (2017) Metabolism of Ibuprofen by *Phragmites australis*: Uptake and Phytodegradation. *Environ Sci Technol* **51**: 4576–4584

Heath RL, Packer L (1968) Photoperoxidation in isolated chloroplasts: I. Kinetics and stoichiometry of fatty acid peroxidation. *Arch Biochem Biophys* **125**: 189–198

Heberer T (2002) Occurrence, fate, and removal of pharmaceutical residues in the aquatic environment: A review of recent research data. *Toxicol Lett* **131**: 5–17

Hossain MA, Mostofa MG, Vivancos PD, Burritt DJ, Fujita M, Tran L-SP (2017) Glutathione in Plant Growth, Development, and Stress Tolerance. doi: 10.1007/978-3-319-66682-2

Huber C, Bartha B, Schröder P (2012) Metabolism of diclofenac in plants – Hydroxylation is followed by glucose conjugation. *J Hazard Mater* **243**: 250–256

Jajic I, Sarna T, Strzalka K (2015) Senescence, Stress, and Reactive Oxygen Species. *Plants (Basel, Switzerland)* **4**: 393–411

Jeffries KM, Brander SM, Britton MT, Fangué NA, Cannon RE (2015) Chronic exposures to low and high concentrations of ibuprofen elicit different gene response patterns in a euryhaline fish. *Environ Sci Pollut Res Int* **22**: 17397–17413

Jin C, Chen Q, Sun R, Zhou Q, Liu J (2009) Eco-toxic effects of sulfadiazine sodium,

sulfamonomethoxine sodium and enrofloxacin on wheat, Chinese cabbage and tomato. *Ecotoxicology* **18**: 878–885

Kampranis SC, Damianova R, Atallah M, Toby G, Kondi G, Tsihchlis PN, Makris AM (2000) A Novel Plant Glutathione S -Transferase/Peroxidase Suppresses Bax Lethality in Yeast. *J Biol Chem* **275**: 29207–29216

Karnjanapiboonwong A, Chase DA, Cañas JE, Jackson WA, Maul JD, Morse AN, Anderson TA (2011) Uptake of 17 α -ethynylestradiol and triclosan in pinto bean, *Phaseolus vulgaris*. *Ecotoxicol Environ Saf* **74**: 1336–1342

Kasote DM, Katyare SS, Hegde M V, Bae H (2015) Significance of antioxidant potential of plants and its relevance to therapeutic applications. *Int J Biol Sci* **11**: 982–91

Kaur G, Asthir B (2015) Proline: a key player in plant abiotic stress tolerance. *Biol Plant* **59**: 609–619

Khan MH, Panda SK (2007) Alterations in root lipid peroxidation and antioxidative responses in two rice cultivars under NaCl-salinity stress. *Acta Physiol Plant* **30**: 81–89

Khetan SK, Collins TJ (2007) Human Pharmaceuticals in the Aquatic Environment: A Challenge to Green Chemistry. *Chem Rev* **107**: 2319–2364

Kim SD, Cho J, Kim IS, Vanderford BJ, Snyder SA (2007) Occurrence and removal of pharmaceuticals and endocrine disruptors in South Korean surface, drinking, and waste waters. *Water Res* **41**: 1013–1021

Kimura S, Sinha N (2008) Tomato (*Solanum lycopersicum*): A Model Fruit-Bearing Crop. *CSH Protoc* **2008**: pdb.emo105

Komives T, Gullner G (2005) Phase I xenobiotic metabolic systems in plants. *Z Naturforsch C* **60**: 179–185

Kösesakal T, Ünal M (2012) Effects of zinc toxicity on seed germination and plant growth in tomato (*Lycopersicon esculentum* Mill.). *Fresenius Environ Bull* **21**: 315–324

Kotyza J, Soudek P, Kafka Z, Vaněk T (2010) Phytoremediation of Pharmaceuticals—Preliminary Study. *Int J Phytoremediation* **12**: 306–316

Kummerova M, Zezulka S, Babula P, Triska J (2016) Possible ecological risk of two pharmaceuticals diclofenac and paracetamol demonstrated on a model plant *Lemna minor*. *J Hazard Mater* **302**: 351–361

Labrou NE, Papageorgiou AC, Pavli O, Flietakis E (2015) Plant GSTome: structure

and functional role in xenome network and plant stress response. *Curr Opin Biotechnol* **32**: 186–194

Lamoureux GL, Rusness DG, Schroder P (1993) Metabolism of a Diphenylether Herbicide to a Volatile Thioanisole and a Polar Sulfonic Acid Metabolite in Spruce (*Picea*). *Pestic Biochem Physiol* **47**: 8–20

Li X, Feng Y, Boersma L (1994) Partition of photosynthates between shoot and root in spring wheat (*Triticum aestivum* L.) as a function of soil water potential and root temperature. *Plant Soil* **164**: 43–50

Liang X, Zhang L, Natarajan SK, Becker DF (2013) Proline mechanisms of stress survival. *Antioxid Redox Signal* **19**: 998–1011

Livak KJ, Schmittgen TD (2001) Analysis of Relative Gene Expression Data Using Real-Time Quantitative PCR and the $2^{-\Delta\Delta CT}$ Method. *Methods* **25**: 402–408

Lonappan L, Brar SK, Das RK, Verma M, Surampalli RY (2016) Diclofenac and its transformation products: Environmental occurrence and toxicity - A review. *Environ Int* **96**: 127–138

Lopez-Serna R, Perez S, Ginebreda A, Petrovic M, Barcelo D (2010) Fully automated determination of 74 pharmaceuticals in environmental and waste waters by online solid phase extraction-liquid chromatography-electrospray-tandem mass spectrometry. *Talanta* **83**: 410–424

Løvdaal T, Lillo C (2009) Reference gene selection for quantitative real-time PCR normalization in tomato subjected to nitrogen, cold, and light stress. *Anal Biochem* **387**: 238–242

Luu D-T, Maurel C (2005) Aquaporins in a challenging environment: molecular gears for adjusting plant water status. *Plant, Cell Environ* **28**: 85–96

Matamoros V, Arias CA, Nguyen LX, Salvadó V, Brix H (2012a) Occurrence and behavior of emerging contaminants in surface water and a restored wetland. *Chemosphere* **88**: 1083–1089

Matamoros V, Nguyen LX, Arias CA, Salvadó V, Brix H (2012b) Evaluation of aquatic plants for removing polar microcontaminants: A microcosm experiment. *Chemosphere* **88**: 1257–1264

McGettigan P, Henry D (2013) Use of non-steroidal anti-inflammatory drugs that elevate cardiovascular risk: an examination of sales and essential medicines lists in low-, middle-

, and high-income countries. PLoS Med **10**: e1001388

McRae NK, Glover CN, Burket SR, Brooks BW, Gaw S (2018) Acute exposure to an environmentally relevant concentration of diclofenac elicits oxidative stress in the culturally important galaxiid fish *Galaxias maculatus*. Environ Toxicol Chem **37**: 224–235

Mehinto AC, Hill EM, Tyler CR (2010) Uptake and Biological Effects of Environmentally Relevant Concentrations of the Nonsteroidal Anti-inflammatory Pharmaceutical Diclofenac in Rainbow Trout (*Oncorhynchus mykiss*). Environ Sci Technol **44**: 2176–2182

Meissner R, Jacobson Y, Melamed S, Levyatuv S, Shalev G, Ashri A, Elkind Y, Levy A (1997) A new model system for tomato genetics. Plant J **12**: 1465–1472

Mhamdi A, Queval G, Chaouch S, Vanderauwera S, Van Breusegem F, Noctor G (2010) Catalase function in plants: a focus on Arabidopsis mutants as stress-mimic models. J Exp Bot **61**: 4197–4220

Michelini L, Reichel R, Werner W, Ghisi R, Thiele-Bruhn S (2012) Sulfadiazine Uptake and Effects on *Salix fragilis* L. and *Zea mays* L. Plants. Water, Air, Soil Pollut **223**: 5243–5257

Miller A-F (2012) Superoxide dismutases: Ancient enzymes and new insights. FEBS Lett **586**: 585–595

Mittler R (2002) Oxidative stress, antioxidants and stress tolerance. Trends Plant Sci **7**: 405–410

Mobin M, Khan NA (2007) Photosynthetic activity, pigment composition and antioxidative response of two mustard (*Brassica juncea*) cultivars differing in photosynthetic capacity subjected to cadmium stress. J Plant Physiol **164**: 601–610

Mohapatra D, Cledón M, Brar K, Y. Surampalli R (2016) Application of Wastewater and Biosolids in Soil: Occurrence and Fate of Emerging Contaminants. Water, Air, Soil Pollut. doi: 10.1007/s11270-016-2768-4

Moons A (2005) Regulatory and Functional Interactions of Plant Growth Regulators and Plant Glutathione S-Transferases (GSTs). Vitam Horm **72**: 155–202

Murshed R, Lopez-Lauri F, Sallanon H (2008) Microplate quantification of enzymes of the plant ascorbate–glutathione cycle. Anal Biochem **383**: 320–322

National Center for Environmental Assessments (2011) Exposure Factors Handbook

2011 Edition (Final Report). U.S. Environ. Prot. Agency, Washington, DC

Noctor G, Arisi A-CM, Jouanin L, Kunert KJ, Rennenberg H, Foyer CH (1998) Glutathione: biosynthesis, metabolism and relationship to stress tolerance explored in transformed plants. *J Exp Bot* **49**: 623–647

Noctor G, Mhamdi A, Chaouch S, Han Y, Neukermans J, Marquez-Garcia B, Queval G, Foyer CH (2012) Glutathione in plants: an integrated overview. *Plant Cell Environ* **35**: 454–484

Oaks JL, Gilbert M, Virani MZ, Watson RT, Meteyer CU, Rideout BA, Shivaprasad HL, Ahmed S, Iqbal Chaudhry MJ, Arshad M, et al (2004) Diclofenac residues as the cause of vulture population decline in Pakistan. *Nature* **427**: 630–633

Overturf MD, Anderson JC, Pandelides Z, Beyger L, Holdway DA (2015) Pharmaceuticals and personal care products: A critical review of the impacts on fish reproduction. *Crit Rev Toxicol* **45**: 469–491

Öztetik E (2008) A Tale of Plant Glutathione S-Transferases: Since 1970. *Bot Rev* **74**: 419–437

Pan M, Chu LM (2016) Phytotoxicity of veterinary antibiotics to seed germination and root elongation of crops. *Ecotoxicol Environ Saf* **126**: 228–237

Pereira A, Silva L, S.M. Laranjeiro C, M. Meisel L, Lino C, Pena A (2017) Human pharmaceuticals in Portuguese rivers: The impact of water scarcity in the environmental risk. *Sci Total Environ* **609**: 1182–1191

Pierattini EC, Francini A, Huber C, Sebastiani L, Schröder P (2018) Poplar and diclofenac pollution: A focus on physiology, oxidative stress and uptake in plant organs. *Sci Total Environ* **636**: 944–952

Pino MR, Muñiz S, Val J, Navarro E (2016) Phytotoxicity of 15 common pharmaceuticals on the germination of *Lactuca sativa* and photosynthesis of *Chlamydomonas reinhardtii*. *Environ Sci Pollut Res* **23**: 22530–22541

Pinto AÁF (2017) 2,4-dichlorophenoxy acetic acid-mediated stress in tomato plants: a biochemical and molecular approach. University of Porto

Quan L-J, Zhang B, Shi W-W, Li H-Y (2008) Hydrogen peroxide in plants: a versatile molecule of the reactive oxygen species network. *J Integr Plant Biol* **50**: 2–18

Rejeb K, Lefebvre-De Vos D, Le Disquet I, Leprince A-S, Bordenave M, Maldiney R,

- Jdey A, Abdelly C, Savouré A** (2015) Hydrogen peroxide produced by NADPH oxidases increases proline accumulation during salt or mannitol stress in *Arabidopsis thaliana*. *New Phytol* **208**: 1138–1148
- Ricci G, Bello M Lo, Caccuri AM, Galiazzo F, Federici G** (1984) Detection of glutathione transferase activity on polyacrylamide gels. *Anal Biochem* **143**: 226–230
- Rouhier N, Lemaire SD, Jacquot J-P** (2008) The Role of Glutathione in Photosynthetic Organisms: Emerging Functions for Glutaredoxins and Glutathionylation. *Annu Rev Plant Biol* **59**: 143–166
- Rucińska-Sobkowiak R** (2016) Water relations in plants subjected to heavy metal stresses. *Acta Physiol Plant* **38**: 257
- Salgado R, Noronha JP, Oehmen A, Carvalho G, Reis MAM** (2010) Analysis of 65 pharmaceuticals and personal care products in 5 wastewater treatment plants in Portugal using a simplified analytical methodology. *Water Sci Technol* **62**: 2862–2871
- Sandermann H** (1992) Plant metabolism of xenobiotics. *Trends Biochem Sci* **17**: 82–4
- Sandermann HJ** (1994) Higher plant metabolism of xenobiotics: the “green liver” concept. *Pharmacogenetics* **4**: 225–241
- Sasan M, Maryam E, Fateme M, Maryam S, Babak S, Hassan M** (2011) Plant glutathione S-transferase classification, structure and evolution. *African J Biotechnol* **10**: 8160–8165
- Schmidt W, Redshaw CH** (2015) Evaluation of biological endpoints in crop plants after exposure to non-steroidal anti-inflammatory drugs (NSAIDs): implications for phytotoxicological assessment of novel contaminants. *Ecotoxicol Environ Saf* **112**: 212–222
- Schröder P, Collins C** (2002) Conjugating Enzymes Involved in Xenobiotic Metabolism of Organic Xenobiotics in Plants. *Int J Phytoremediation* **4**: 247–265
- Schröder P, Huber C V, Bartha B** (2013) Insight in the Metabolism of Diclofenac in Plants – P 450 Mediated Hydroxylation Is Followed by Glucosyl Transfer Reactions.
- Schröder P, Juuti S, Roy S, Sandermann H, Sutinen S** (1997) Exposure to chlorinated acetic acids: Responses of peroxidase and glutathione S-transferase activity in pine needles. *Environ Sci Pollut Res* **4**: 163–171
- Schwaiger J, Ferling H, Mallow U, Wintermayr H, Negele RD** (2004) Toxic effects of

the non-steroidal anti-inflammatory drug diclofenac. Part I: histopathological alterations and bioaccumulation in rainbow trout. *Aquat Toxicol* **68**: 141–150

Sengupta D, Ramesh G, Mudalkar S, Kumar KRR, Kirti PB, Reddy AR (2012) Molecular Cloning and Characterization of γ -Glutamyl Cysteine Synthetase (V γ ECS) from Roots of *Vigna radiata* (L.) Wilczek Under Progressive Drought Stress and Recovery. *Plant Mol Biol Report* **30**: 894–903

Sevilla F, Camejo D, Ortiz-Espín A, Calderón A, Lázaro JJ, Jiménez A (2015) The thioredoxin/peroxiredoxin/sulfiredoxin system: current overview on its redox function in plants and regulation by reactive oxygen and nitrogen species. *J Exp Bot* **66**: 2945–2955

Sharma P, Jha AB, Dubey RS, Pessarakli M (2012) Reactive Oxygen Species, Oxidative Damage, and Antioxidative Defense Mechanism in Plants under Stressful Conditions. *J Bot* **2012**: 1–26

Sharma R, Sahoo A, Devendran R, Jain M (2014) Over-expression of a rice tau class glutathione s-transferase gene improves tolerance to salinity and oxidative stresses in *Arabidopsis*. *PLoS One* **9**: e92900

Shimabukuro RH (1976) Glutathione conjugation of herbicides in plants and animals and its role in herbicidal selectivity. *Asian-Pacific Weed Sci Soc* **183**: e186

Sies H (1993) Strategies of antioxidant defense. *Eur J Biochem* **215**: 213–219

Snyder SA (2008) Occurrence, Treatment, and Toxicological Relevance of EDCs and Pharmaceuticals in Water. *Ozone Sci Eng* **30**: 65–69

Soares C, Branco-Neves S, de Sousa A, Pereira R, Fidalgo F (2016) Ecotoxicological relevance of nano-NiO and acetaminophen to *Hordeum vulgare* L.: Combining standardized procedures and physiological endpoints. *Chemosphere* **165**: 442–452

Soares C, Branco-Neves S, de Sousa A, Teixeira J, Pereira R, Fidalgo F (2018) Can nano-SiO₂ reduce the phytotoxicity of acetaminophen? – A physiological, biochemical and molecular approach. *Environ Pollut* **241**: 900–911

de Sousa A, AbdElgawad H, Asard H, Pinto A, Soares C, Branco-Neves S, Braga T, Azenha M, Selim S, Al Jaouni S, et al (2017) Metalaxyl Effects on Antioxidant Defenses in Leaves and Roots of *Solanum nigrum* L. *Front Plant Sci*. doi: 10.3389/fpls.2017.01967

de Sousa A, Teixeira J, Regueiras MT, Azenha M, Silva F, Fidalgo F (2013) Metalaxyl-induced changes in the antioxidant metabolism of *Solanum nigrum* L.

suspension cells. *Pestic Biochem Physiol* **107**: 235–243

Sresty TVS, Madhava Rao KV (1999) Ultrastructural alterations in response to zinc and nickel stress in the root cells of pigeonpea. *Environ Exp Bot* **41**: 3–13

Streibig JC, Walker A, Blair AM, Anderson-Taylor G, Eagle DJ, Friedländer H, Hacker E, Iwanzik W, Kudsk P, Labhart C, et al (2006) Variability of bioassays with metsulfuron-methyl in soil. *Weed Res* **35**: 215–224

Sun C, Dudley S, Trumble J, Gan J (2017) Pharmaceutical and personal care products-induced stress symptoms and detoxification mechanisms in cucumber plants. *Environ Pollut* **234**: 39–47

Susarla S, Medina VF, McCutcheon SC (2002) Phytoremediation: An ecological solution to organic chemical contamination. *Ecol Eng* **18**: 647–658

Sutherland MW (1991) The generation of oxygen radicals during host plant responses to infection. *Physiol Mol Plant Pathol* **39**: 79–93

Taiz L, Zeiger E (2010) *Plant physiology* 5th Ed. Sunderland, MA Sinauer Assoc.

Teixeira J, Sousa A de, Azenha M, Moreira JT, Fidalgo F, Fernando Silva A, Faria JL, Silva AMT (2011) *Solanum nigrum* L. weed plants as a remediation tool for metalaxyl-polluted effluents and soils. *Chemosphere* **85**: 744–750

Ternes TA (1998) Occurrence of drugs in German sewage treatment plants and rivers. *Water Res* **32**: 3245–3260

Thatcher LF, Carrie C, Andersson CR, Sivasithamparam K, Whelan J, Singh KB (2007) Differential Gene Expression and Subcellular Targeting of Arabidopsis Glutathione S-Transferase F8 Is Achieved through Alternative Transcription Start Sites. *J Biol Chem* **282**: 28915–28928

Trapp S, Legind CN (2011) Uptake of Organic Contaminants from Soil into Vegetables and Fruits BT - *Dealing with Contaminated Sites: From Theory towards Practical Application*. In FA Swartjes, ed, Springer Netherlands, Dordrecht, pp 369–408

Tripathy BC, Oelmüller R (2012) Reactive oxygen species generation and signaling in plants. *Plant Signal Behav* **7**: 1621–1633

Vieira dos Santos C, Rey P (2006) Plant thioredoxins are key actors in the oxidative stress response. *Trends Plant Sci* **11**: 329–34

Wagner U, Edwards R, Dixon DP, Mauch F (2002) Probing the Diversity of the

Arabidopsis glutathione S-Transferase Gene Family. *Plant Mol Biol* **49**: 515–532

Walker A, Cotterill EG, Welch SJ (1989) Adsorption and degradation of chlorsulfuron and metsulfuron-methyl in soils from different depths. *Weed Res* **29**: 281–287

Wink M (1997) Compartmentation of Secondary Metabolites and Xenobiotics in Plant Vacuoles. *Adv Bot Res* **25**: 141–169

Xu J, Duan X, Yang J, Beeching JR, Zhang P (2013) Enhanced Reactive Oxygen Species Scavenging by Overproduction of Superoxide Dismutase and Catalase Delays Postharvest Physiological Deterioration of Cassava Storage Roots. *Plant Physiol* **161**: 1517–1528

Yan Q, Gao X, Guo J, Zhu Z, Feng G (2016) Insights into the molecular mechanism of the responses for *Cyperus alternifolius* to PhACs stress in constructed wetlands. *Chemosphere* **164**: 278–289

Yang S-L, Lan S-S, Gong M (2009) Hydrogen peroxide-induced proline and metabolic pathway of its accumulation in maize seedlings. *J Plant Physiol* **166**: 1694–1699

Yannarelli GG, Fernández-Alvarez AJ, Santa-Cruz DM, Tomaro ML (2007) Glutathione reductase activity and isoforms in leaves and roots of wheat plants subjected to cadmium stress. *Phytochemistry* **68**: 505–512

Yu T a. o., Li YS, Chen XF, Hu J, Chang X u. n., Zhu YG (2003) Transgenic tobacco plants overexpressing cotton glutathione S-transferase (GST) show enhanced resistance to methyl viologen. *J Plant Physiol* **160**: 1305–1311

Zagorchev L, Seal CE, Kranner I, Odjakova M (2013) A Central Role for Thiols in Plant Tolerance to Abiotic Stress. *Int J Mol Sci* **14**: 7405–7432

Zar JH (1996) Biostatistical analysis. Prentice Hall

Zhang H, Lian C, Shen Z (2009) Proteomic identification of small, copper-responsive proteins in germinating embryos of *Oryza sativa*. *Ann Bot* **103**: 923–930

Zhang Z, Xie Q, Jobe TO, Kau AR, Wang C, Li Y, Qiu B, Wang Q, Mendoza-Cózatl DG, Schroeder JI (2016) Identification of AtOPT4 as a Plant Glutathione Transporter. *Mol Plant* **9**: 481–484

Zhou Y-H, Yu J-Q, Mao W-H, Huang L-F, Song X-S, Nogués S (2006) Genotypic Variation of Rubisco Expression, Photosynthetic Electron Flow and Antioxidant Metabolism in the Chloroplasts of Chill-exposed Cucumber Plants. *Plant Cell Physiol* **47**:

192–199

Zhu J-K (2016) Abiotic Stress Signaling and Responses in Plants. *Cell* **167**: 313–324

Zlatev ZS, Lidon FC, Ramalho JC, Yordanov IT (2006) Comparison of resistance to drought of three bean cultivars. *Biol Plant* **50**: 389–394